

Contents

| | |
|--|-----------|
| 1 Radial Density Function | 2 |
| 1.1 Calculation of Distances with Periodicity | 2 |
| 1.2 Adding Noise For Atom Vibration | 3 |
| 1.3 Cubane Example | 3 |
| 1.3.1 Cubane Radial Density Functions | 4 |
| 1.4 Experimental and Theoretical RDFs for Known Structures | 6 |
| 1.4.1 Ga As | 6 |
| 1.4.2 In As | 7 |
| 1.4.3 Si Lattice | 7 |
| 2 Smoothing Analysis | 8 |
| 3 Matching Algorithm Evaluation | 11 |
| 3.1 Noise Analysis | 13 |
| 3.1.1 Peak Counts | 14 |
| 3.1.2 Peak Locations | 16 |
| 3.1.3 Noise Peak Heights | 17 |
| 3.1.4 Sample Noisy Image | 19 |
| 4 Recognition Using Eigenfaces | 21 |
| 4.1 Mean Image | 21 |
| 4.2 Variance Explained by Principal Components | 23 |
| 4.3 Eigenfaces | 24 |
| 4.4 Data in Eigenspace | 27 |
| 4.4.1 Eigenspace Outliers | 32 |
| 4.5 Experimental Image Recognition | 37 |
| 4.5.1 3 Principal Components | 37 |
| 4.5.2 10 Principal Components | 48 |
| 4.5.3 128 Principal Components | 59 |
| 4.6 Synthetic Experimental Image Recognition | 70 |

| | | |
|----------|--|-----------|
| 5 | Recognition Using Sparse Representations | 72 |
| 5.1 | Experimental Image Recognition | 72 |
| 5.2 | Synthetic Experimental Image Recognition | 83 |
| 6 | Code | 84 |
| 7 | Sources | 84 |

1 Radial Density Function

1.1 Calculation of Distances with Periodicity

Suppose a large chemical structure has uncountably many atoms but the follow a periodic pattern of n atoms every p Angstroms. The atom locations within a period are given by a_1, a_2, \dots, a_n where $a_i \in \mathbb{R}^3$. The radial density function is the distribution of pairwise distances between these atoms.

The distances d between atoms a_i and a_j where $i \neq j$, atom a_i has been displaced by x , and atom a_j has been displaced by y per the periodicity is

$$\begin{aligned} d^2 &= \langle a_i + x - (a_j + y), a_i + x - (a_j + y) \rangle \\ &= \langle a_i - a_j, a_i - a_j \rangle + \langle x - y, x - y \rangle + 2\langle a_i - a_j, x - y \rangle \end{aligned}$$

where $x = (k_1 p, k_2 p, k_3 p)$ for $k_i \in \mathbb{Z}$ and $y = (l_1 p, l_2 p, l_3 p)$ for $l_i \in \mathbb{Z}$. Here $\langle x, y \rangle$ denotes the inner product between x and y .

Suppose D is a random variable that samples at random the distances, d , in the chemical structure. The radial density function is the probability density function of this random variable. This function can be estimated empirically via a histogram.

The histogram is then normalized by the volume a spherical shell.

$$\begin{aligned} &\frac{4}{3}\pi(r + \Delta r)^3 - \frac{4}{3}\pi r^3 \\ &= \frac{4}{3}(3r^2\Delta r + 3r(\Delta r)^2 + (\Delta r)^3) \\ &\approx 4\pi r^2 \Delta r \end{aligned}$$

where Δr tends to zero.

For a histogram with frequency, f , for bin $[d_i, d_{i+1}]$, we replace f with f/d_i^2 . And then normalize the histogram so that the sum over all bins is one.

1.2 Adding Noise For Atom Vibration

Due to the vibrations of the molecules, the radial density function will not be just the equilibrium positions. We can approximate this fluctuation in distances via a Gaussian filter or Weierstrass transform.

$$F(x) = \frac{1}{\sqrt{4\pi t}} \int_{-\infty}^{\infty} f(y) e^{-\frac{(x-y)^2}{4t}} dy$$

Given that the density function is only defined for a finite number of distances, we use a discrete version of the transform making sure to keep the sum of the weights equal to one.

$$F(d_k) = \frac{\sum_{d_i=d_0}^{d_n} f(d_i) \exp\left(-\frac{(d_k-d_i)^2}{4t}\right)}{\sum_{d_i=d_0}^{d_n} \exp\left(-\frac{(d_k-d_i)^2}{4t}\right)}$$

where d_0 is the minimum distance and d_n is the maximum distance.

1.3 Cubane Example

As an example of the above, below are the calculations for cubane (C_8H_8).

Here are the coordinates of the elements in Angstroms.

```
Element, x, y, z
C, 1.2455, 0.5367, -0.0729
C, 0.9239, -0.9952, 0.0237
C, -0.1226, -0.7041, 1.1548
C, 0.1989, 0.8277, 1.0582
```

C, 0.1226, 0.7042,-1.1548
C,-0.9239, 0.9952,-0.0237
C,-1.2454,-0.5367, 0.0729
C,-0.1989,-0.8277,-1.0582
H, 2.2431, 0.9666,-0.1313
H, 1.6638,-1.7924, 0.0426
H,-0.2209,-1.2683, 2.0797
H, 0.3583, 1.4907, 1.9059
H, 0.2208, 1.2681,-2.0799
H,-1.6640, 1.7922,-0.0427
H,-2.2430,-0.9665, 0.1313
H,-0.3583,-1.4906,-1.9058

1.3.1 Cubane Radial Density Functions

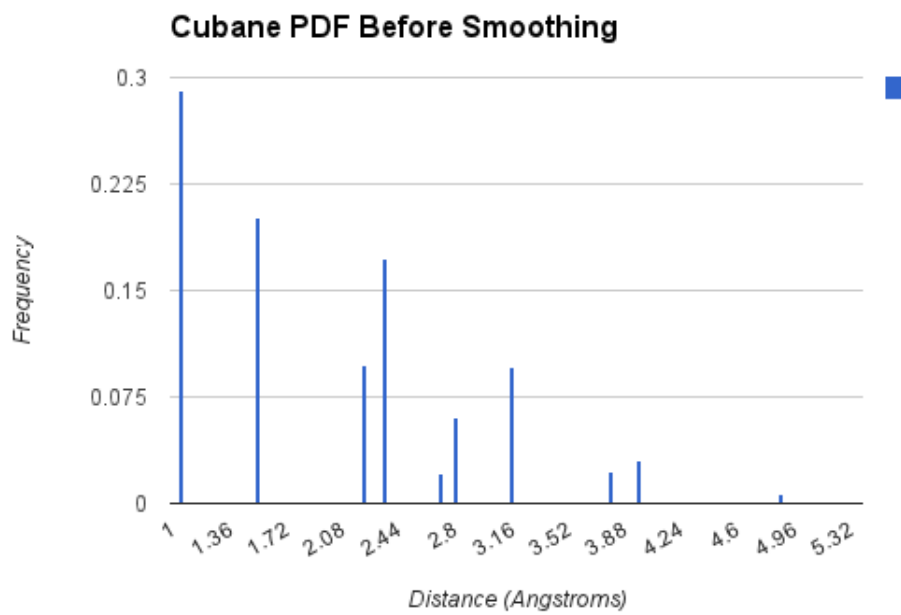


Figure 1: Before Smoothing

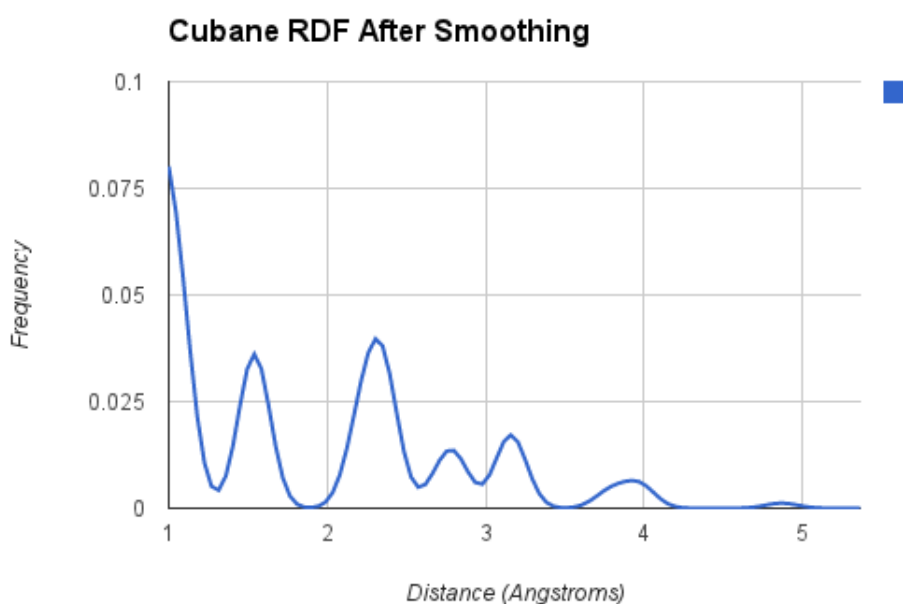


Figure 2: After Smoothing

1.4 Experimental and Theoretical RDFs for Known Structures

For some structures, we are able to theoretically calculate the RDF from atom locations and also have the experimental RDF from Xray scattering. These known matches provide some insight into understanding how the experiments and theory align. The RDF comparison are shown below.

Outside of these structures, there are not many other known matches. There are a few reasons for this. First, if a structures is already known at the atomic level then there is no need to run an xray diffraction experiment. Second, if a structure is periodic as in a lattice, the atomic structure can be determined by xray diffraction which is easier and cheaper than xray scattering.

1.4.1 Ga As

Experimental Data: Pair Distribution Functions Analysis, Valeri Petkov

Calculated Data: Maria Chan

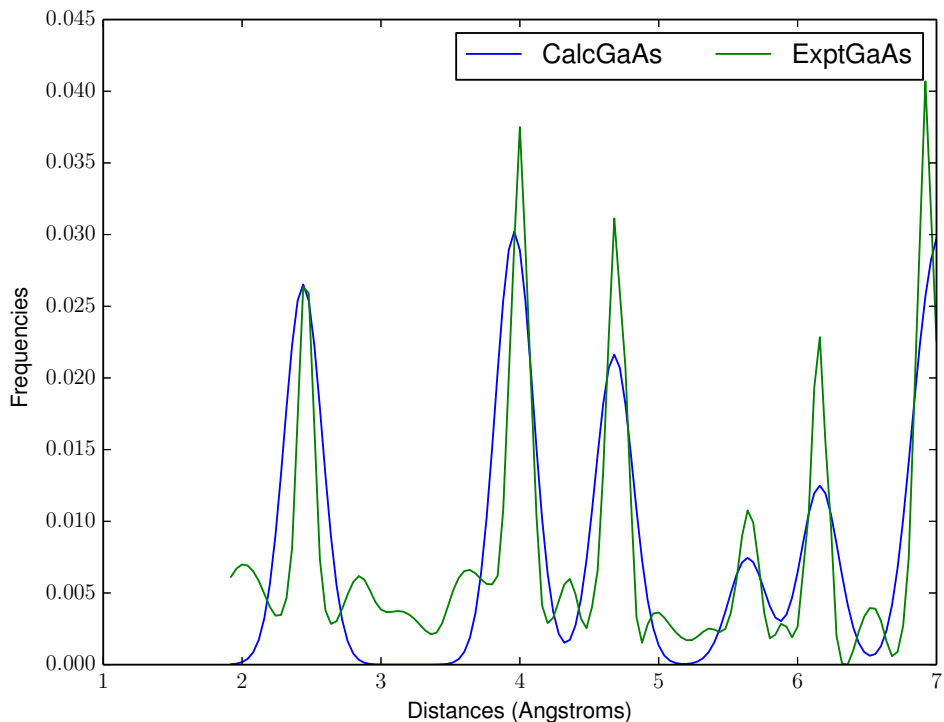


Figure 3: Ga As

1.4.2 In As

Experimental Data: Pair Distribution Functions Analysis, Valeri Petkov

Calculated Data: Maria Chan

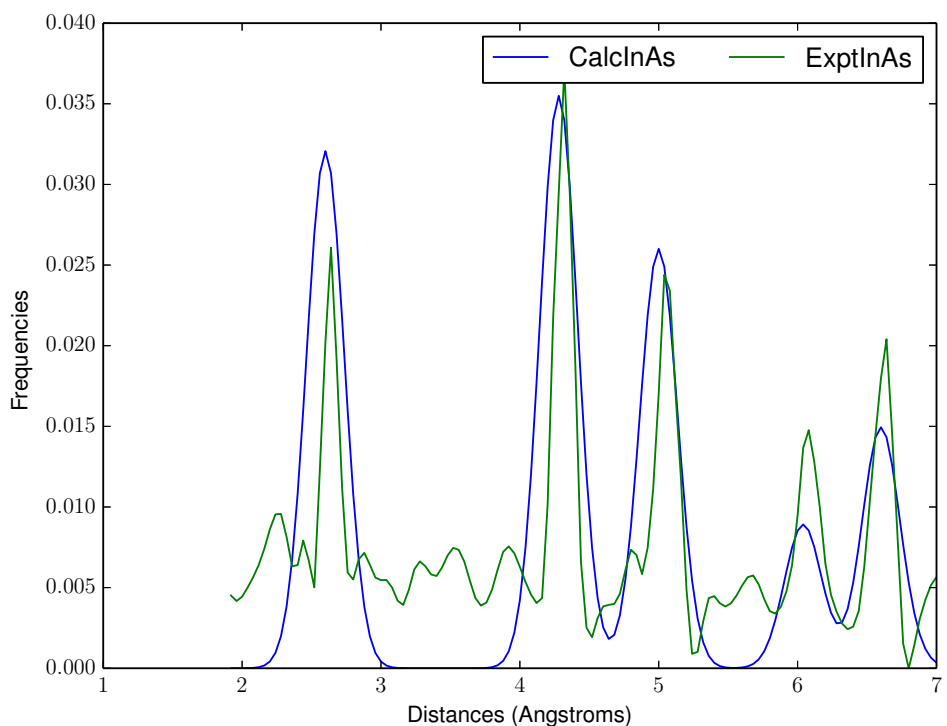


Figure 4: In As

1.4.3 Si Lattice

Experimental Data: J. AM. CHEM. SOC. VOL. 133, NO. 3, 2011, P: 503-512

Calculated Data: <http://materialsproject.org/materials/mp-149/>

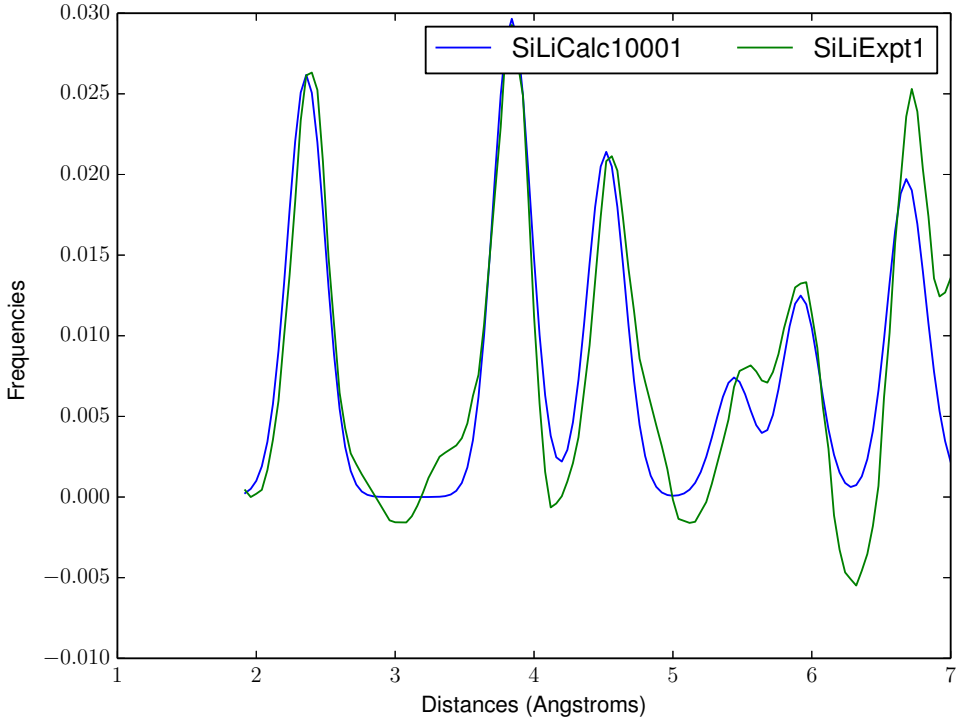


Figure 5: Si Lattice

2 Smoothing Analysis

Consider a function, $\text{SmoothAndNormalize}(i, t)$, that smoothes the image, i , with a smoothing coefficient of t and then normalizes the smoothed image so that the weights sum to one. To calibrate the smoothing coefficient, we focus on the SiLi calculated and experimental matches, SiLiCalc10001 and SiLiExpt1. We want to find the smoothing coefficient, t , that after smoothing and normalization the calculated image is the closest match to the experimental image.

$$\hat{t} = \arg \min_t \|X - \text{SmoothAndNormalize}(C, t)\|_2$$

where $\|\cdot\|_2$ is the L^2 norm, X is the experimental image, and C is the calculated image.

We found that $\hat{t} = 0.0092$.

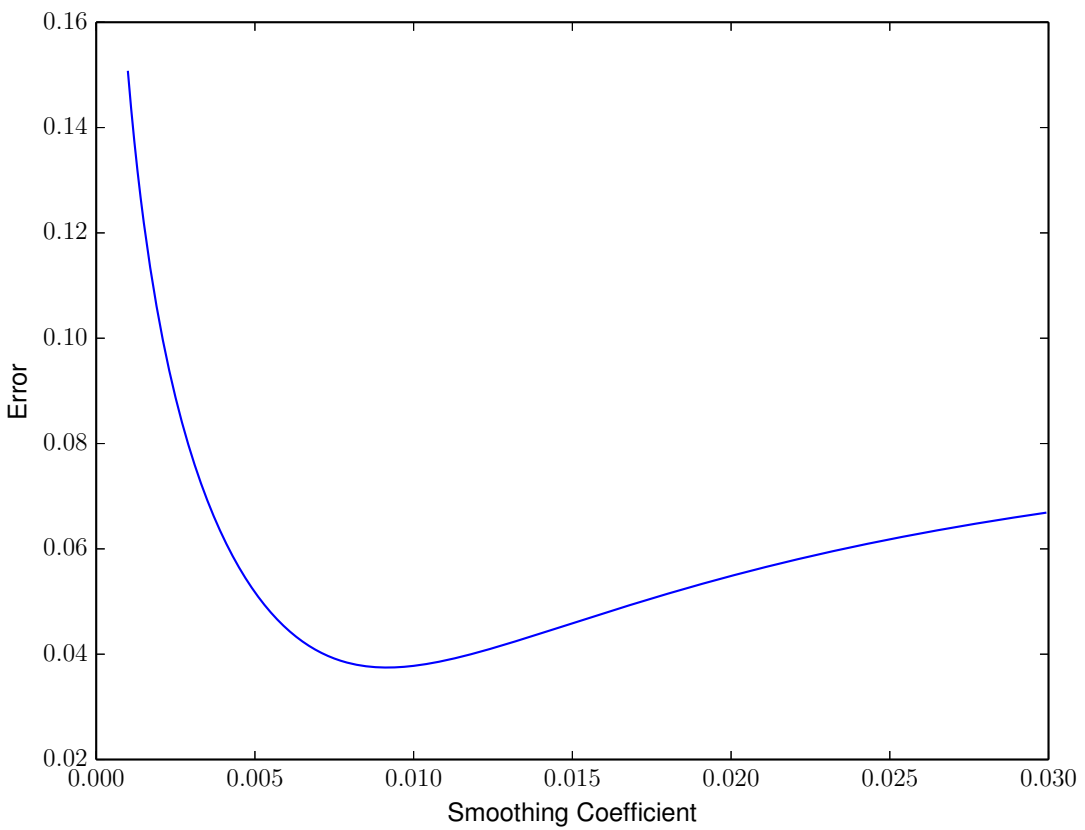


Figure 6: Smoothed - Expt Error vs Smoothing Coefficients

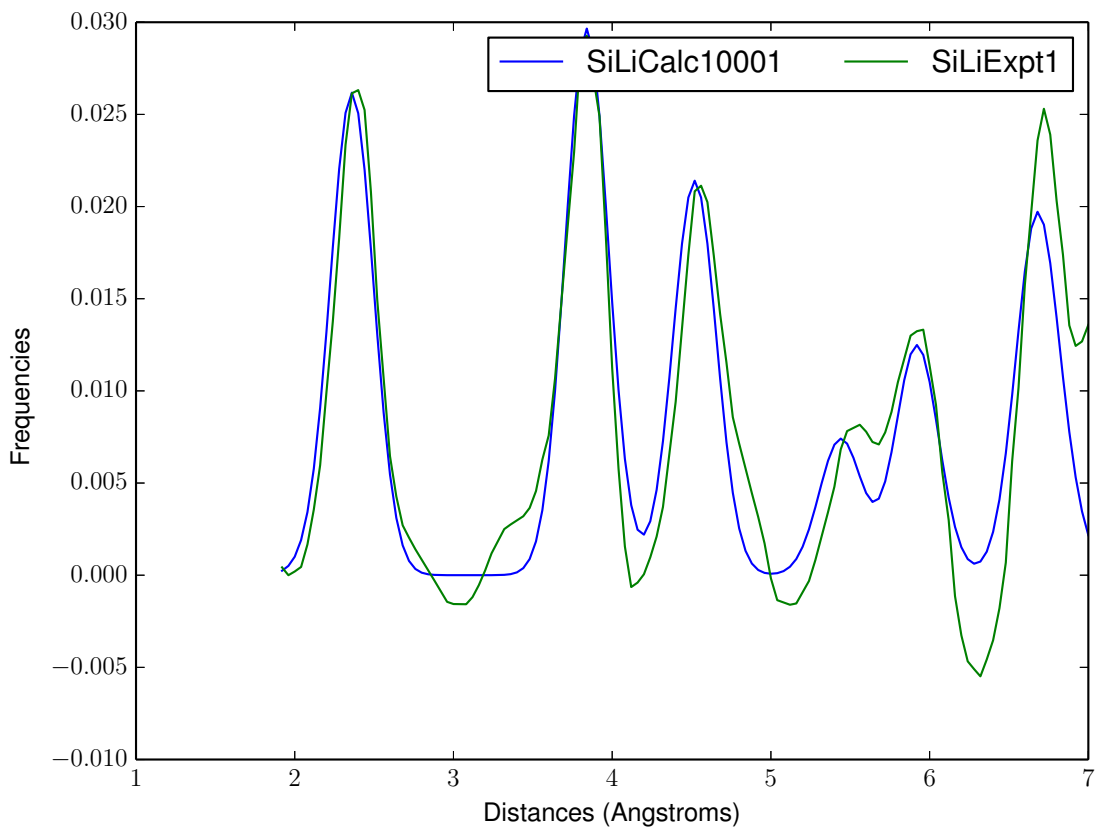


Figure 7: Smoothed SiLiCalc10001 vs SiLiExpt1

3 Matching Algorithm Evaluation

The goal of this project is to invent an algorithm that will find the best matching calculated image for a given experimental image. A more audacious goal is to find an algorithm that can decompose experimental image into a linear combination of a few calculated image.

Before running an experiment, it is possible to theoretically predict the feasible structures that could occur during the experiment. Given this matching algorithm, during the experiment, we could match the experimental results back to the theoretically predicted structures. This would give an 'x-ray vision' into the structures, being able to see that atom locations as the experiment progresses.

One way to evaluate the performance of a proposed matching algorithm is to use the set of known experimental and calculated matches. Taking the set of calculated images as a whole, the algorithm should be able to recover the calculated match given the experimental image.

The problem with this evaluation metric is that there are only three known calculated/experimental matches. This is not a large enough number of samples for good statistics. The reason there are not too many matching pairs is because the known structures at this time are periodic and can be observed experimentally through cheaper x-ray diffraction experiments. Non-periodic structures which are the focus of this project are studied precisely because their exact structures are not known.

An alternative approach to using the calculated and experimental matching pairs directly is to simulate experimental images by adding random noise to a calculated image. The goal then becomes to recover the original calculated image given the simulated experimental image.

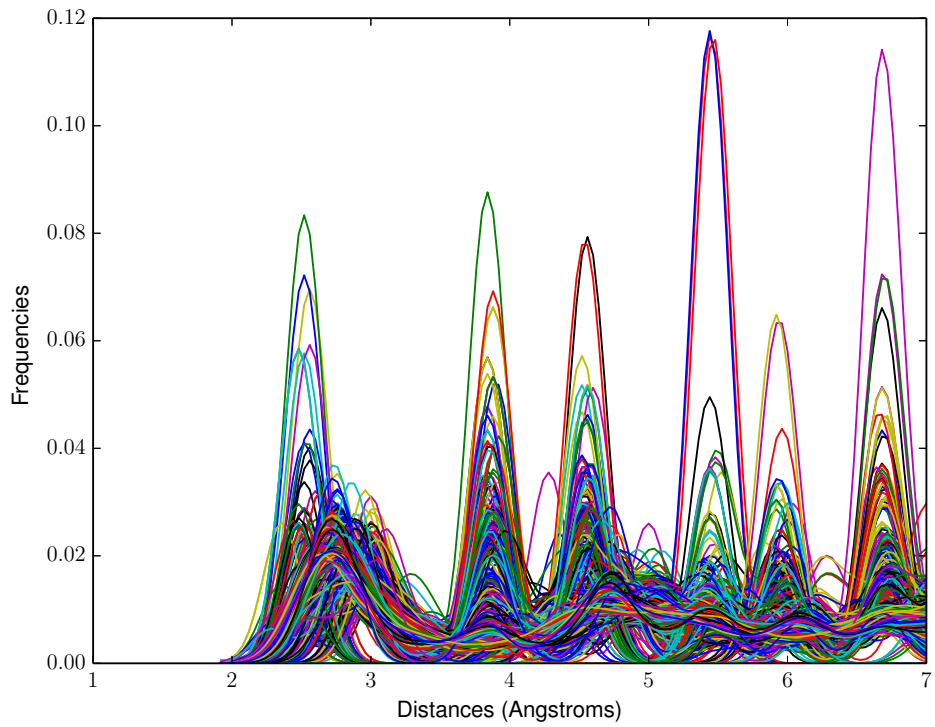


Figure 8: All Calculated Images

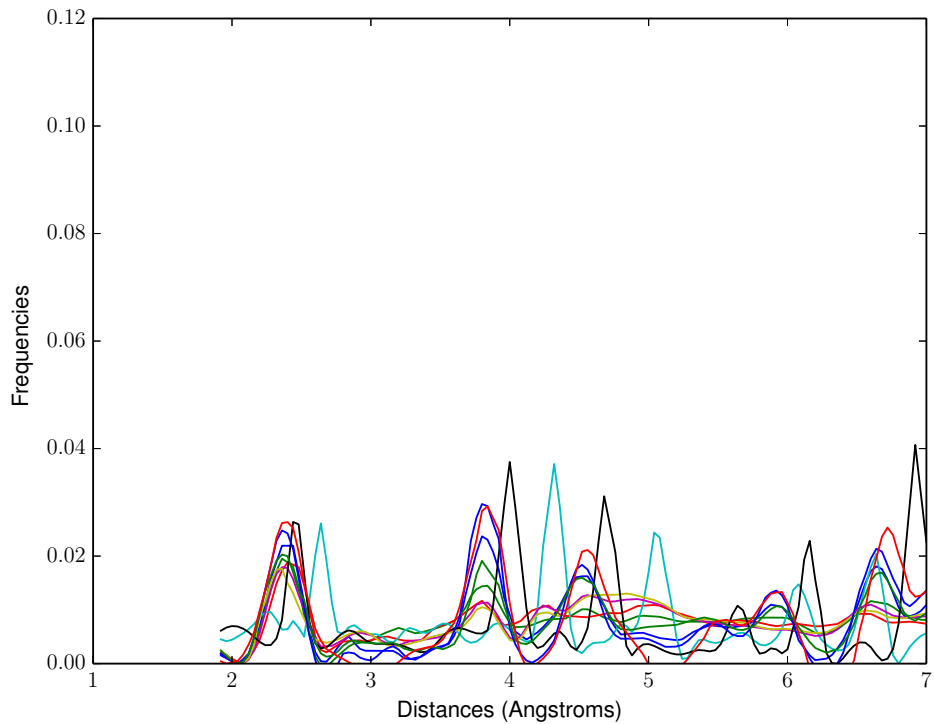


Figure 9: All Experimental Images

3.1 Noise Analysis

The experimental images present three different varieties of noise compared to the calculated images.

- Tilt: Consider the baseline of the image to be the piecewise line connecting the valleys of the image. The experimental images seem to have a non-zero and slanted baseline compared to the calculated images which have a baseline at zero.
- Noise: Between the major peaks of the experimental images, there are also several minor peaks. These minor peaks are not found in the calculated images.
- Peak Heights Difference: The heights of the major peaks vary between the calculated and experimental images.

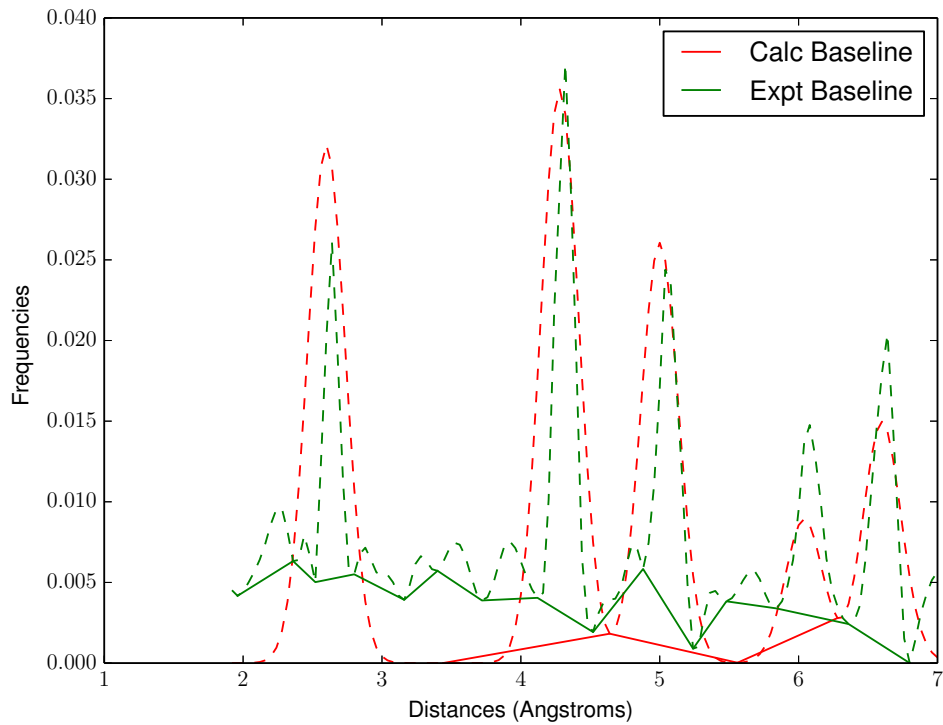


Figure 10: In As

To simulate these features, I first estimated the distributions of the number of peaks, peak locations, and the noise peak heights.

3.1.1 Peak Counts

To estimate the distribution of number of peaks per image, I took all of the experimental images and estimated the number of peaks. Then I visually inspected the histogram to estimate the distribution.

From the histogram, I concluded that the number of peaks is uniformly distributed between 7 and 15.

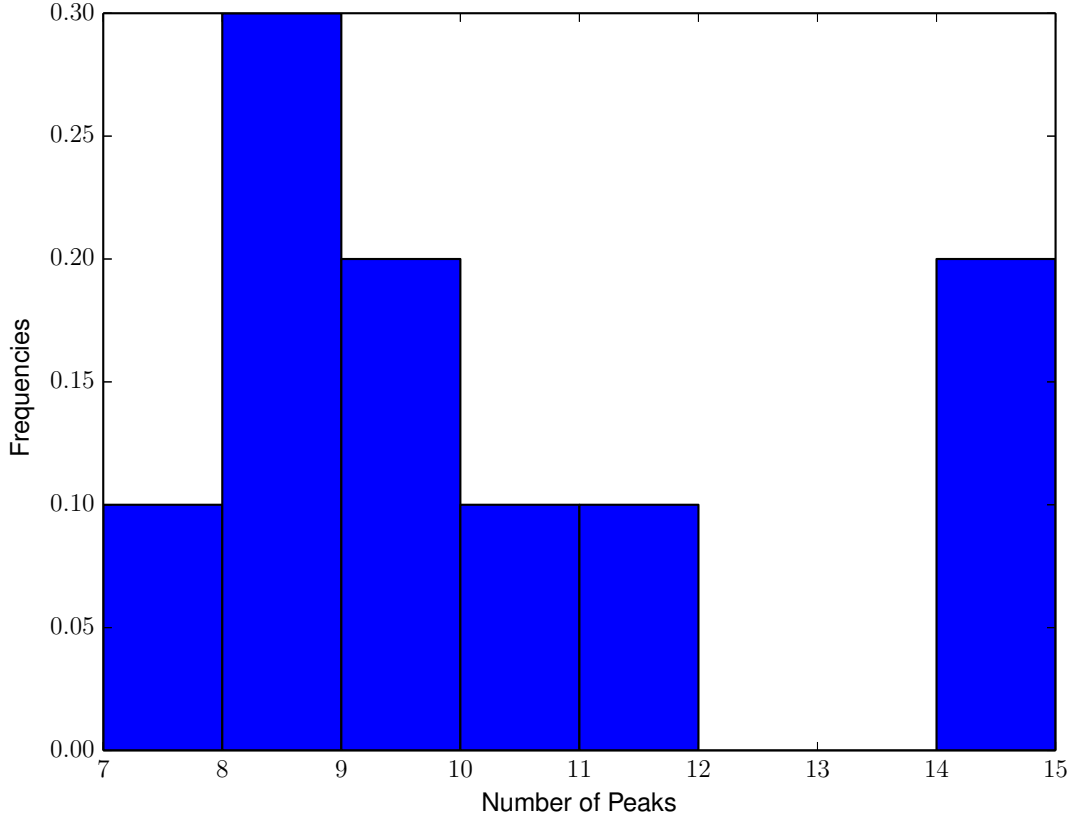


Figure 11: Peak Count Distribution

Note that the estimation is strongly dependent on the maximum length of the image. The raw InAs spectrum goes out to 10 angstroms and has much more than 15 peaks.

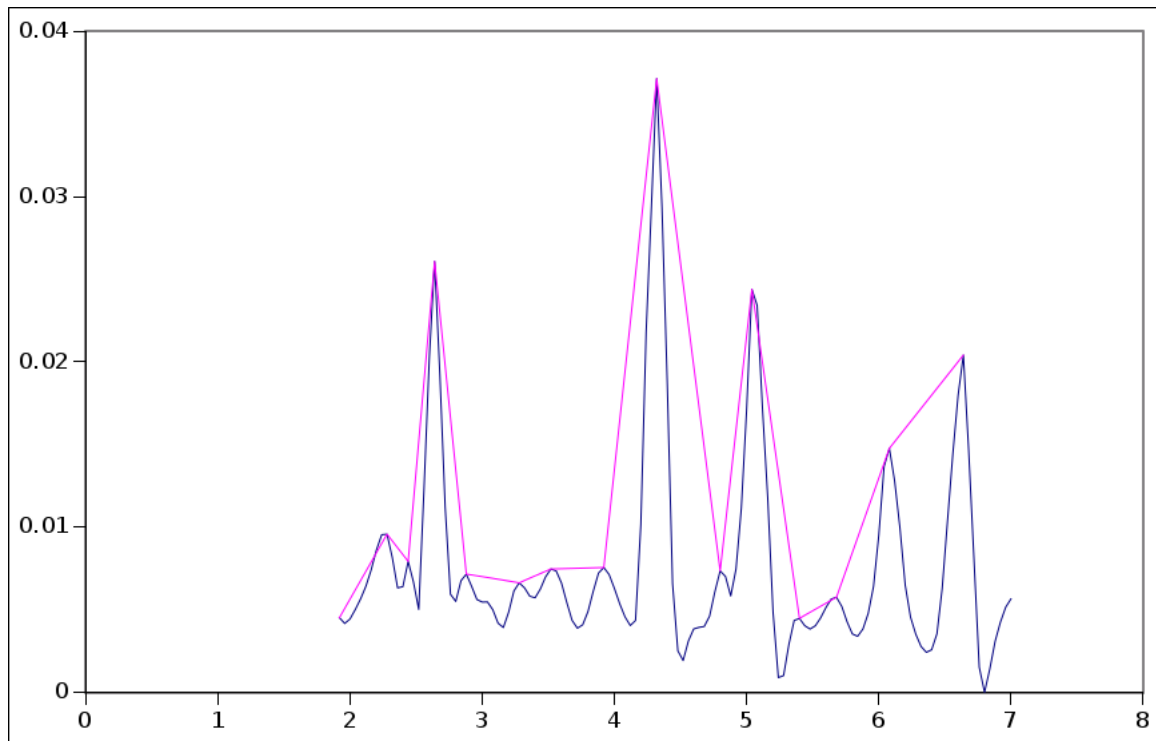


Figure 12: InAs Expt, Max 7 Angstroms

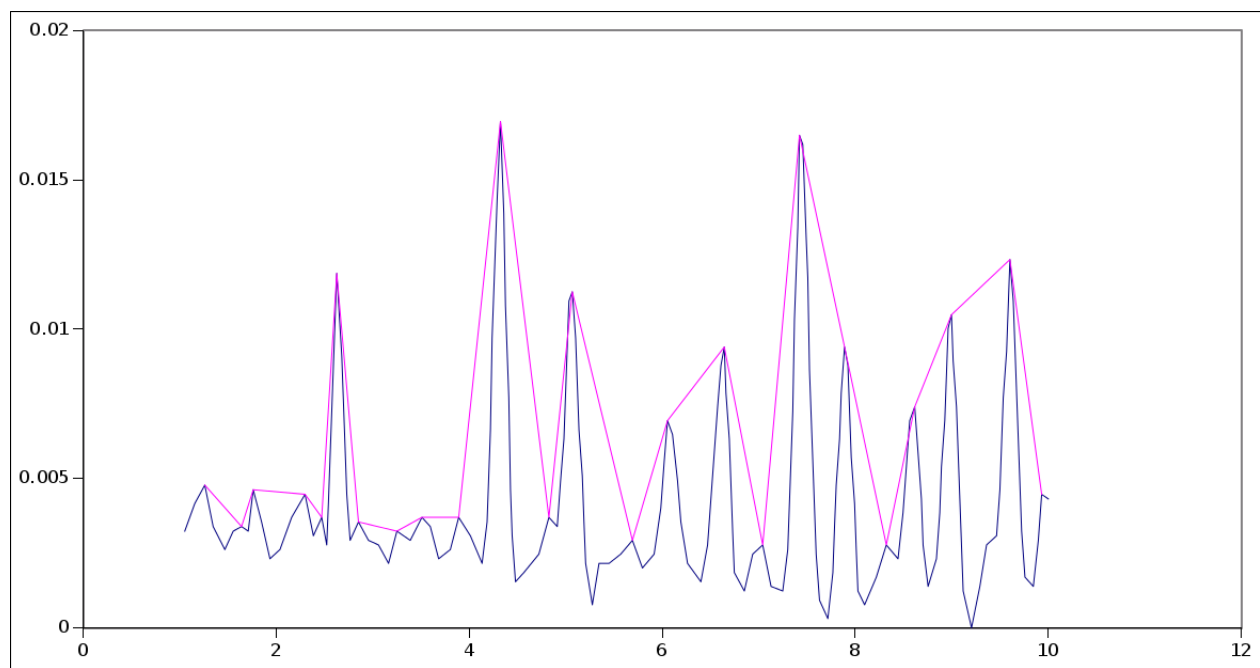


Figure 13: InAs Expt, Max 10 Angstroms

3.1.2 Peak Locations

To estimate the distribution of the location of the peaks, I first took all of the experimental images and calculated the distances of all of the peaks. Then I charted this as a histogram to visually inspect the distribution.

From the histogram, I concluded that the locations are uniformly distributed between 1.96 and 7.

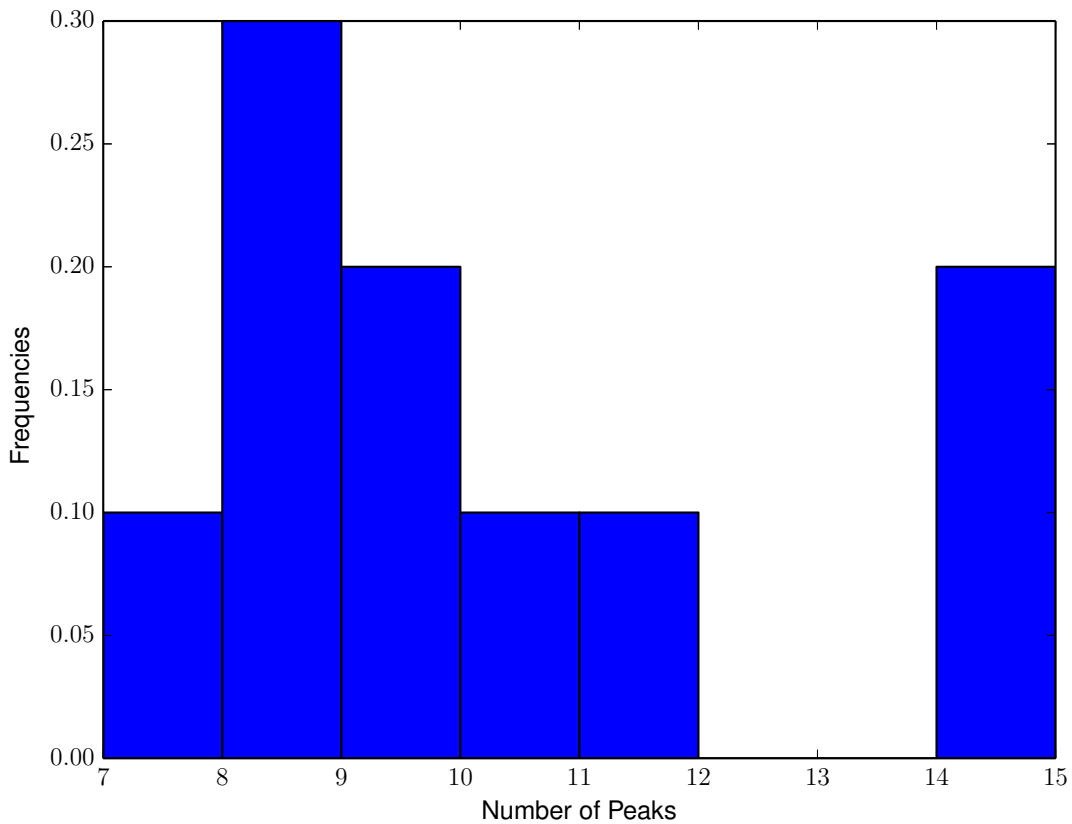


Figure 14: Peak Location Histogram

3.1.3 Noise Peak Heights

To add noise to the image, I random noise directly to the original frequencies. That is, $N = I + R$, where N is a vector of frequencies for the noisified image, I is for the original image, and R is for the random noise.

In light of this, to estimate how much noise to add, I first calculated $E = X - C$, where E is the error or noise to be added, X is the experimental image, and C is the calculated image. I considered the errors at different distances to be independent and thus considered all of the errors to be for any distance. Taking all of the errors together, I estimate the error distribution. From the histogram and cumulative distribution function, I concluded that the error distribution is most similar to a normal distribution. The estimate for the mean is 0.004 and standard deviation is 0.004.

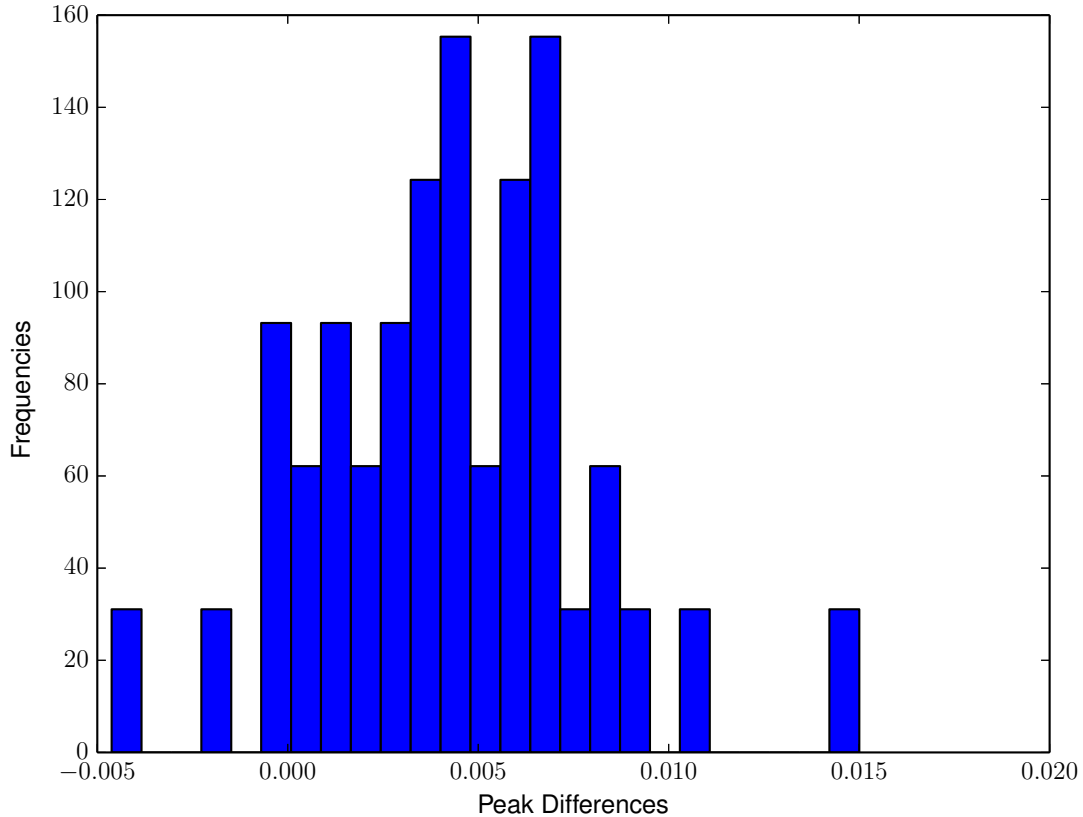


Figure 15: Noise Peak Heights Histogram

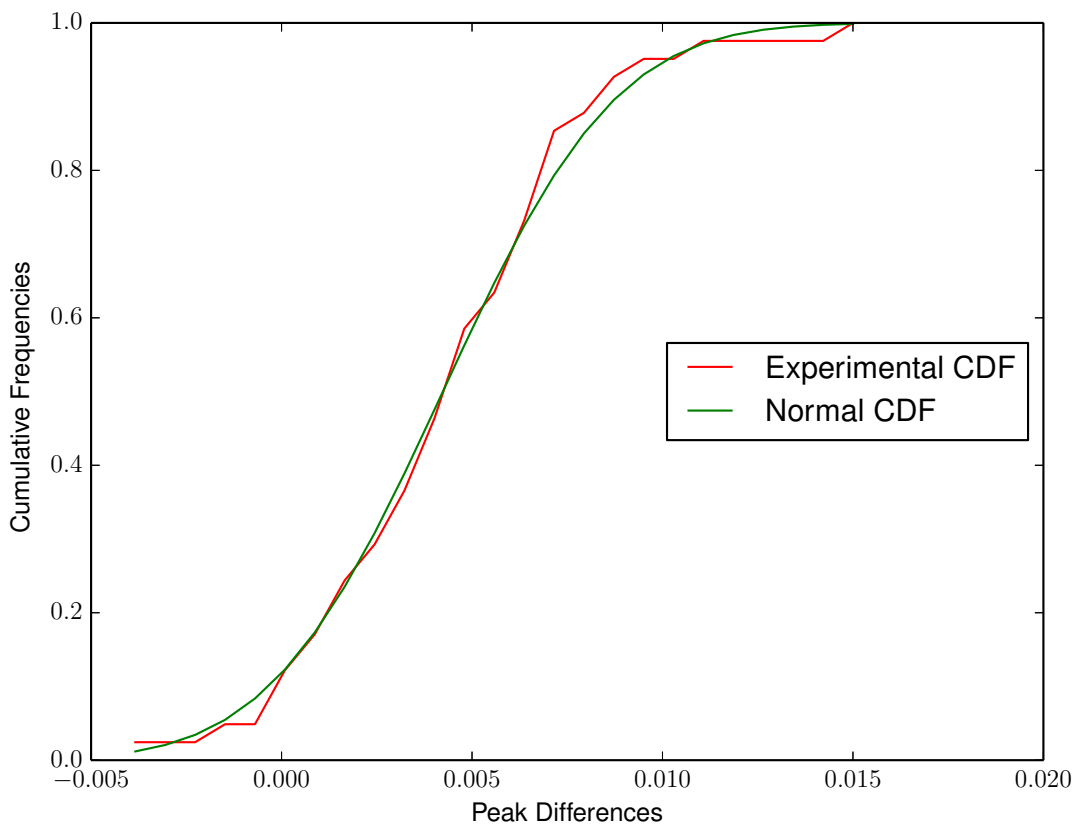


Figure 16: Noise Peak Heights Distribution

3.1.4 Sample Noisy Image

To generate the simulated experimental images, I first sample the number of peaks, the peak locations, and the peak heights from their respective distributions. Then this noise is added to the original image and the resulting image is re-normalized.

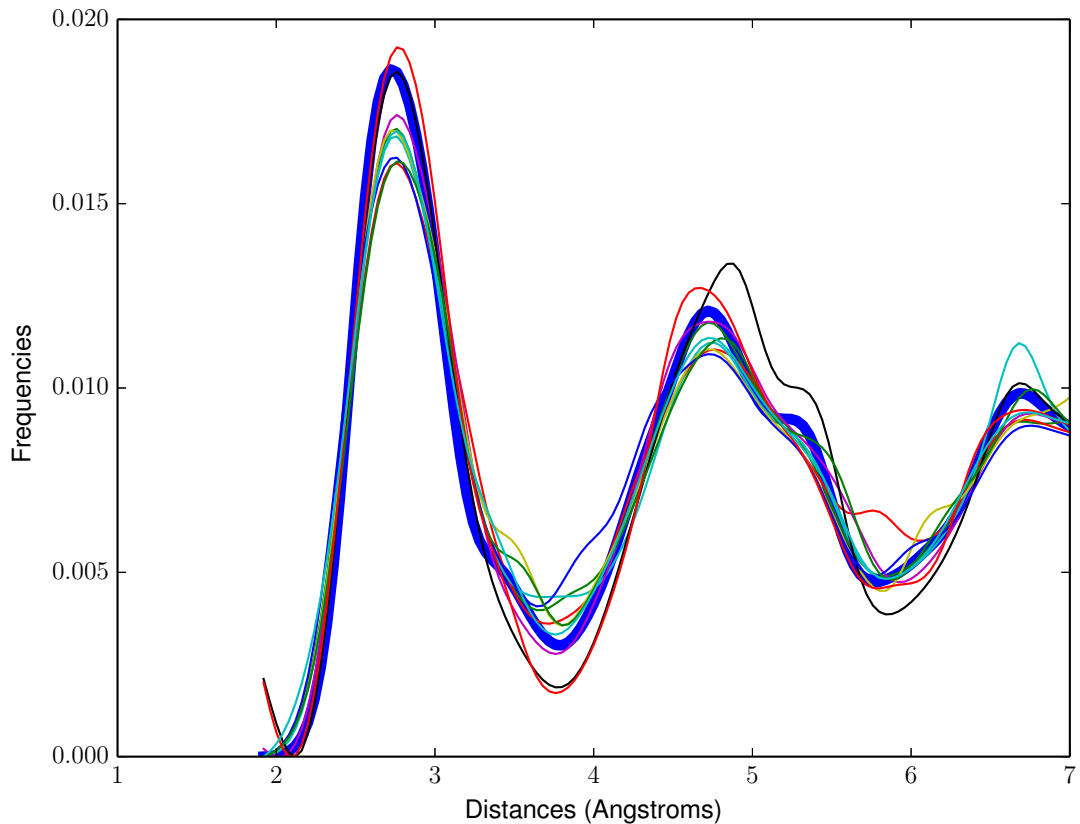


Figure 17: Simulated Experimental Images, 1x Standard Deviation

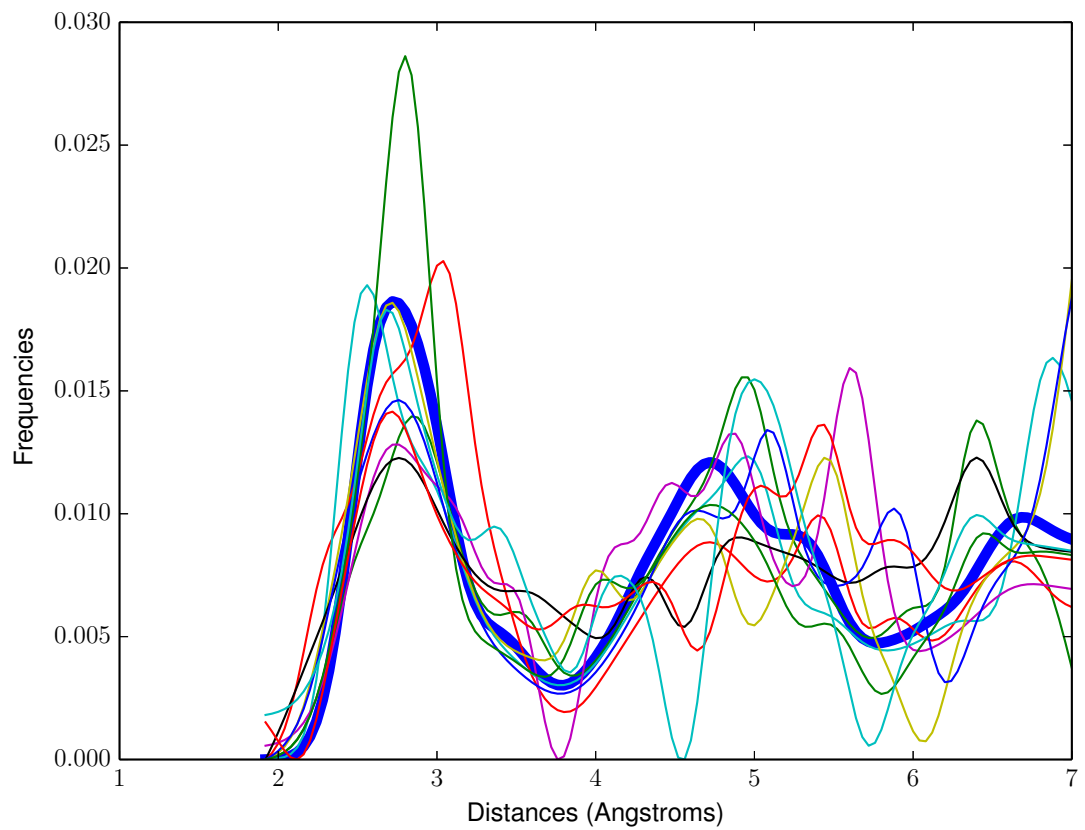


Figure 18: Simulated Experimental Images, 10x Standard Deviation

4 Recognition Using Eigenfaces

In this section, we apply the approach outlined in Turk and Pentland's "Eigenfaces for Recognition".

Let $C = [c_1 \dots c_n]^T$ be the calculated images and Ψ be the column-wise means of the C .

First compute the principal components of C by singular value decomposition.

$$\text{Cov}(C) \sim (C - \Psi)^T (C - \Psi) = W \Sigma^2 W^T$$

Here W are matrices that contain the loadings of C . Each column has different principal components and the rows span the dimensions of the images.

The first L loadings, T_L , are computed with the first L principal components. Let W_L be a matrix with the first L columns of W . Then $T_L = (C - \Psi)W_L$.

Suppose X is the target image that we are trying to find a best match for. First compute the loadings, S_L , for X as $S_L = (X - \Psi)W_L$. Then use the L^p norm to find the closest image in PCA space.

$$\hat{i} = \arg \min_i \|T_L(i, :) - S_L\|_p$$

4.1 Mean Image

Below shows the mean image, Ψ , over all of the calculated images.

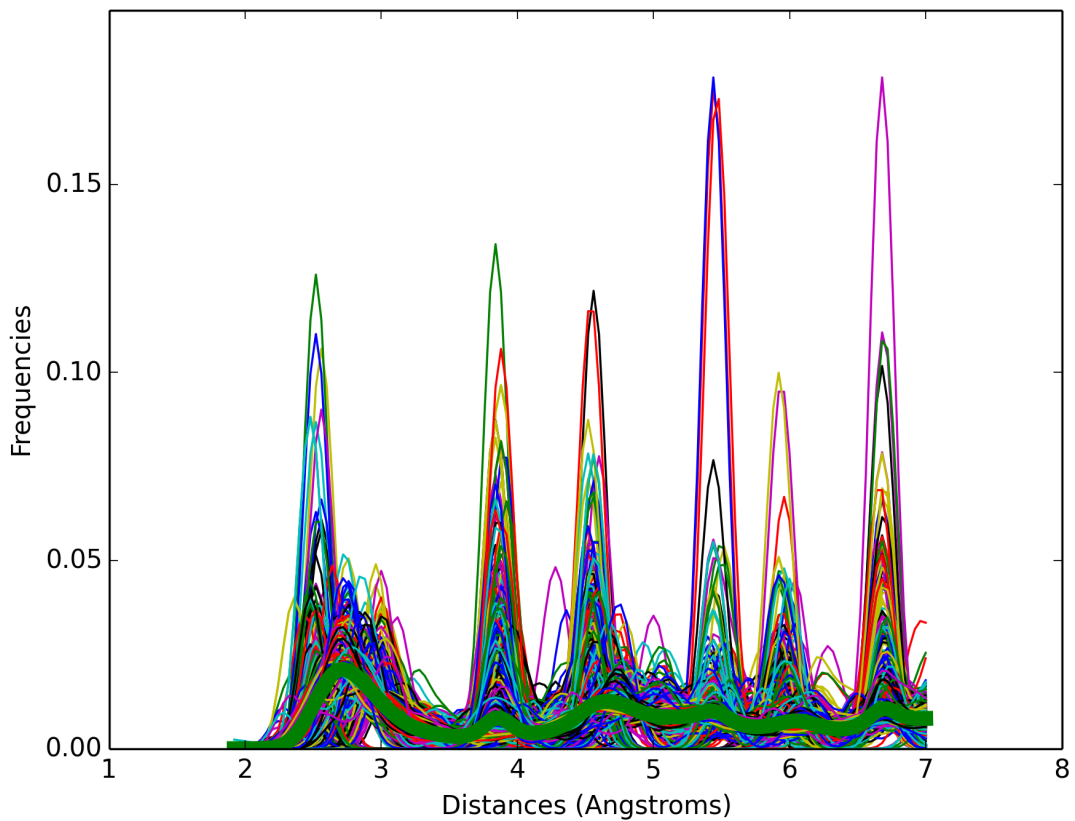


Figure 19: All Calculated Images with Mean

4.2 Variance Explained by Principal Components

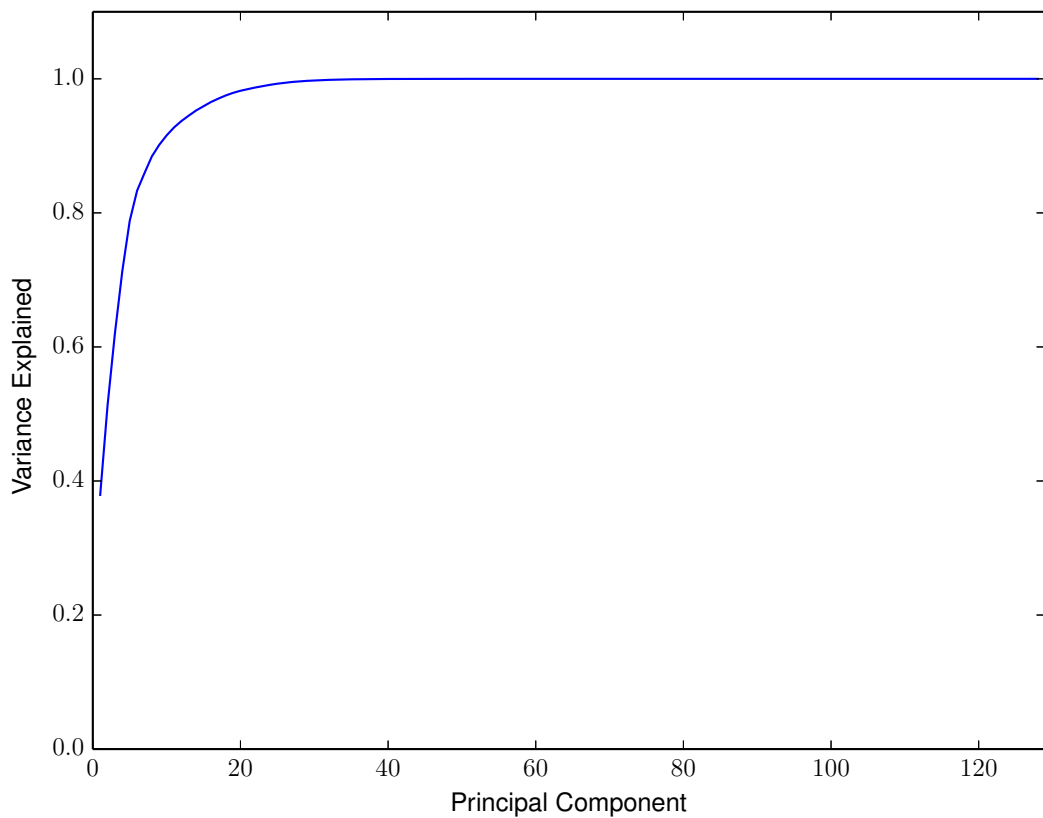


Figure 20: Cumulative Variance Explained by Principal Components

4.3 Eigenfaces

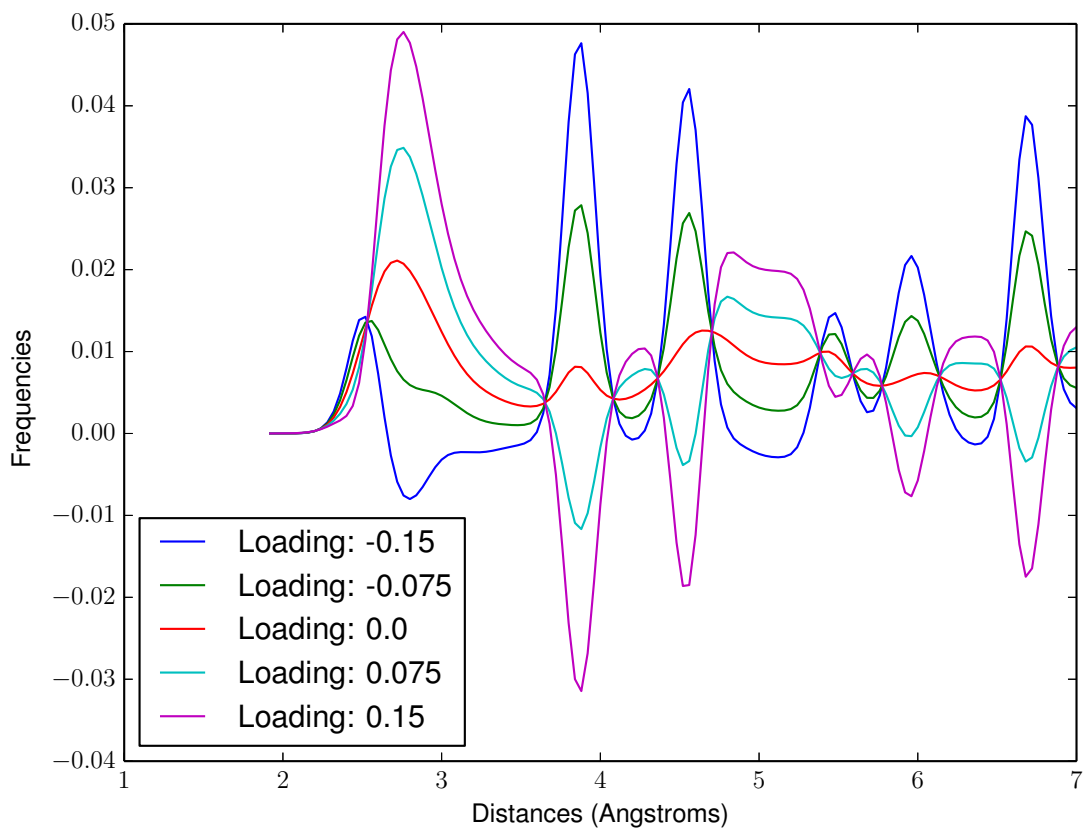


Figure 21: First Eigenface

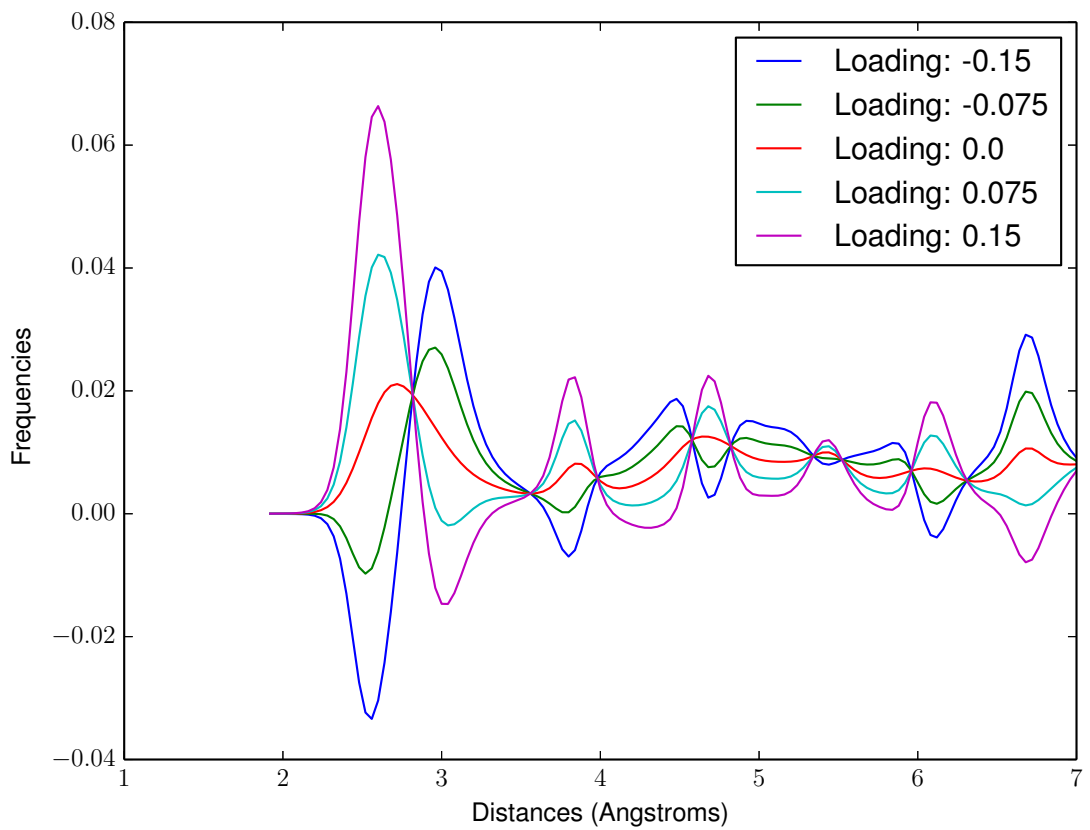


Figure 22: Second Eigenface

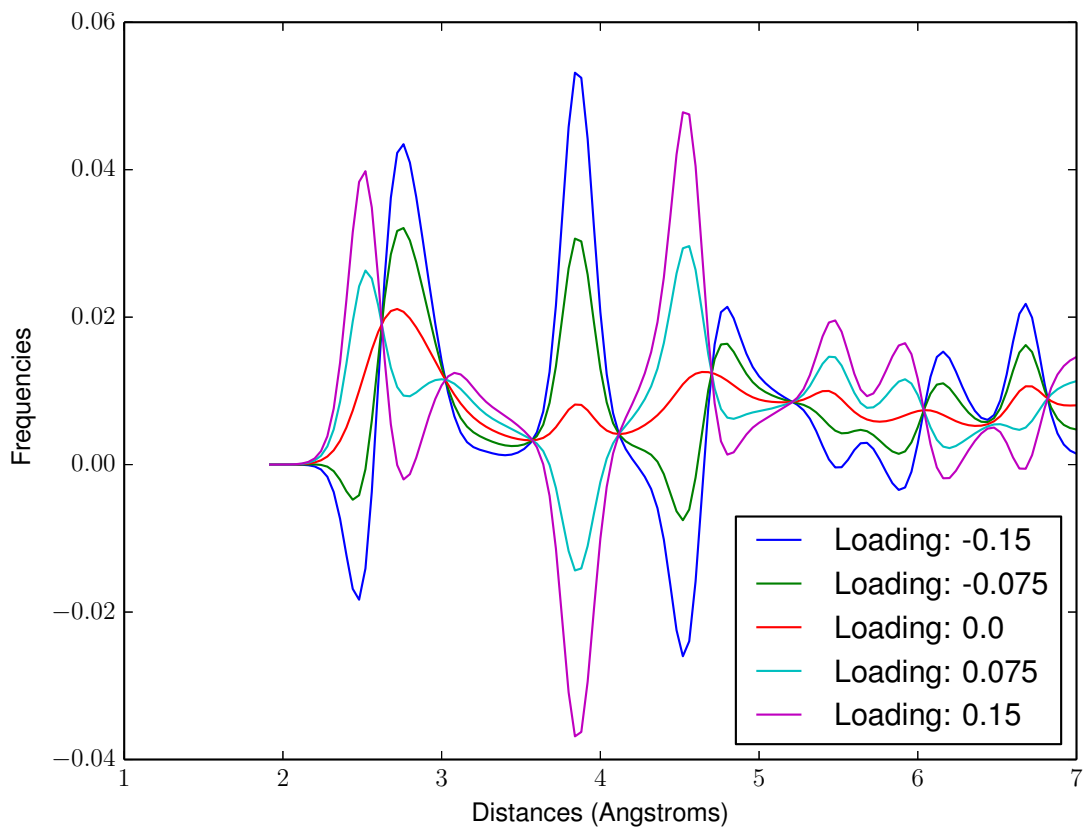


Figure 23: Third Eigenface

4.4 Data in Eigenspace

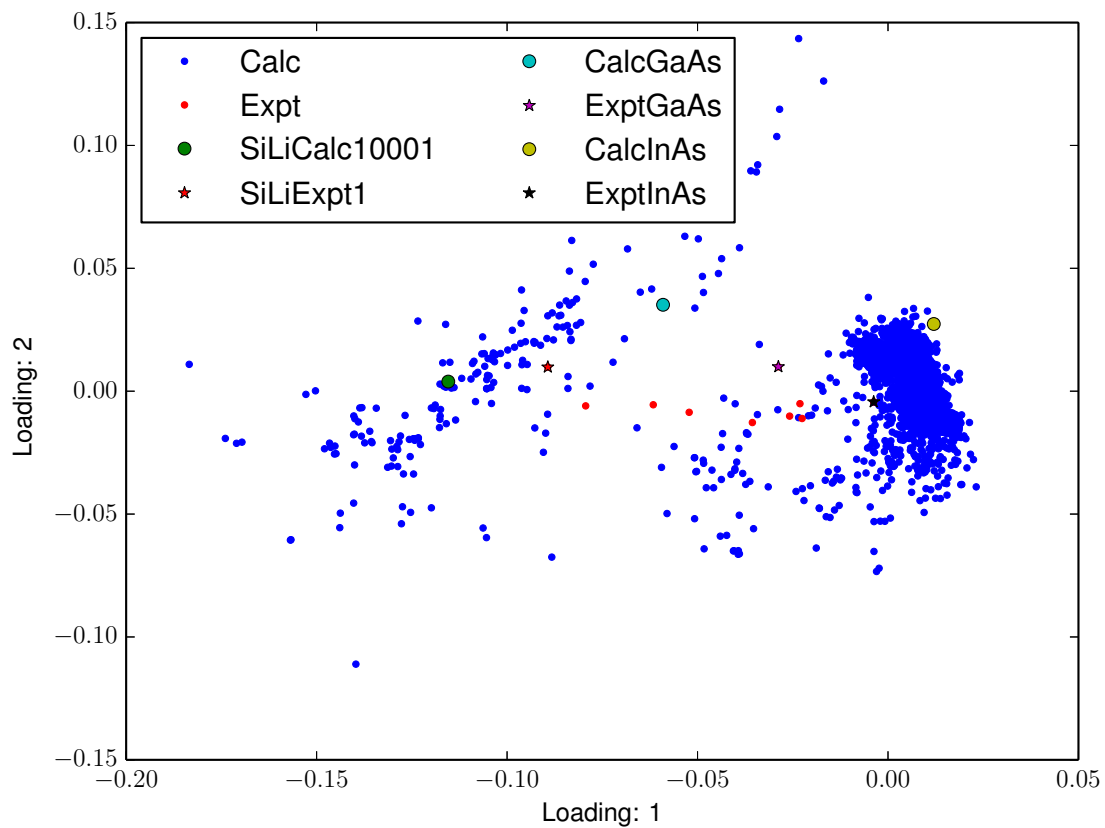


Figure 24: Loading 1 vs Loading 2

| Label | Loading 1 | Loading 2 |
|--------------|------------------|------------------|
| SiLiExpt1 | -0.0893 | 0.00982 |
| SiLiExpt2 | -0.0794 | -0.006 |
| SiLiExpt3 | -0.0616 | -0.0055 |
| SiLiExpt4 | -0.0522 | -0.0086 |
| SiLiExpt5 | -0.0356 | -0.0128 |
| ExptGaAs | -0.0288 | 0.00994 |
| SiLiExpt7 | -0.0258 | -0.0101 |
| SiLiExpt6 | -0.0231 | -0.0051 |
| SiLiExpt8 | -0.0226 | -0.0111 |
| ExptInAs | -0.0038 | -0.0044 |

Table 1: Experimental Data Sorted by Loading 1

| Label | Loading 1 | Loading 2 |
|--------------|------------------|------------------|
| SiLiExpt5 | -0.0356 | -0.0128 |
| SiLiExpt8 | -0.0226 | -0.0111 |
| SiLiExpt7 | -0.0258 | -0.0101 |
| SiLiExpt4 | -0.0522 | -0.0086 |
| SiLiExpt2 | -0.0794 | -0.006 |
| SiLiExpt3 | -0.0616 | -0.0055 |
| SiLiExpt6 | -0.0231 | -0.0051 |
| ExptInAs | -0.0038 | -0.0044 |
| SiLiExpt1 | -0.0893 | 0.00982 |
| ExptGaAs | -0.0288 | 0.00994 |

Table 2: Experimental Data Sorted by Loading 2

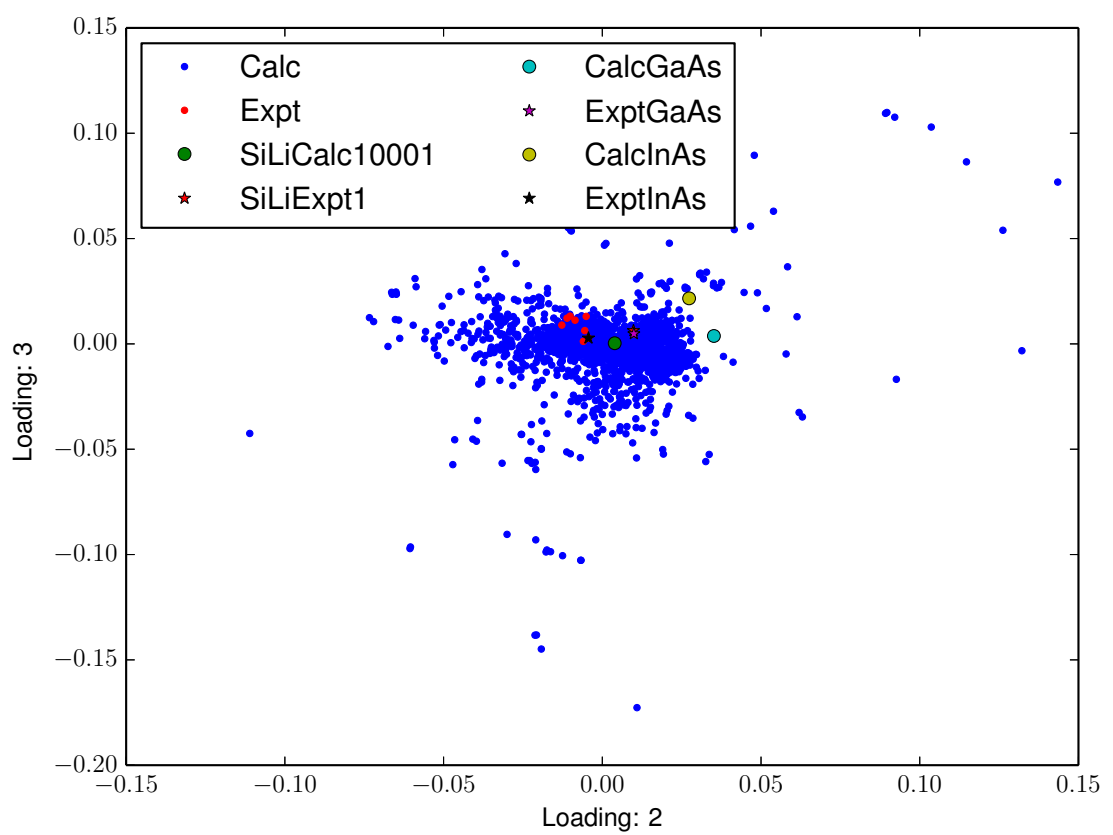


Figure 25: Loading 2 vs Loading 3

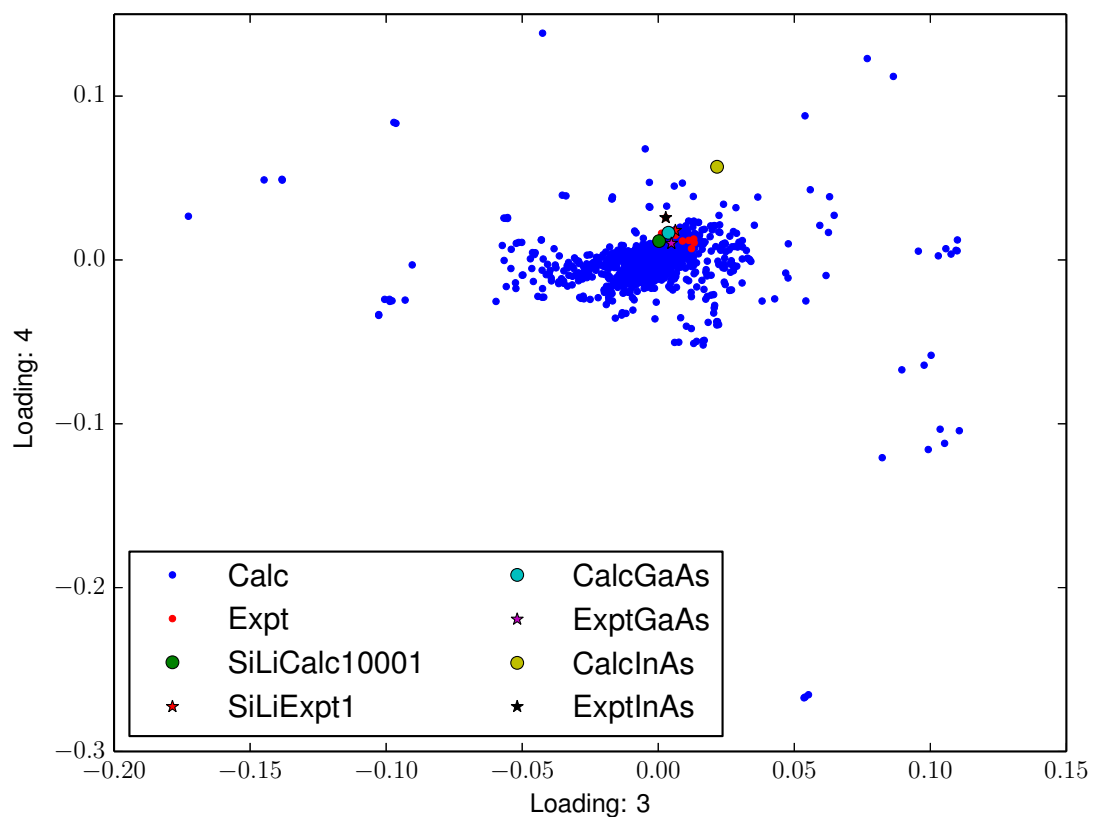


Figure 26: Loading 3 vs Loading 4

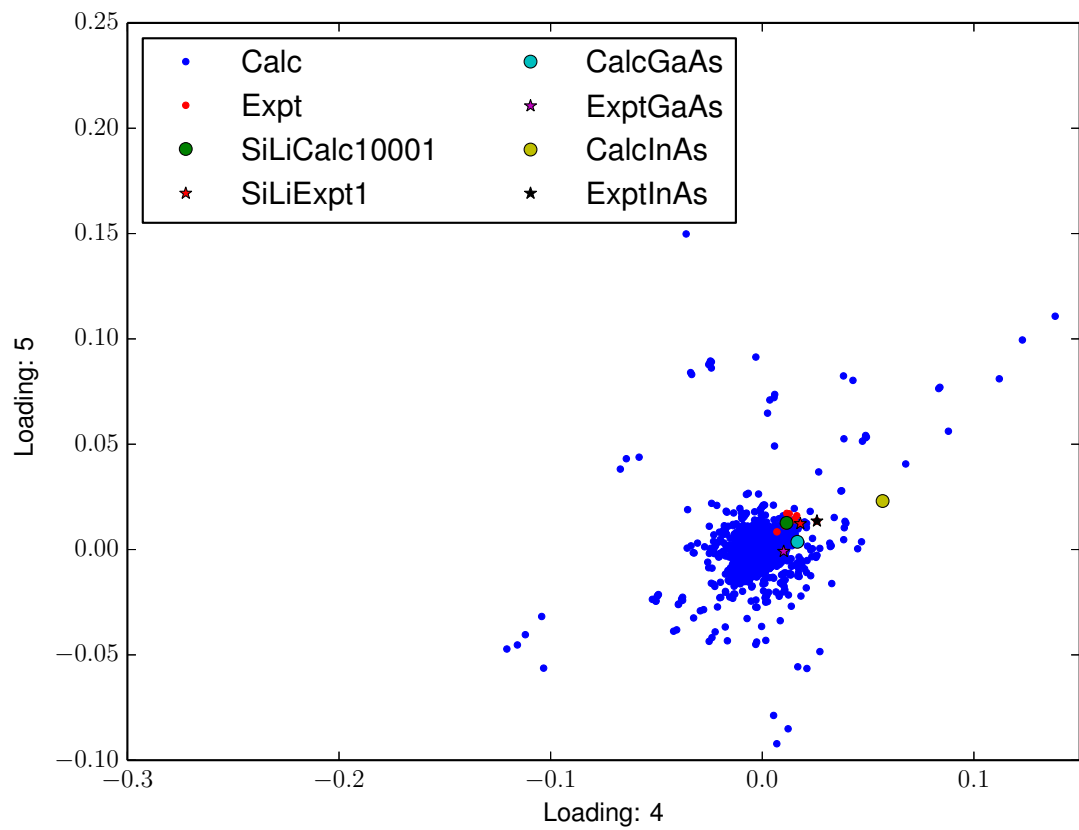


Figure 27: Loading 4 vs Loading 5

4.4.1 Eigenspace Outliers

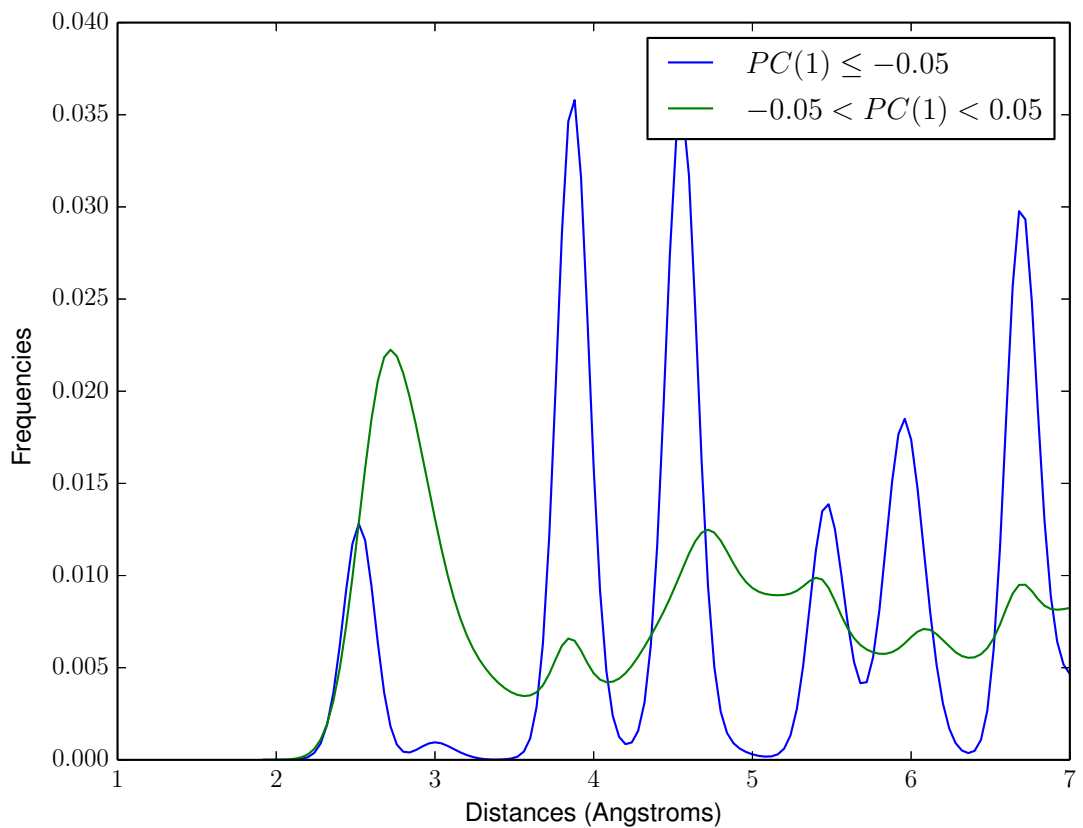


Figure 28: First Principal Component Outliers

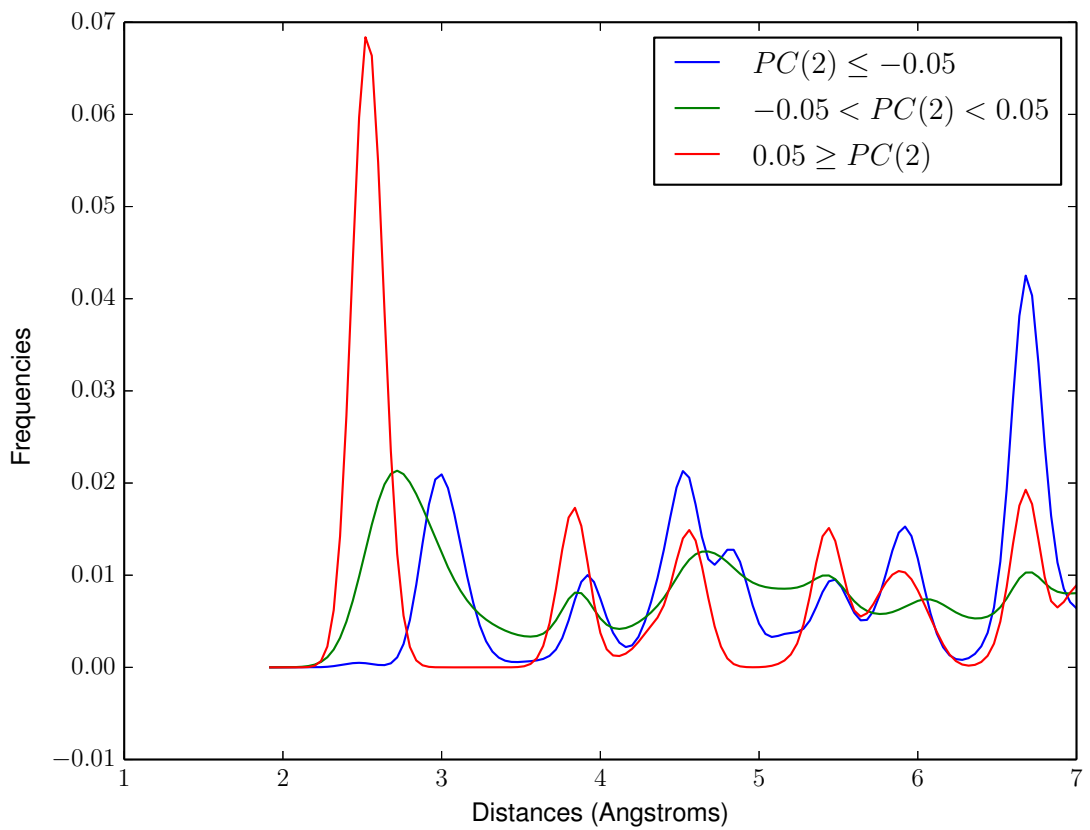


Figure 29: Second Principal Component Outliers

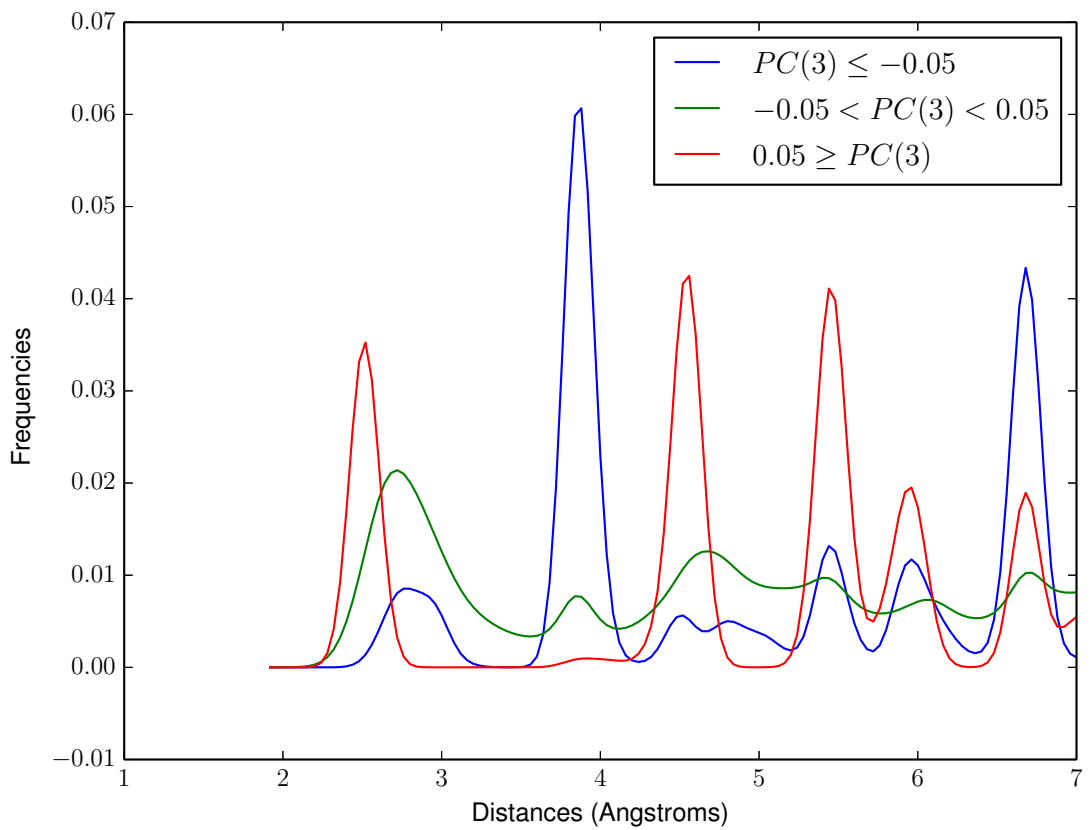


Figure 30: Third Principal Component Outliers

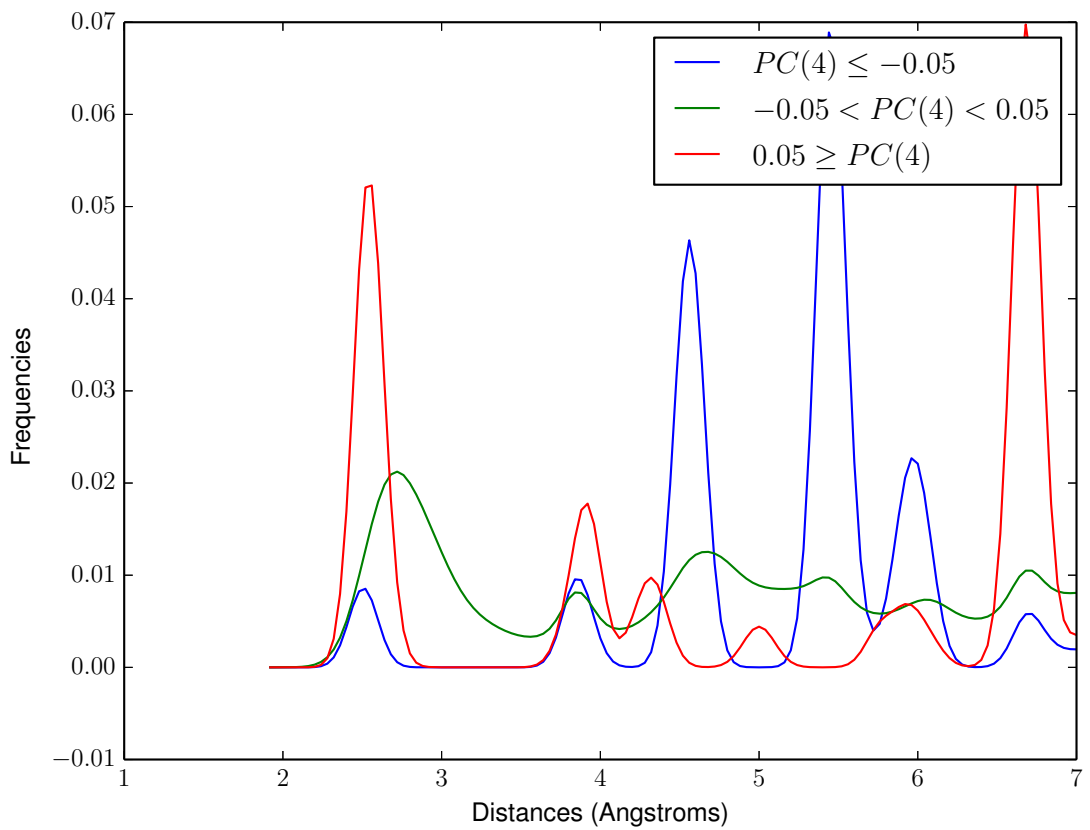


Figure 31: Fourth Principal Component Outliers

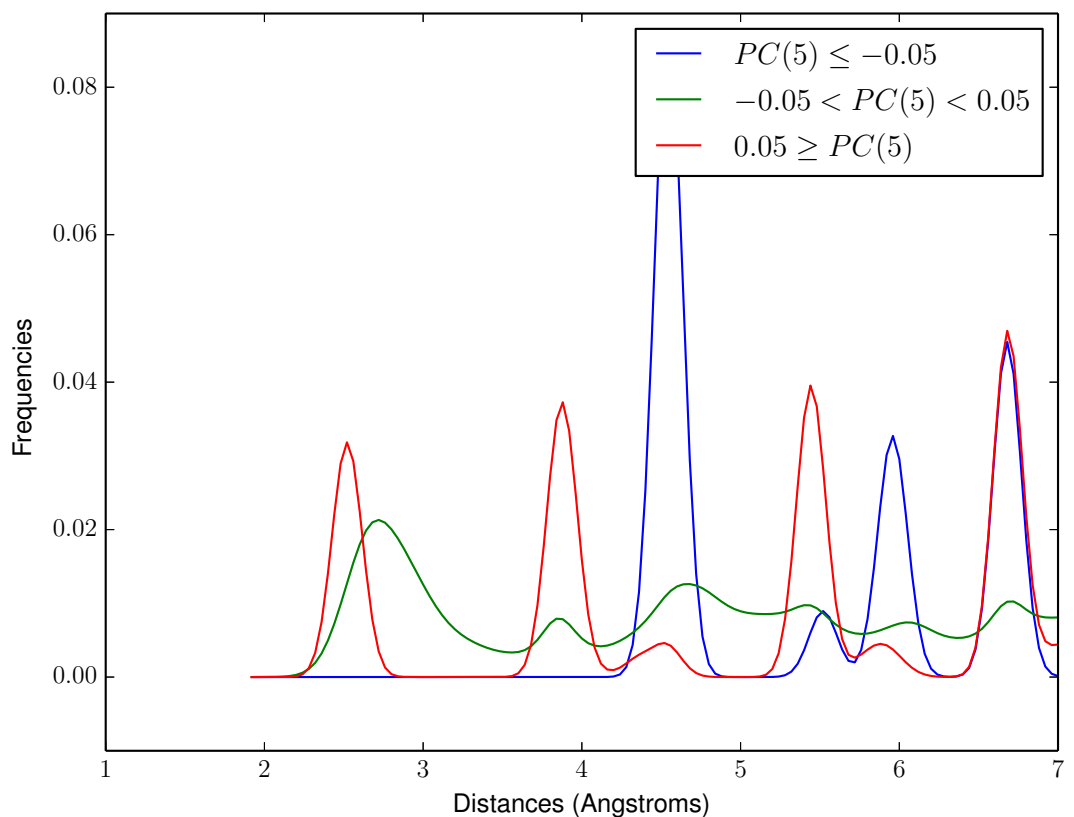


Figure 32: Fifth Principal Component Outliers

4.5 Experimental Image Recognition

4.5.1 3 Principal Components

| Image | Best Match | 2 | 3 | 4 | 5 |
|------------------|-------------------|---------------|---------------|---------------|---------------|
| ExptGaAs | SiLiCalc11436 | SiLiCalc11634 | SiLiCalc11967 | SiLiCalc12738 | SiLiCalc10225 |
| ExptInAs | SiLiCalc10643 | SiLiCalc10560 | SiLiCalc10693 | SiLiCalc10617 | SiLiCalc10621 |
| SiLiExpt1 | SiLiCalc10208 | SiLiCalc10315 | SiLiCalc10317 | SiLiCalc10188 | SiLiCalc10187 |
| SiLiExpt2 | SiLiCalc10317 | SiLiCalc10287 | SiLiCalc10320 | SiLiCalc10283 | SiLiCalc10273 |
| SiLiExpt3 | SiLiCalc10287 | SiLiCalc10239 | SiLiCalc10259 | SiLiCalc10317 | SiLiCalc10232 |
| SiLiExpt4 | SiLiCalc10229 | SiLiCalc10225 | SiLiCalc10232 | SiLiCalc10239 | SiLiCalc10259 |
| SiLiExpt5 | SiLiCalc10225 | SiLiCalc10256 | SiLiCalc10232 | SiLiCalc10229 | SiLiCalc10231 |
| SiLiExpt6 | SiLiCalc10322 | SiLiCalc10225 | SiLiCalc10247 | SiLiCalc10229 | SiLiCalc10256 |
| SiLiExpt7 | SiLiCalc10225 | SiLiCalc10322 | SiLiCalc10256 | SiLiCalc10247 | SiLiCalc10229 |
| SiLiExpt8 | SiLiCalc10225 | SiLiCalc10322 | SiLiCalc10247 | SiLiCalc10337 | SiLiCalc10256 |

Table 3: Recognition with 3 Principal Components

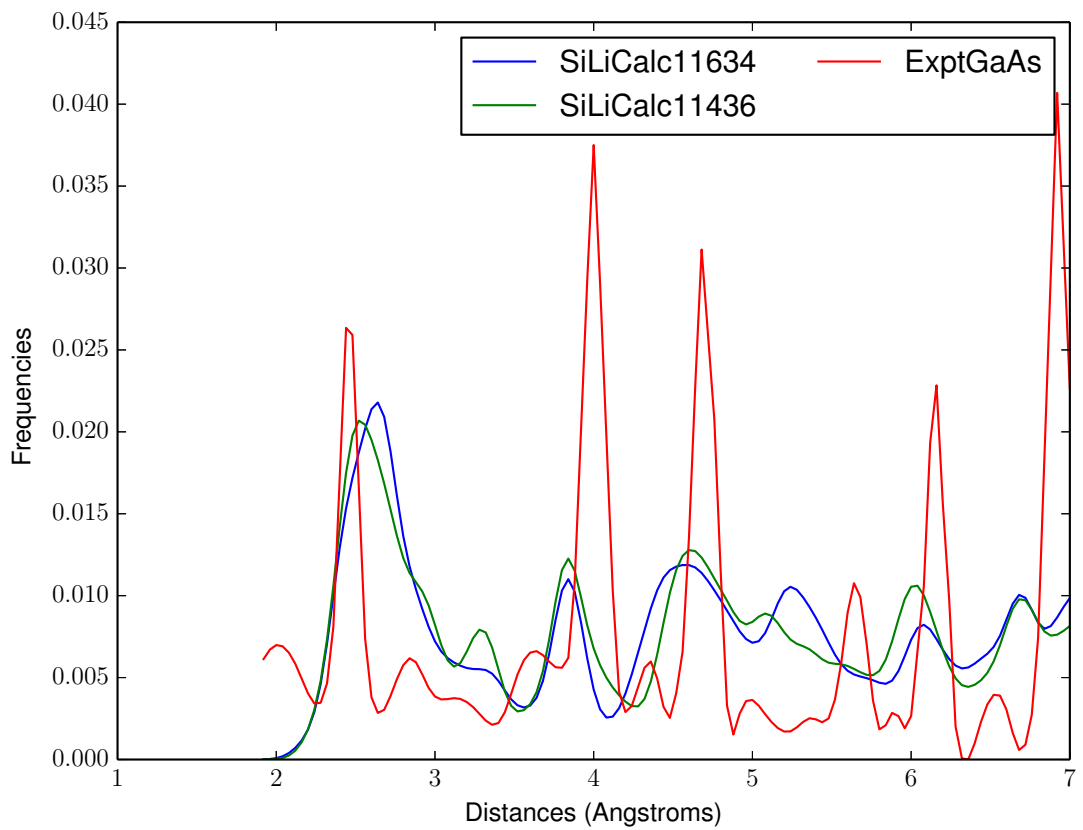


Figure 33: PCA Matches: ExptGaAs, SiLiCalc11436, SiLiCalc11634

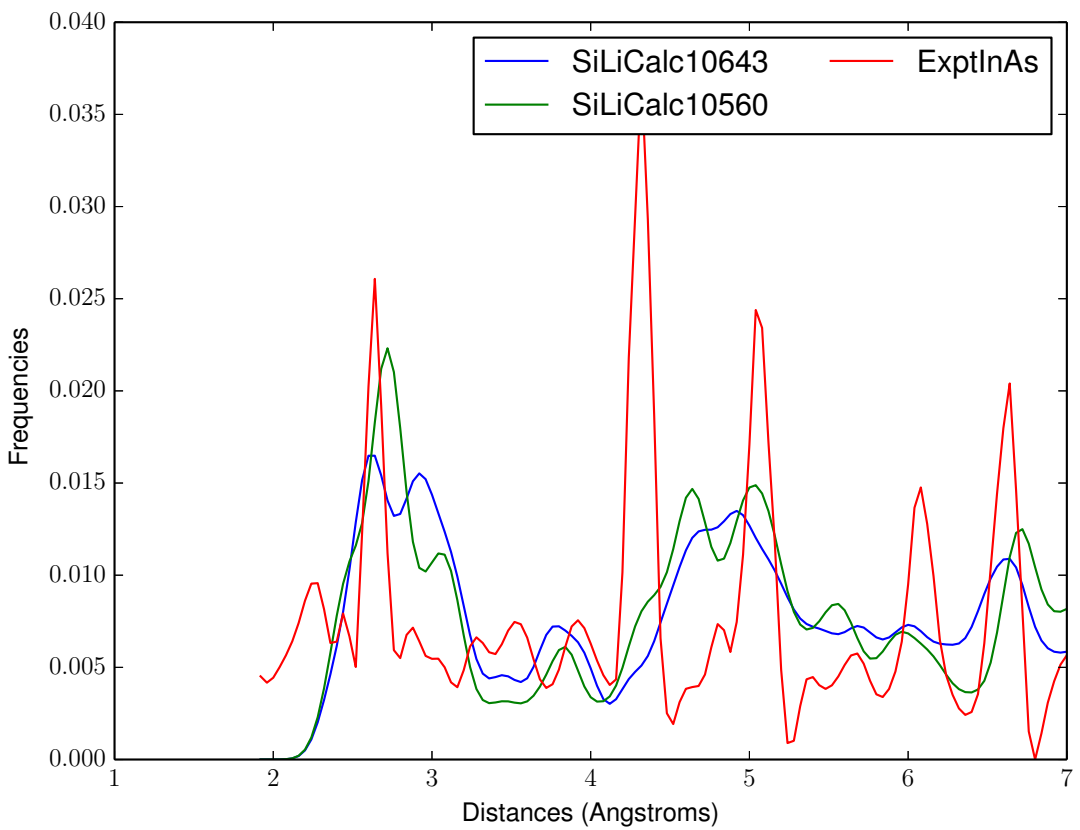


Figure 34: PCA Matches: ExptInAs, SiLiCalc10643, SiLiCalc10560

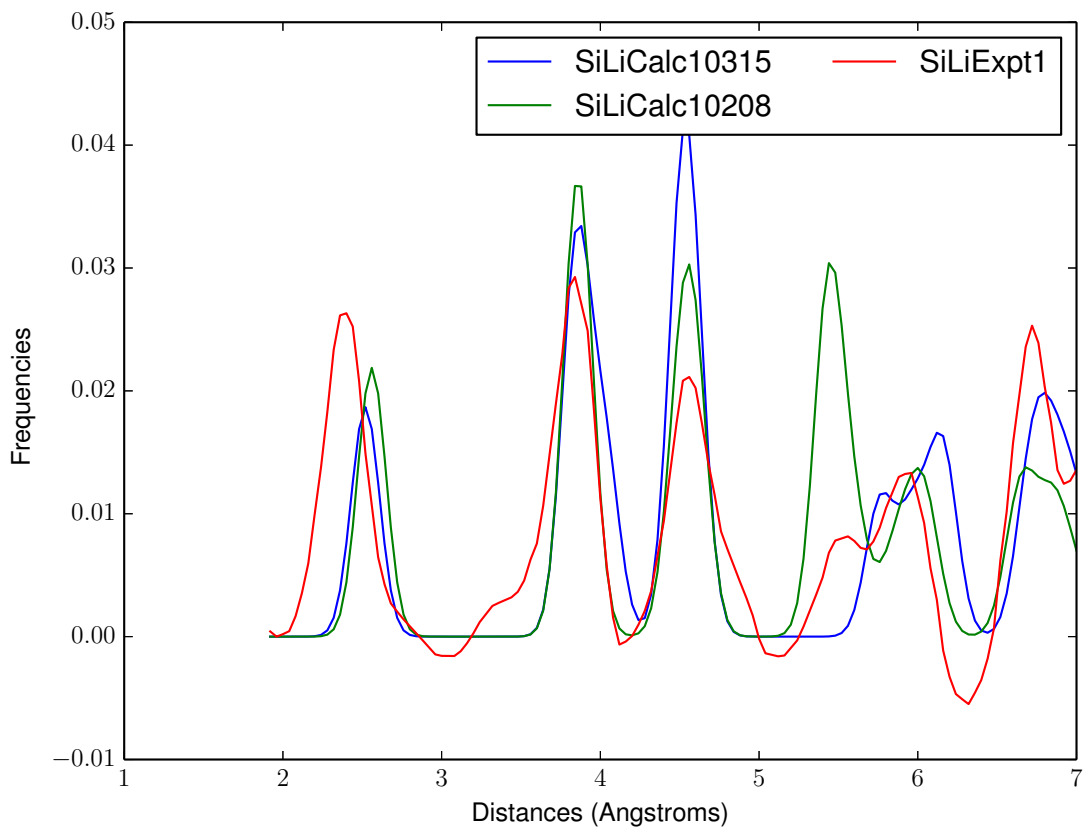


Figure 35: PCA Matches: SiLiExpt1, SiLiCalc10208, SiLiCalc10315

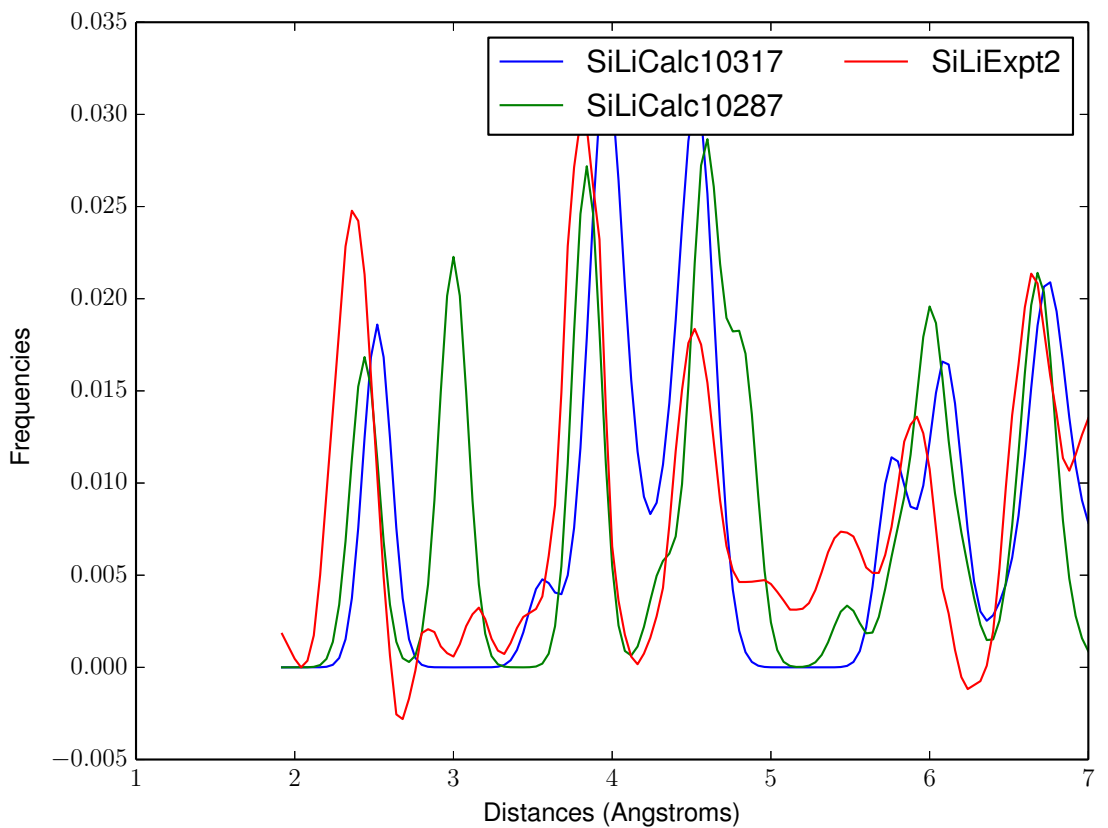


Figure 36: PCA Matches: SiLiExpt2, SiLiCalc10317, SiLiCalc10287

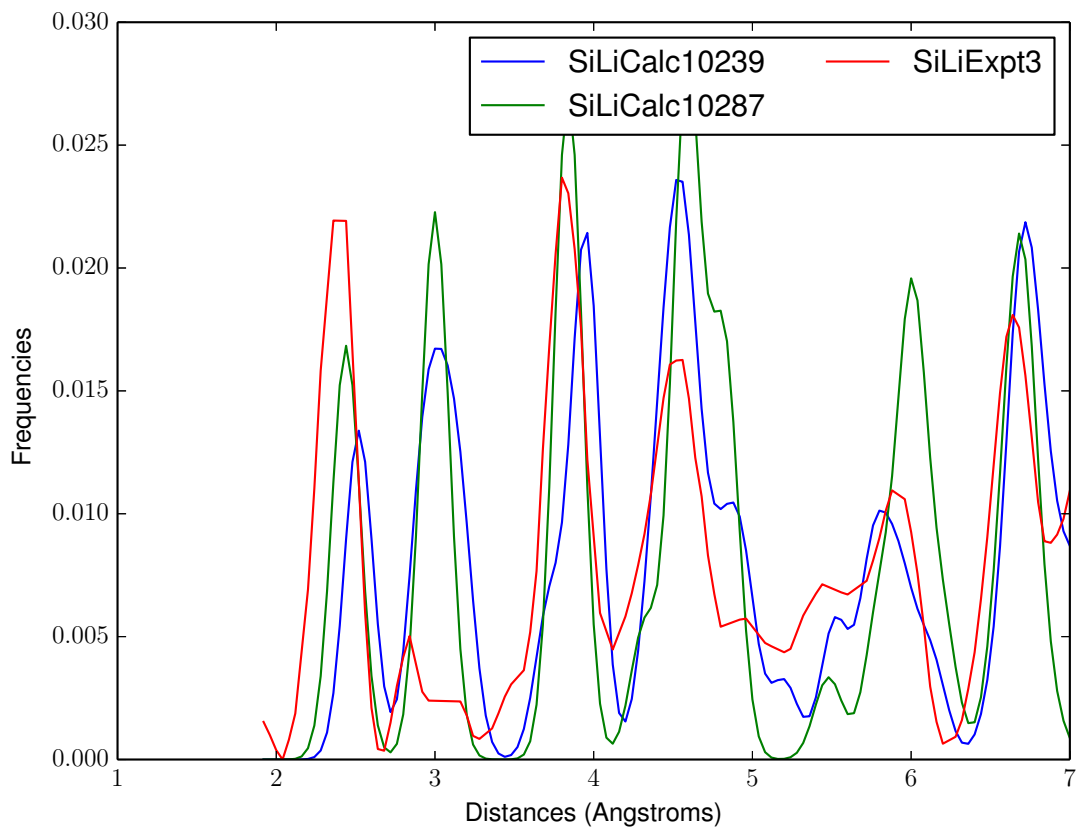


Figure 37: PCA Matches: SiLiExpt3, SiLiCalc10287, SiLiCalc10239

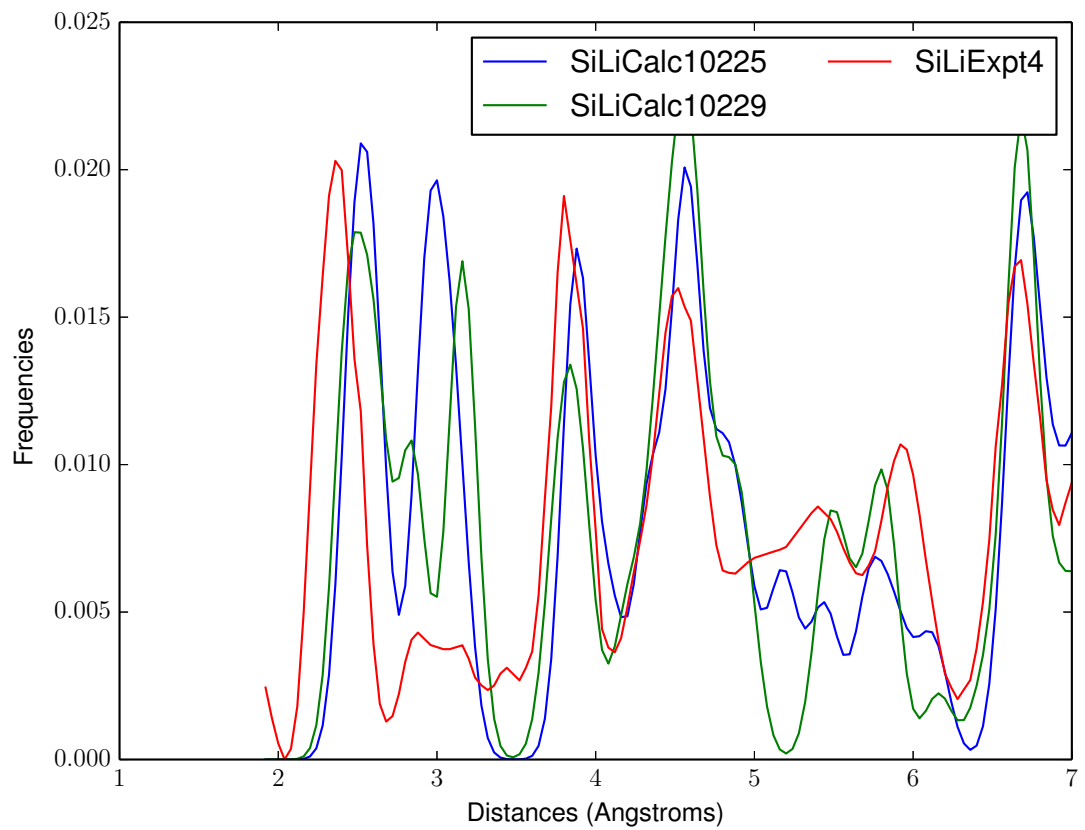


Figure 38: PCA Matches: SiLiExpt4, SiLiCalc10229, SiLiCalc10225

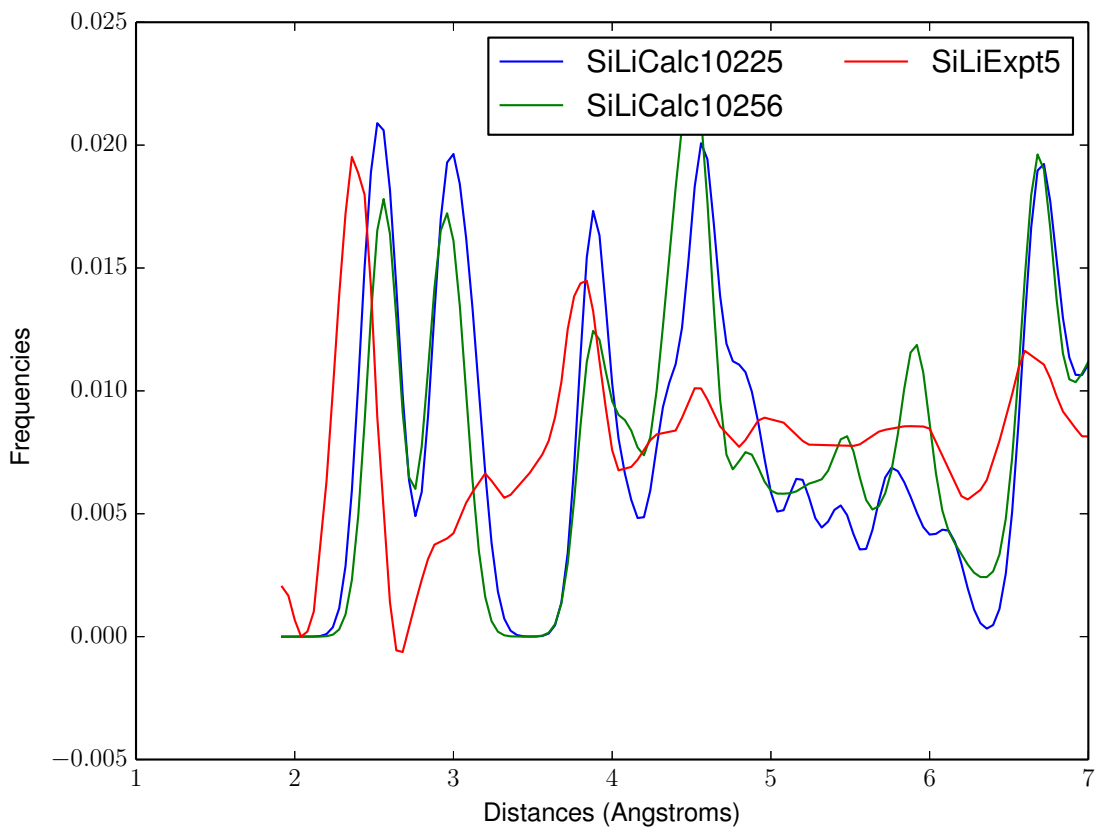


Figure 39: PCA Matches: SiLiExpt5, SiLiCalc10225, SiLiCalc10256

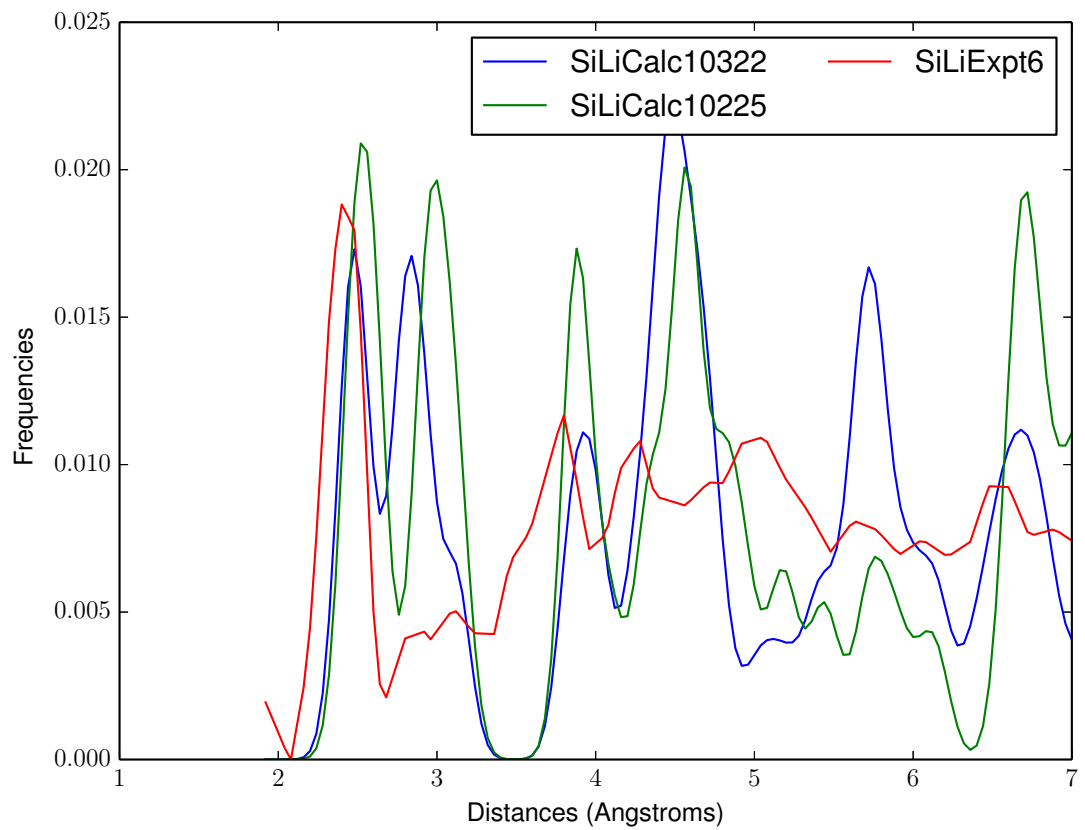


Figure 40: PCA Matches: SiLiExpt6, SiLiCalc10322, SiLiCalc10225

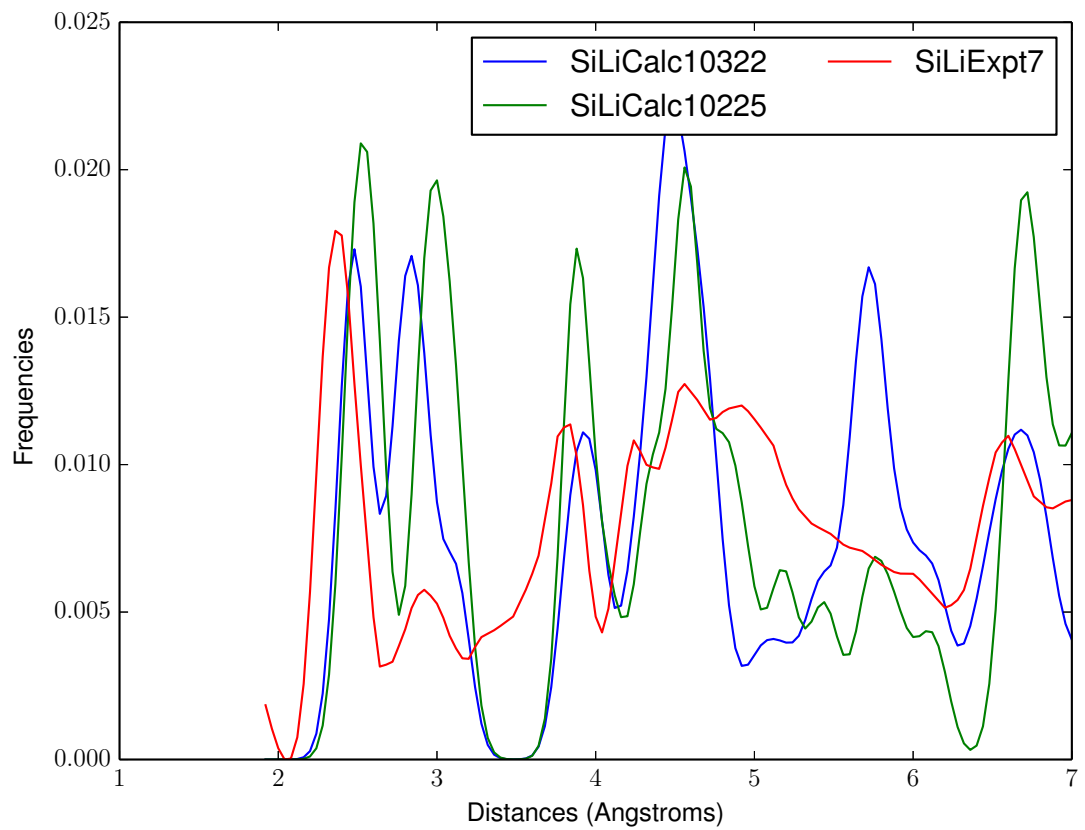


Figure 41: PCA Matches: SiLiExpt7, SiLiCalc10225, SiLiCalc10322

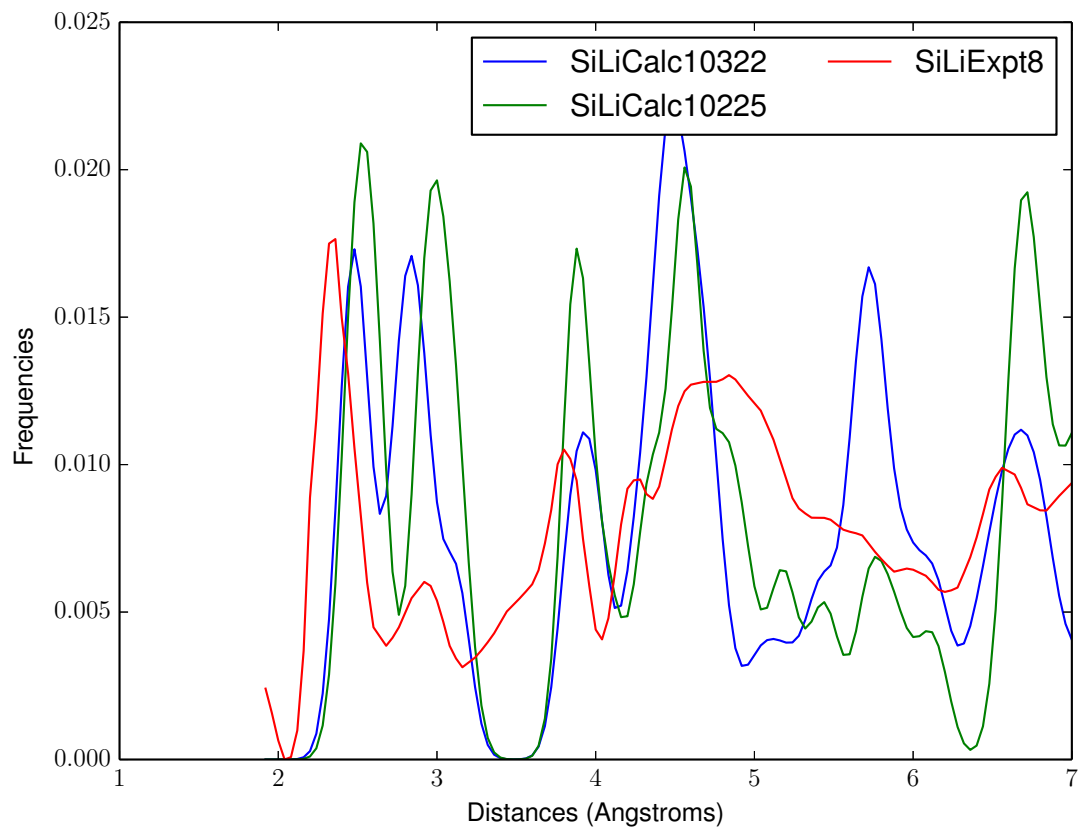


Figure 42: PCA Matches: SiLiExpt8, SiLiCalc10225, SiLiCalc10322

4.5.2 10 Principal Components

| Image | Best Match | 2 | 3 | 4 | 5 |
|------------------|-------------------|---------------|----------------------|---------------|---------------|
| ExptGaAs | CalcGaAs | SiLiCalc10329 | SiLiCalc11337 | SiLiCalc11436 | SiLiCalc10571 |
| ExptInAs | SiLiCalc10646 | SiLiCalc10805 | SiLiCalc10792 | SiLiCalc10836 | SiLiCalc10767 |
| SiLiExpt1 | SiLiCalc10213 | SiLiCalc10215 | SiLiCalc10001 | SiLiCalc10003 | SiLiCalc10313 |
| SiLiExpt2 | SiLiCalc10001 | SiLiCalc10003 | SiLiCalc10209 | SiLiCalc10317 | SiLiCalc10313 |
| SiLiExpt3 | SiLiCalc10257 | SiLiCalc10317 | SiLiCalc10259 | SiLiCalc10258 | SiLiCalc10256 |
| SiLiExpt4 | SiLiCalc10257 | SiLiCalc10258 | SiLiCalc10256 | SiLiCalc10229 | SiLiCalc10232 |
| SiLiExpt5 | SiLiCalc10445 | SiLiCalc10616 | SiLiCalc11436 | SiLiCalc10329 | SiLiCalc11337 |
| SiLiExpt6 | SiLiCalc10445 | SiLiCalc10616 | SiLiCalc11436 | SiLiCalc10693 | SiLiCalc11337 |
| SiLiExpt7 | SiLiCalc10445 | SiLiCalc10693 | SiLiCalc11337 | SiLiCalc10616 | SiLiCalc10482 |
| SiLiExpt8 | SiLiCalc10445 | SiLiCalc10693 | SiLiCalc10329 | SiLiCalc11337 | SiLiCalc10482 |

Table 4: Recognition with 10 Principal Components

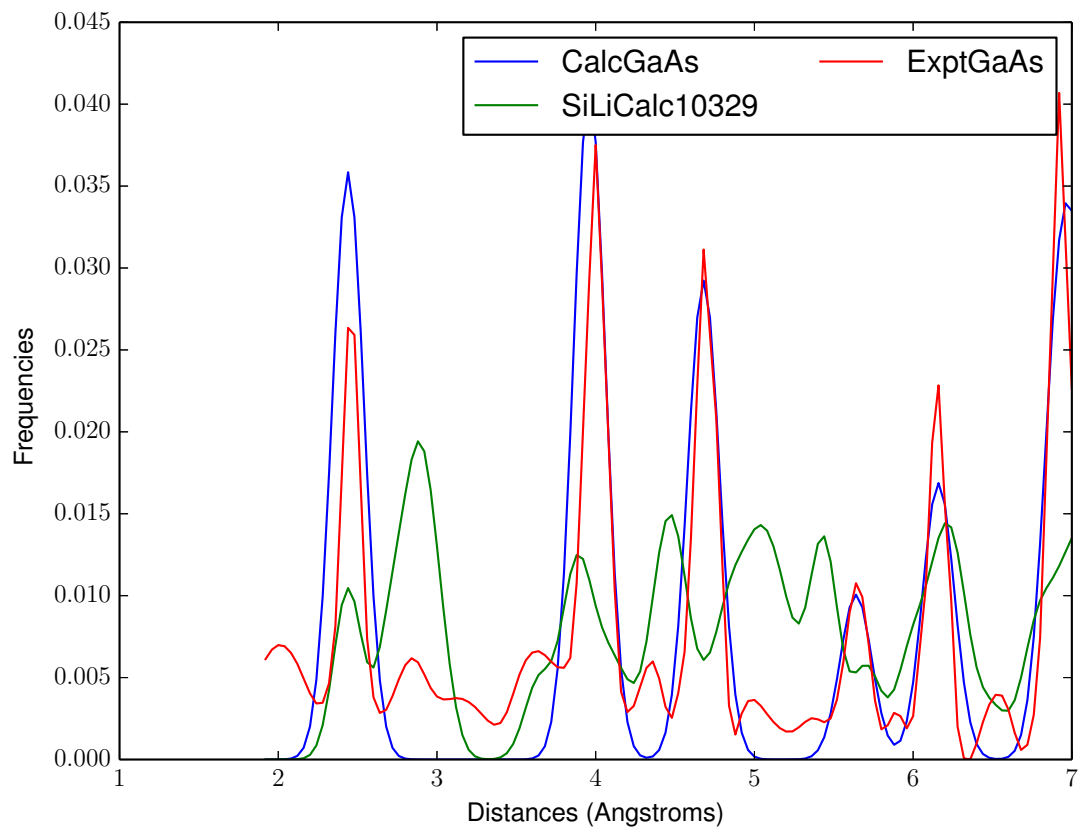


Figure 43: PCA Matches: ExptGaAs, CalcGaAs, SiLiCalc10329

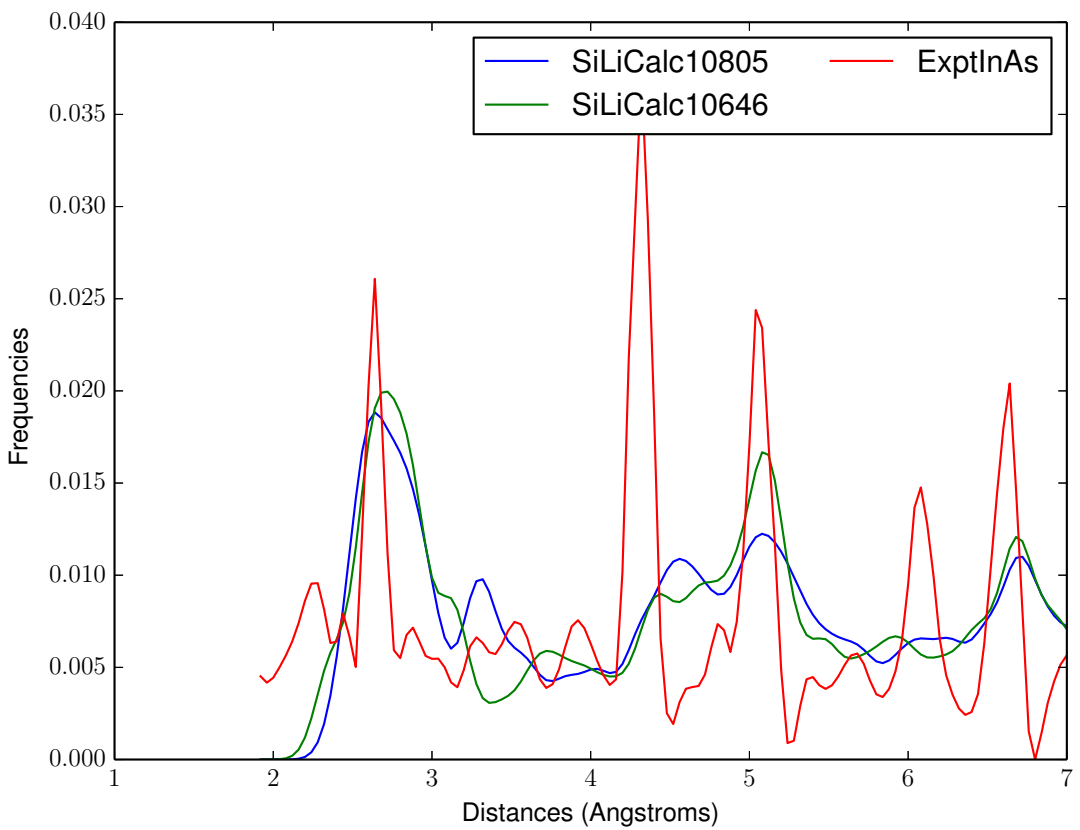


Figure 44: PCA Matches: ExptInAs, SiLiCalc10646, SiLiCalc10805

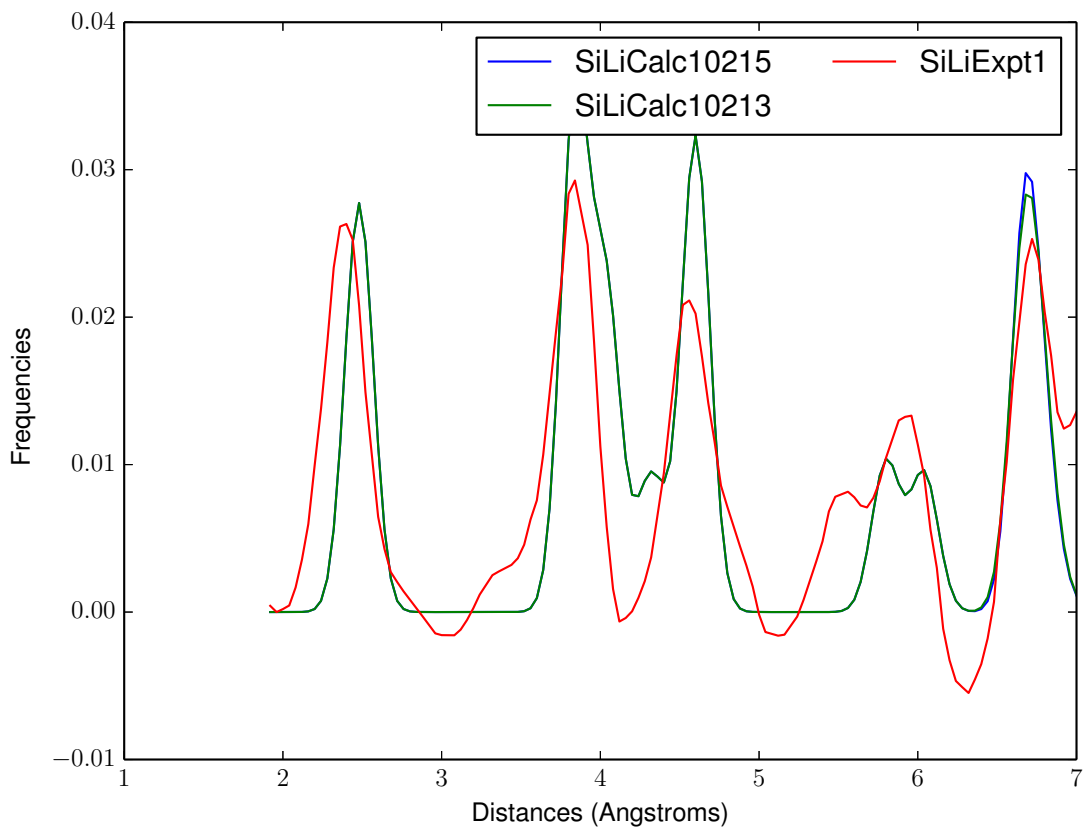


Figure 45: PCA Matches: SiLiExpt1, SiLiCalc10213, SiLiCalc10215

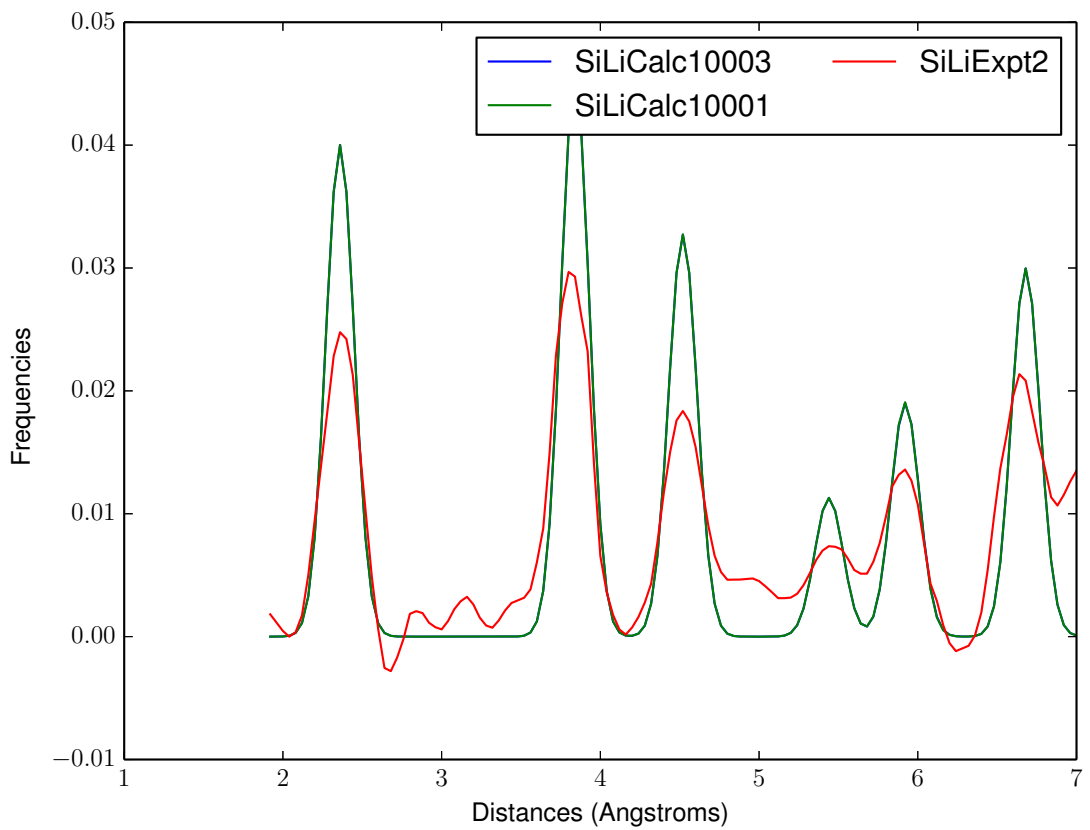


Figure 46: PCA Matches: SiLiExpt2, SiLiCalc10001, SiLiCalc10003

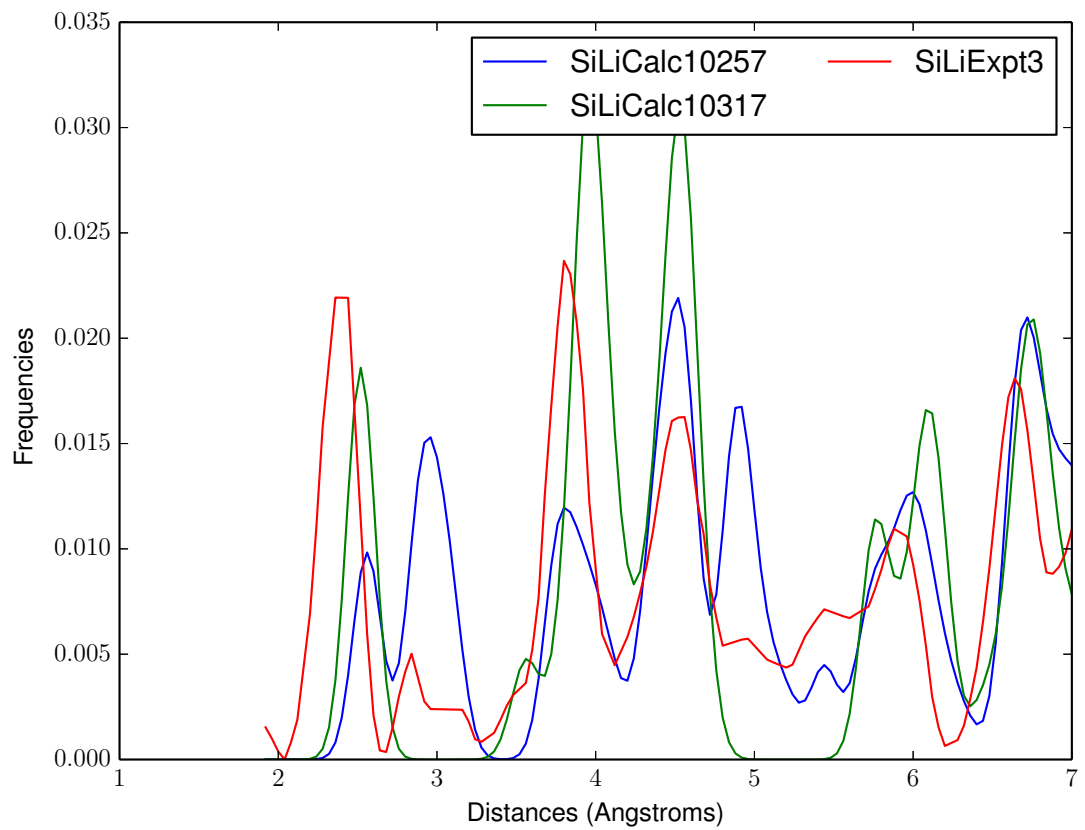


Figure 47: PCA Matches: SiLiExpt3, SiLiCalc10257, SiLiCalc10317

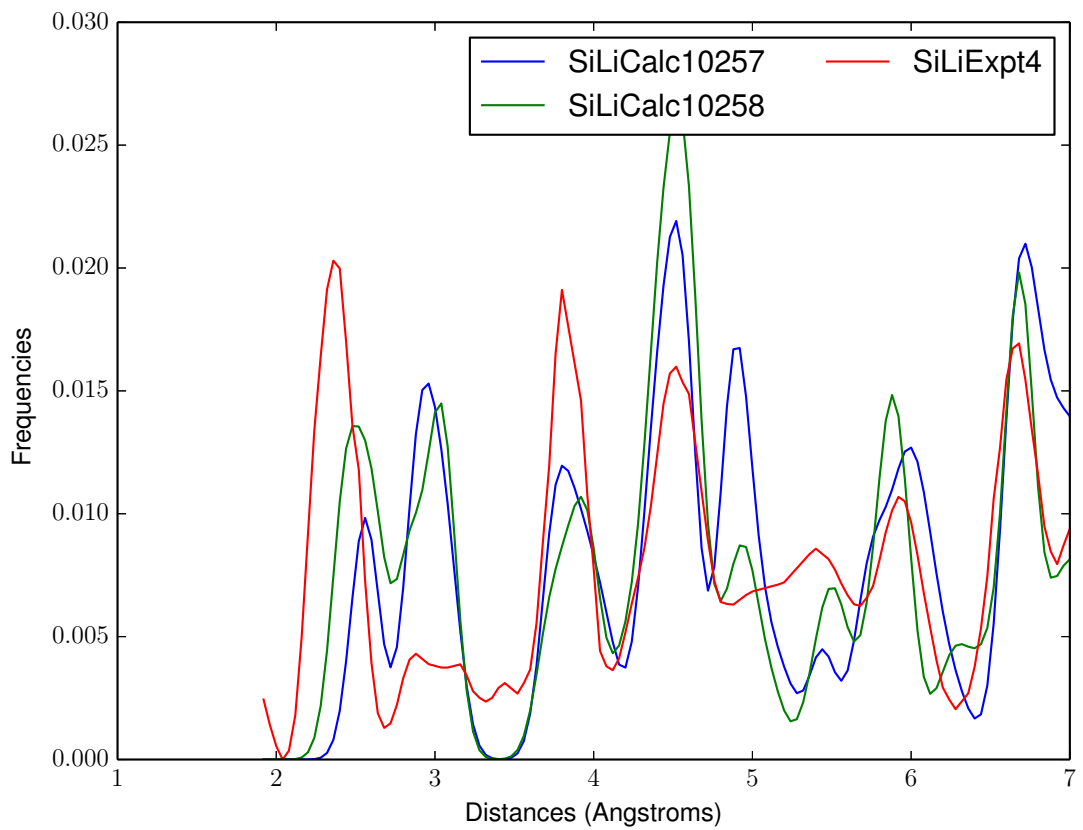


Figure 48: PCA Matches: SiLiExpt4, SiLiCalc10257, SiLiCalc10258

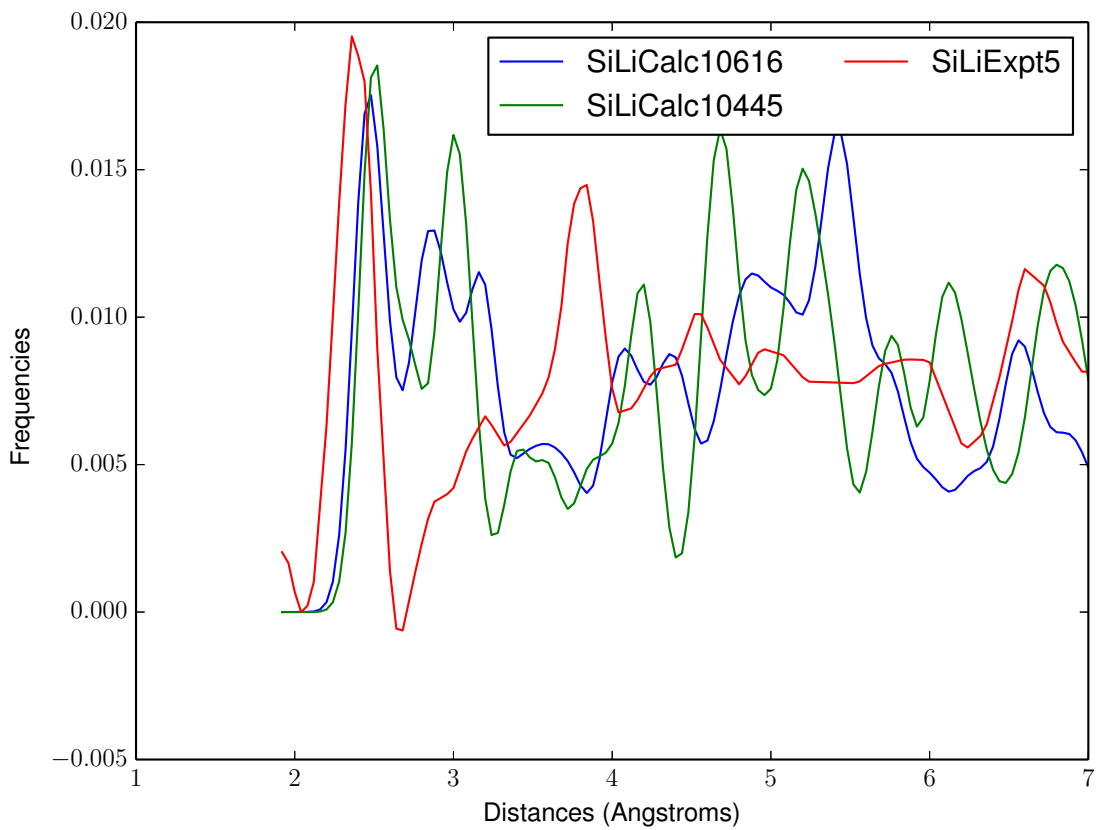


Figure 49: PCA Matches: SiLiExpt5, SiLiCalc10445, SiLiCalc10616

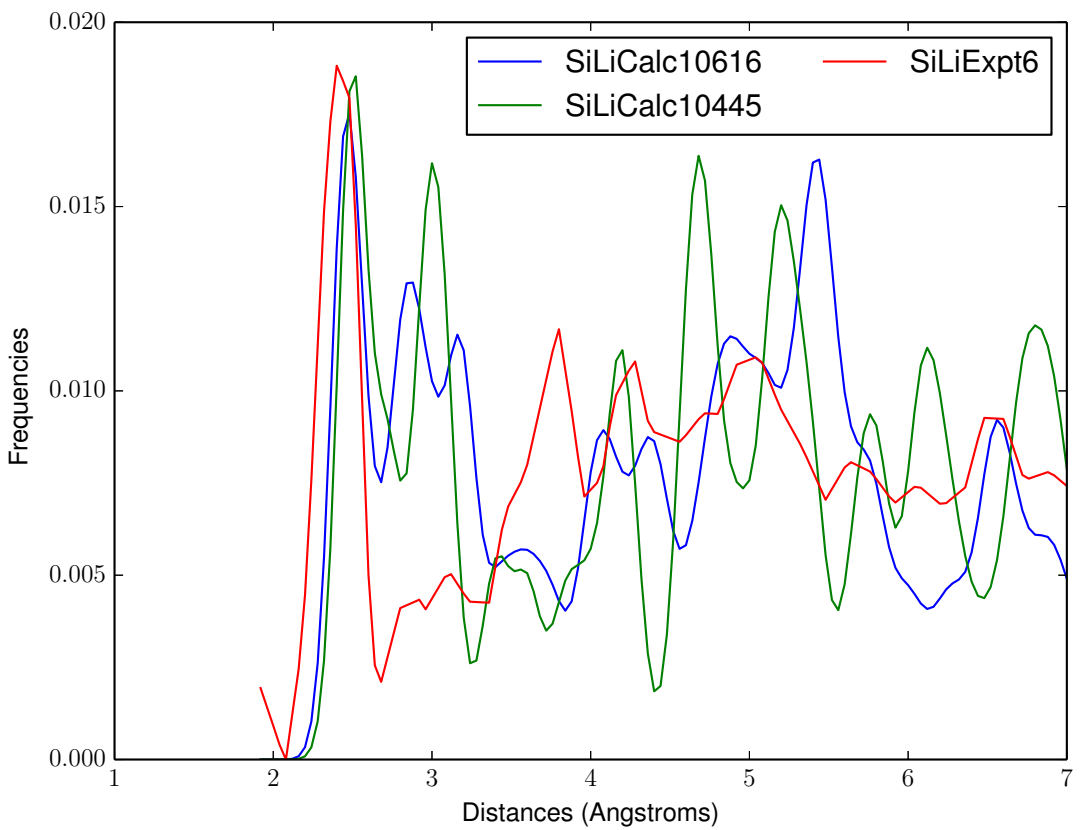


Figure 50: PCA Matches: SiLiExpt6, SiLiCalc10445, SiLiCalc10616

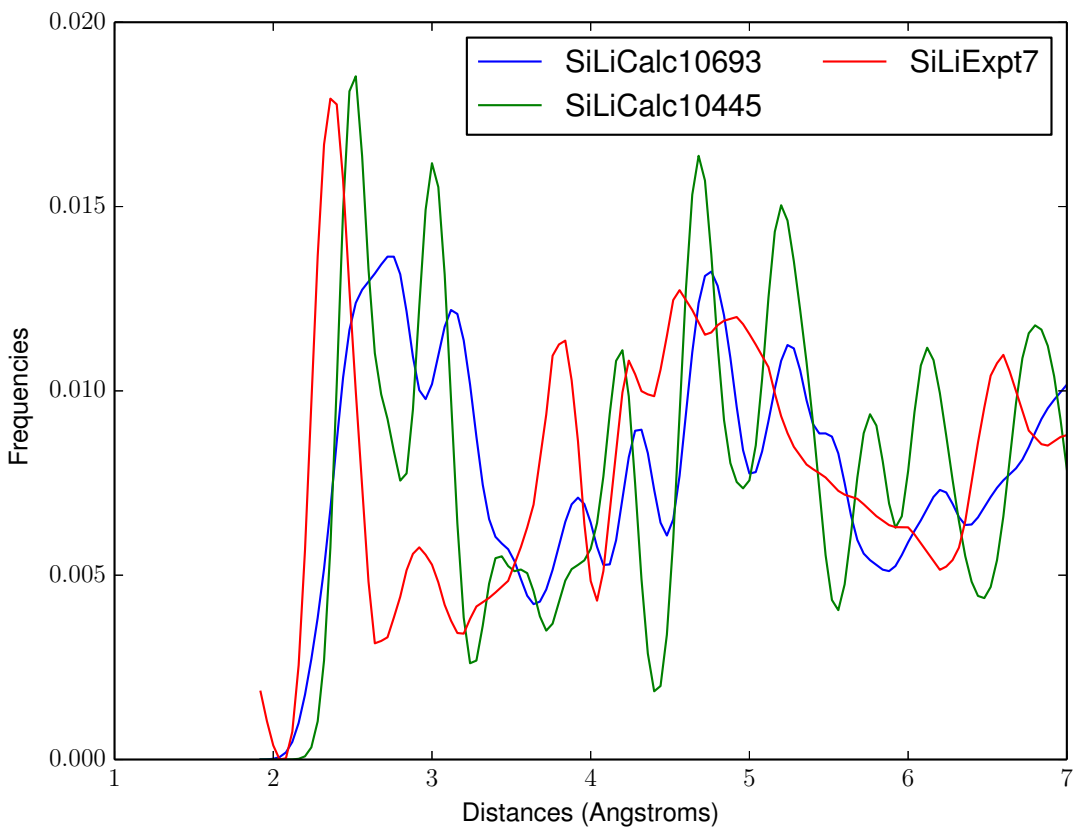


Figure 51: PCA Matches: SiLiExpt7, SiLiCalc10445, SiLiCalc10693

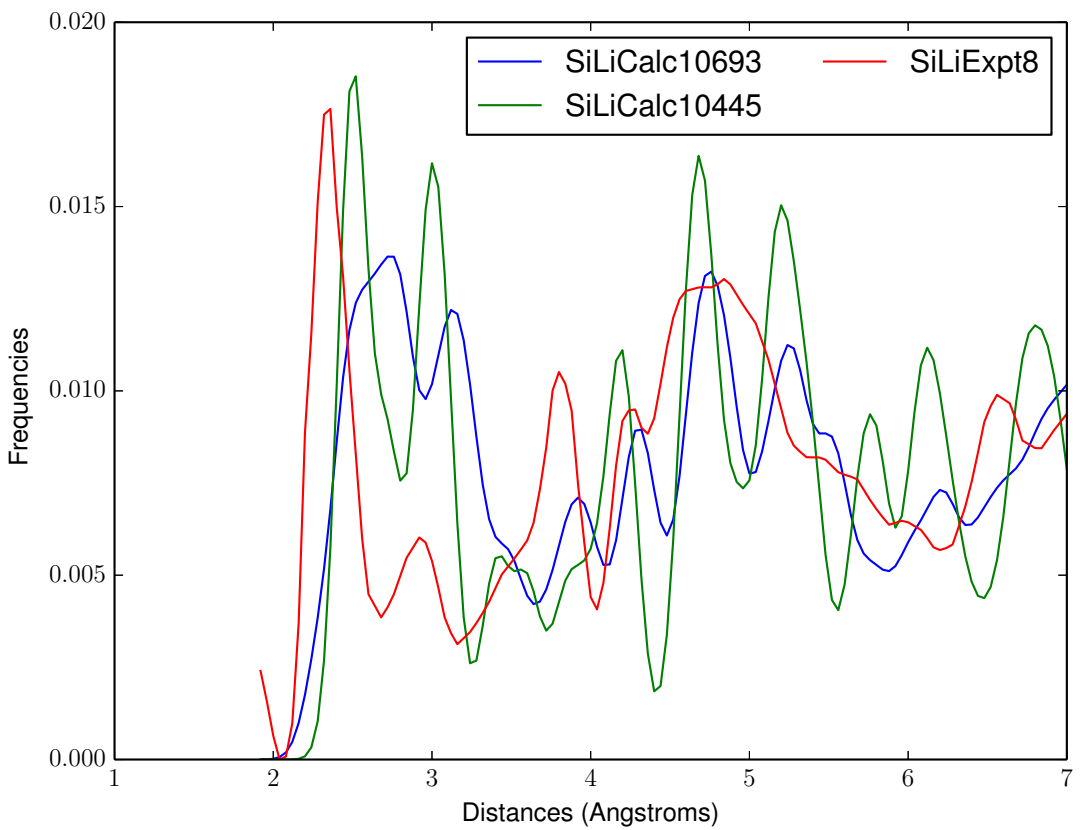


Figure 52: PCA Matches: SiLiExpt8, SiLiCalc10445, SiLiCalc10693

4.5.3 128 Principal Components

| Image | Best Match | 2 | 3 | 4 | 5 |
|------------------|-------------------|----------------------|---------------|---------------|---------------|
| ExptGaAs | CalcGaAs | SiLiCalc10445 | SiLiCalc11436 | SiLiCalc10693 | SiLiCalc11337 |
| ExptInAs | SiLiCalc10429 | SiLiCalc10602 | SiLiCalc10838 | SiLiCalc10901 | SiLiCalc10607 |
| SiLiExpt1 | SiLiCalc10194 | SiLiCalc10001 | SiLiCalc10003 | SiLiCalc10136 | SiLiCalc10147 |
| SiLiExpt2 | SiLiCalc10001 | SiLiCalc10003 | SiLiCalc10194 | SiLiCalc10136 | SiLiCalc10147 |
| SiLiExpt3 | SiLiCalc10258 | SiLiCalc10229 | SiLiCalc10245 | SiLiCalc11436 | SiLiCalc10259 |
| SiLiExpt4 | SiLiCalc10258 | SiLiCalc11436 | SiLiCalc10229 | SiLiCalc11337 | SiLiCalc11634 |
| SiLiExpt5 | SiLiCalc10616 | SiLiCalc11337 | SiLiCalc10693 | SiLiCalc11436 | SiLiCalc11336 |
| SiLiExpt6 | SiLiCalc10616 | SiLiCalc10693 | SiLiCalc11337 | SiLiCalc11436 | SiLiCalc11336 |
| SiLiExpt7 | SiLiCalc10693 | SiLiCalc11337 | SiLiCalc10482 | SiLiCalc10616 | SiLiCalc10651 |
| SiLiExpt8 | SiLiCalc10693 | SiLiCalc10651 | SiLiCalc11337 | SiLiCalc10482 | SiLiCalc10616 |

Table 5: Recognition with 128 Principal Components

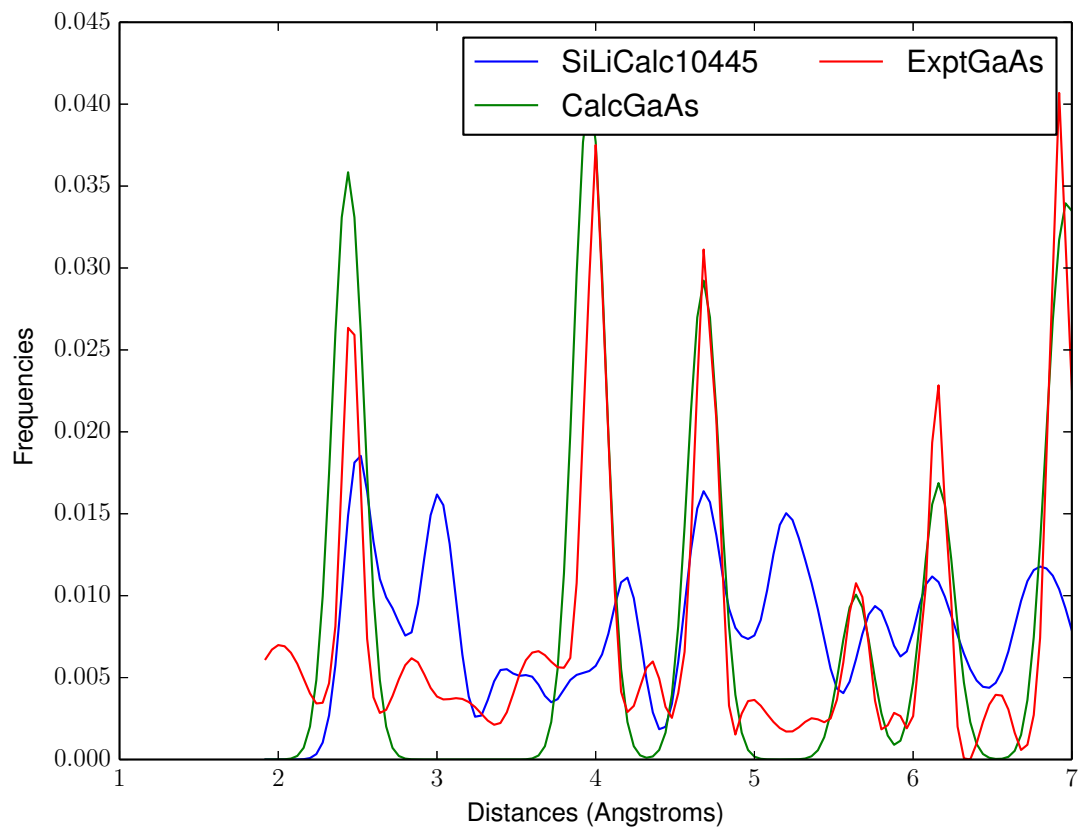


Figure 53: PCA Matches: ExptGaAs, CalcGaAs, SiLiCalc10445

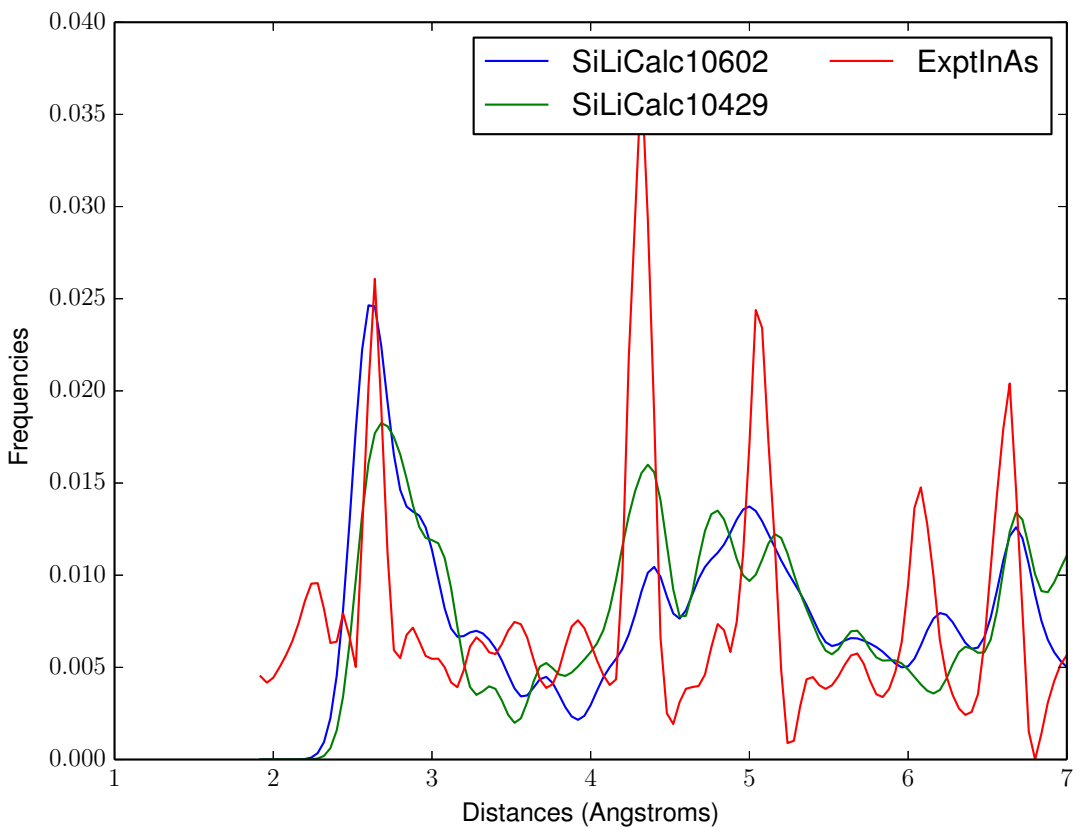


Figure 54: PCA Matches: ExptInAs, SiLiCalc10429, SiLiCalc10602

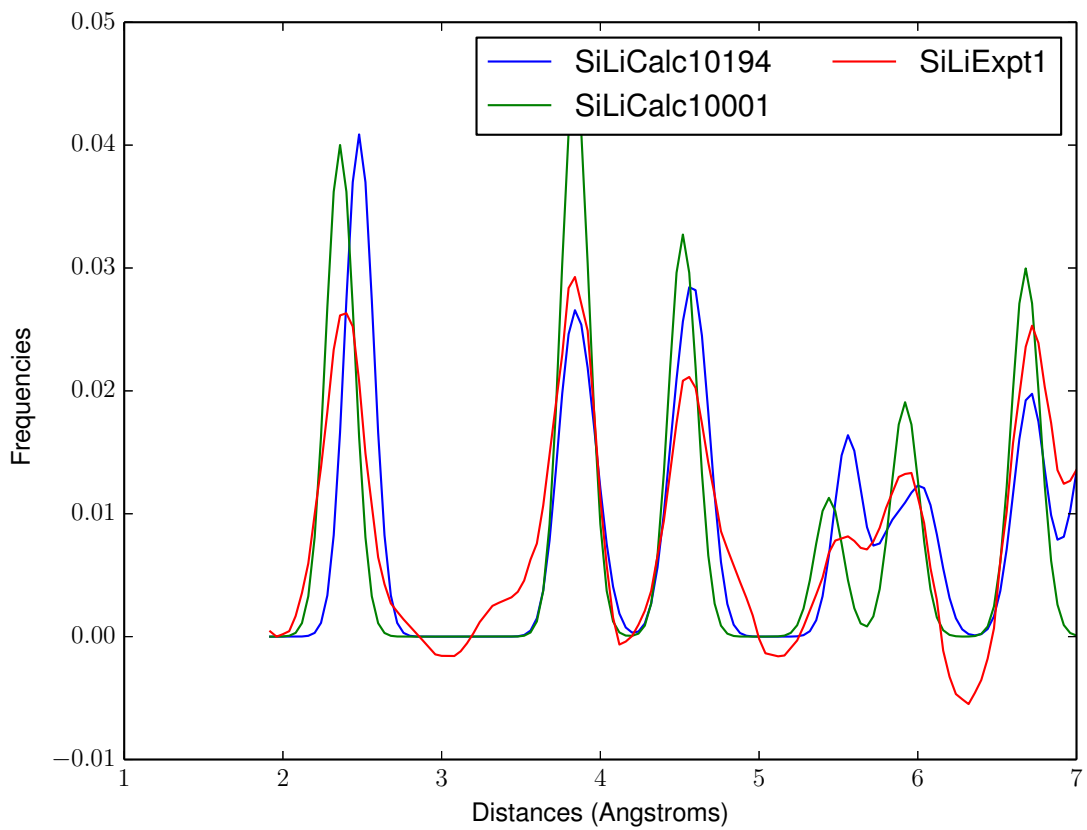


Figure 55: PCA Matches: SiLiExpt1, SiLiCalc10194, SiLiCalc10001

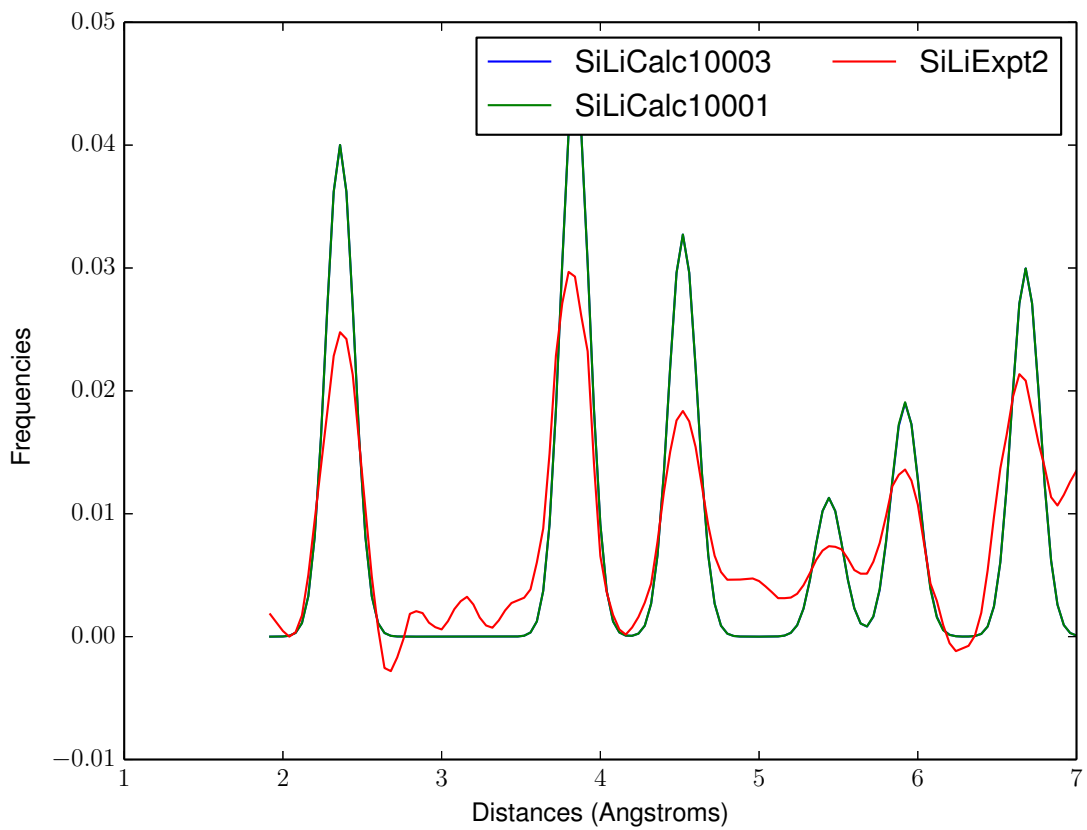


Figure 56: PCA Matches: SiLiExpt2, SiLiCalc10001, SiLiCalc10003

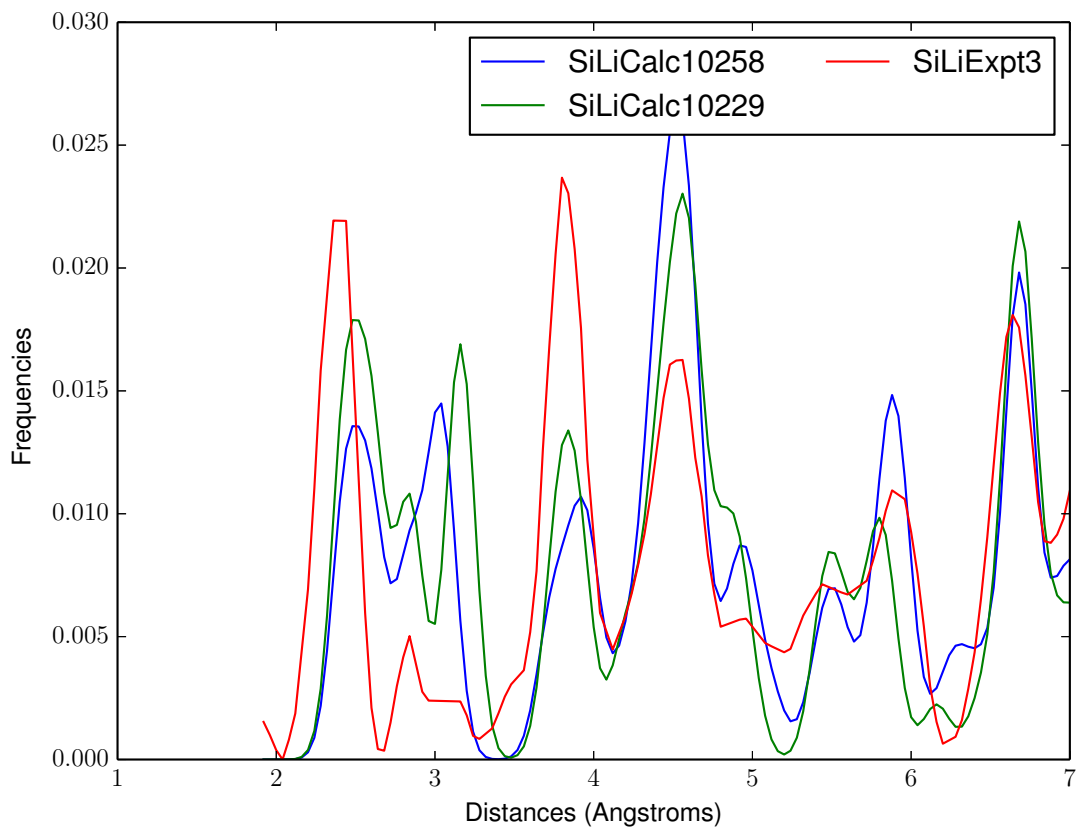


Figure 57: PCA Matches: SiLiExpt3, SiLiCalc10258, SiLiCalc10229

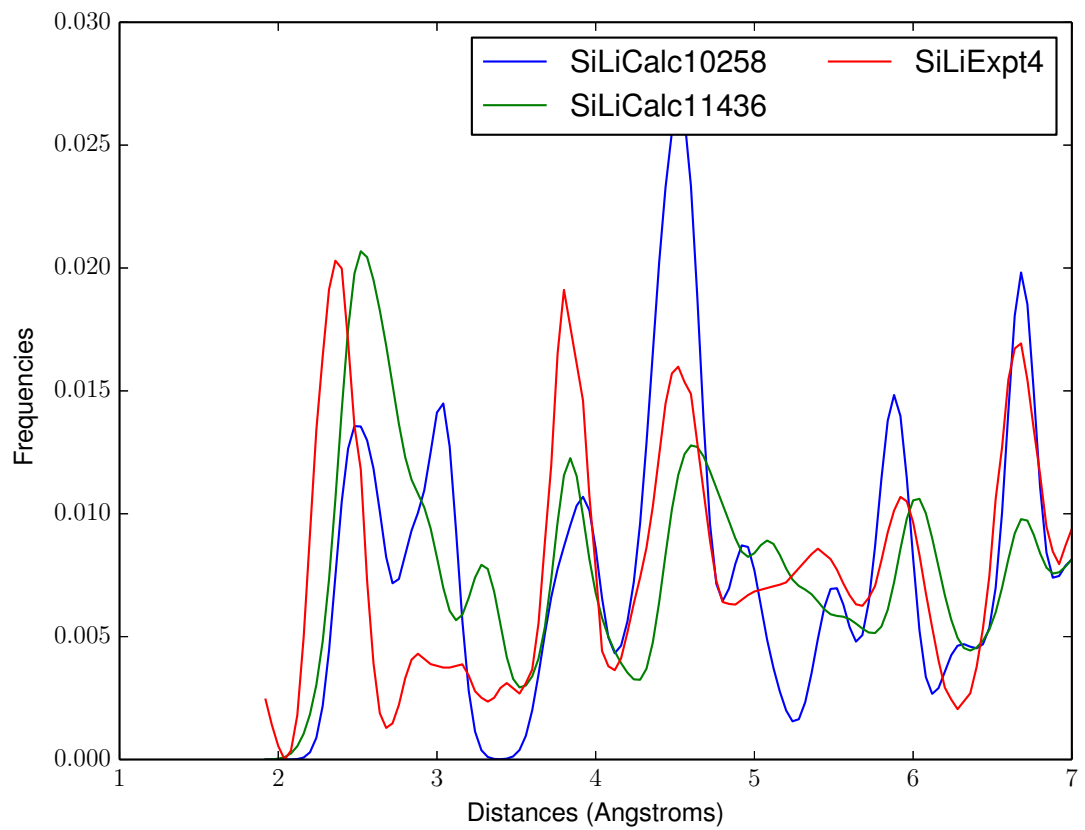


Figure 58: PCA Matches: SiLiExpt4, SiLiCalc10258, SiLiCalc11436

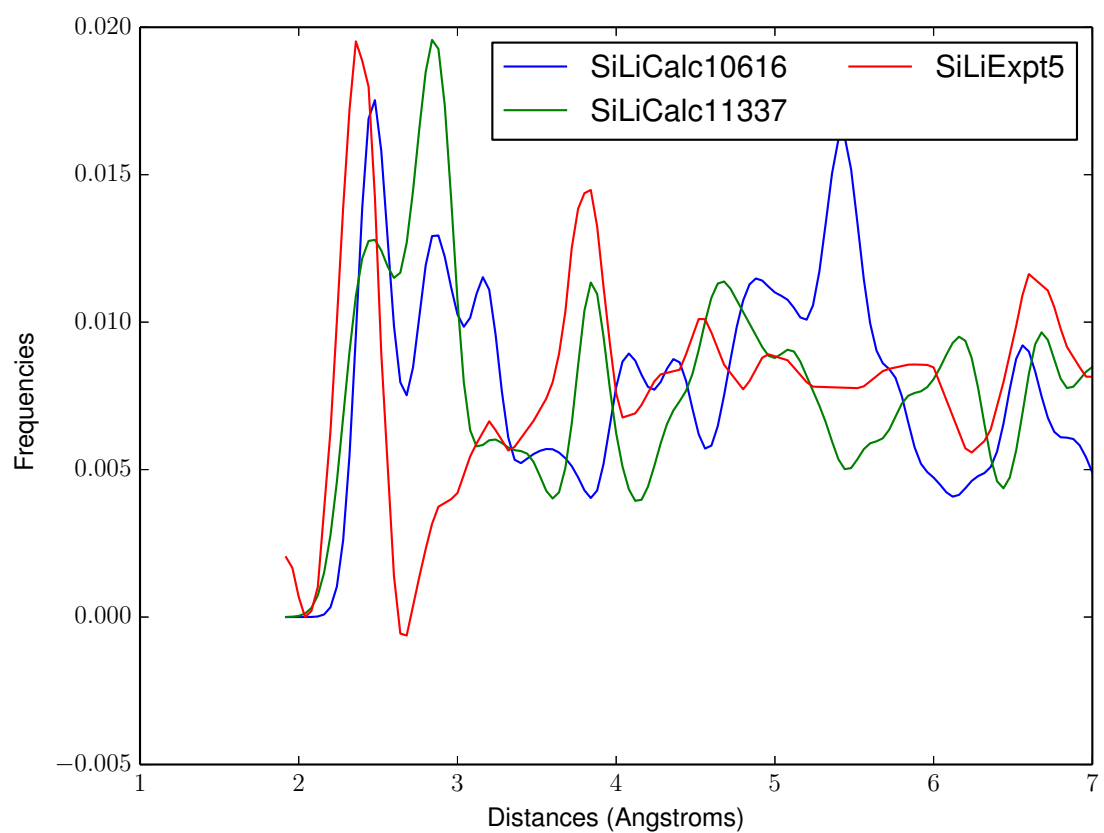


Figure 59: PCA Matches: SiLiExpt5, SiLiCalc10616, SiLiCalc11337

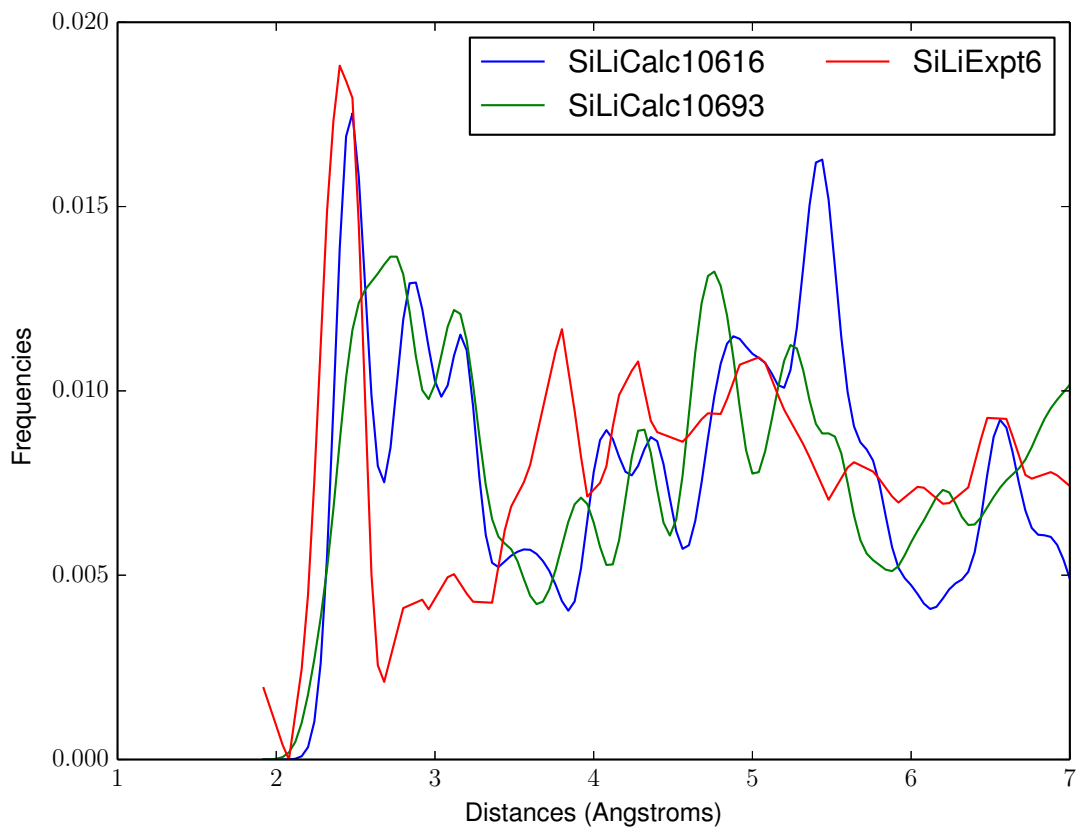


Figure 60: PCA Matches: SiLiExpt6, SiLiCalc10616, SiLiCalc10693

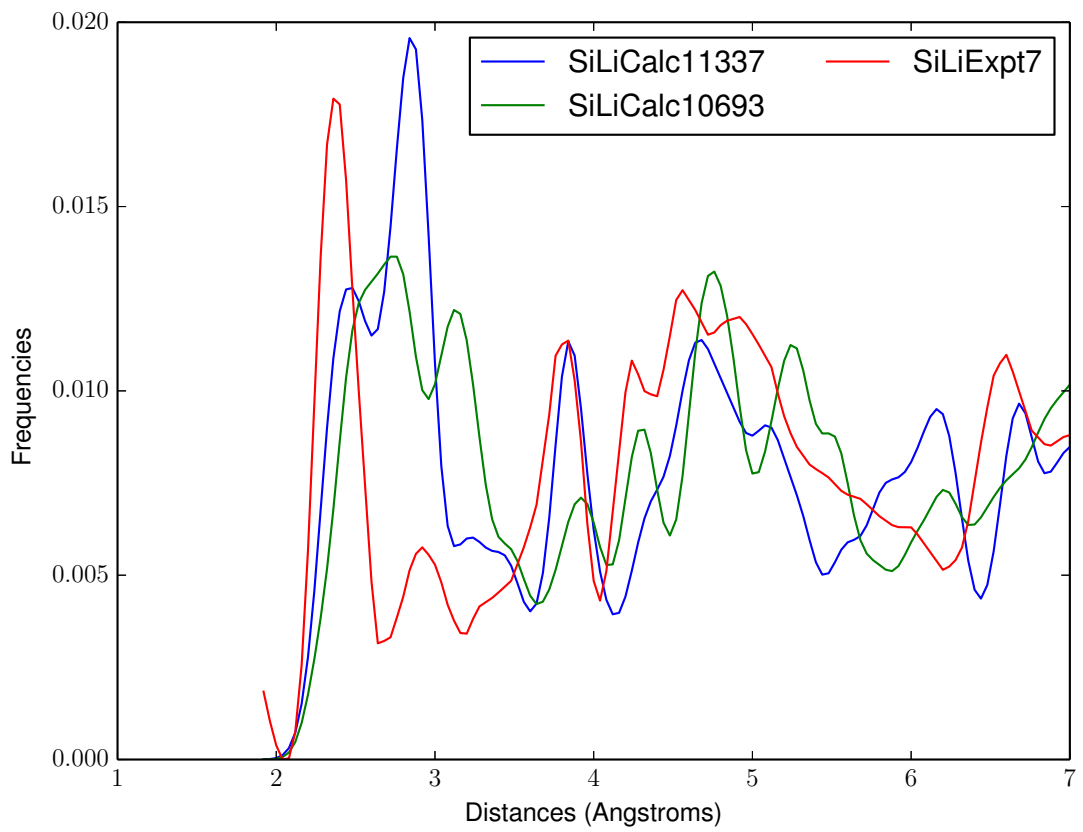


Figure 61: PCA Matches: SiLiExpt7, SiLiCalc10693, SiLiCalc11337

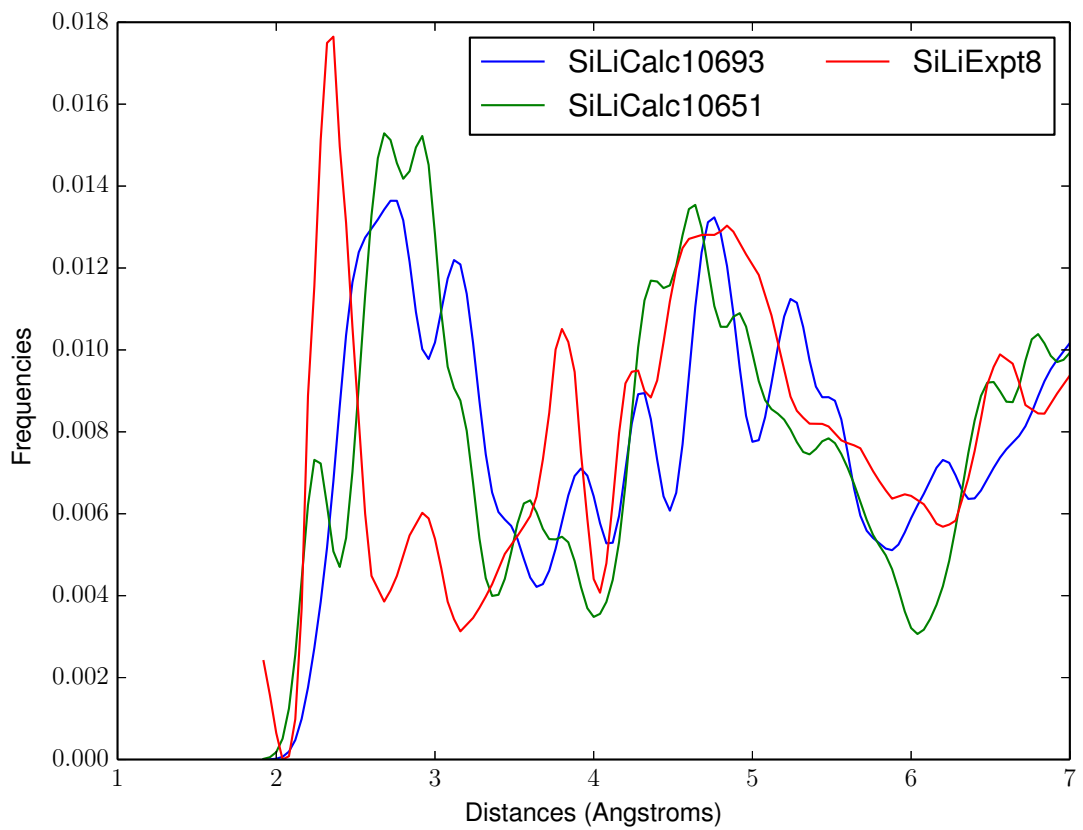


Figure 62: PCA Matches: SiLiExpt8, SiLiCalc10693, SiLiCalc10651

4.6 Synthetic Experimental Image Recognition

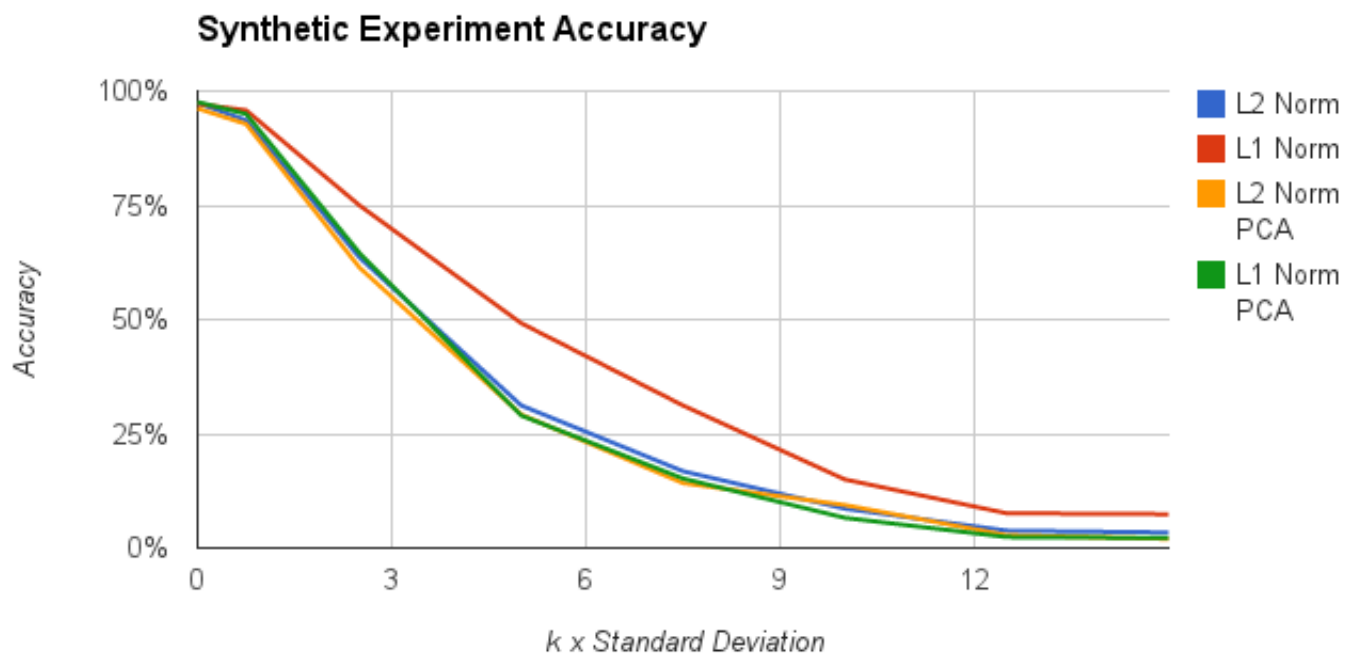


Figure 63: Synthetic Experimental Images Accuracy

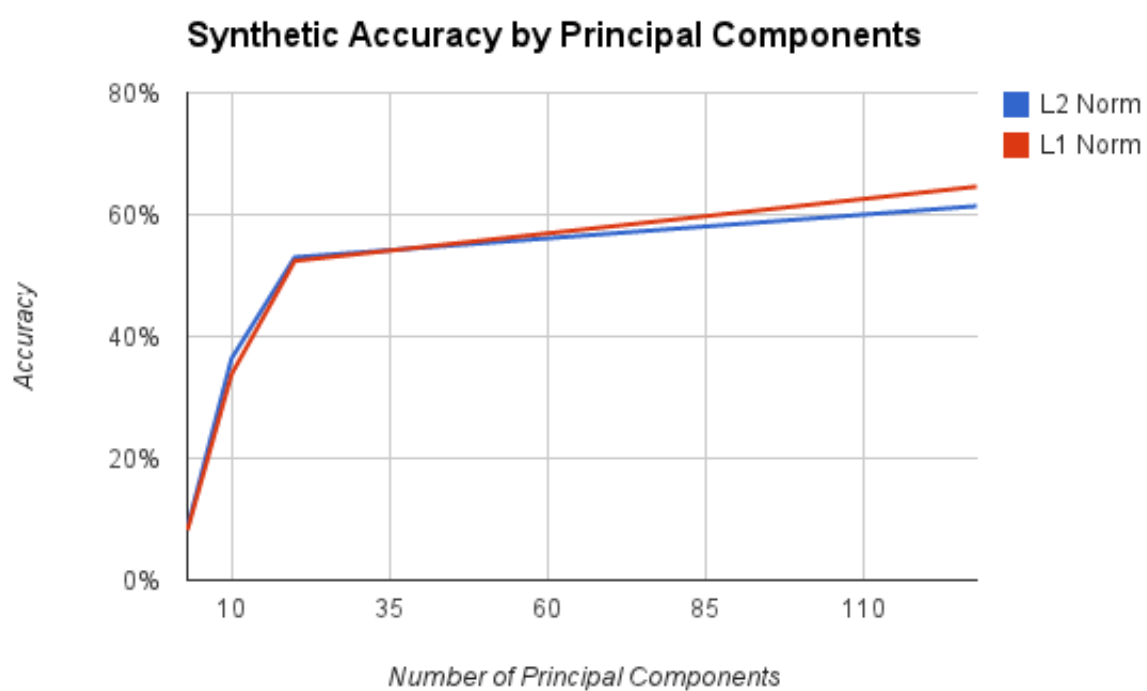


Figure 64: Accuracy vs Number of Principal Components

5 Recognition Using Sparse Representations

5.1 Experimental Image Recognition

| Experiment | Match |
|------------|---------------|
| ExptGaAs | CalcGaAs |
| ExptInAs | CalcInAs |
| SiLiExpt1 | SiLiCalc10001 |
| SiLiExpt2 | SiLiCalc10001 |
| SiLiExpt3 | SiLiCalc10001 |
| SiLiExpt4 | SiLiCalc10003 |
| SiLiExpt5 | SiLiCalc10003 |
| SiLiExpt6 | SiLiCalc10616 |
| SiLiExpt7 | SiLiCalc10382 |
| SiLiExpt8 | SiLiCalc10382 |

Table 6: Experimental Image Recognition

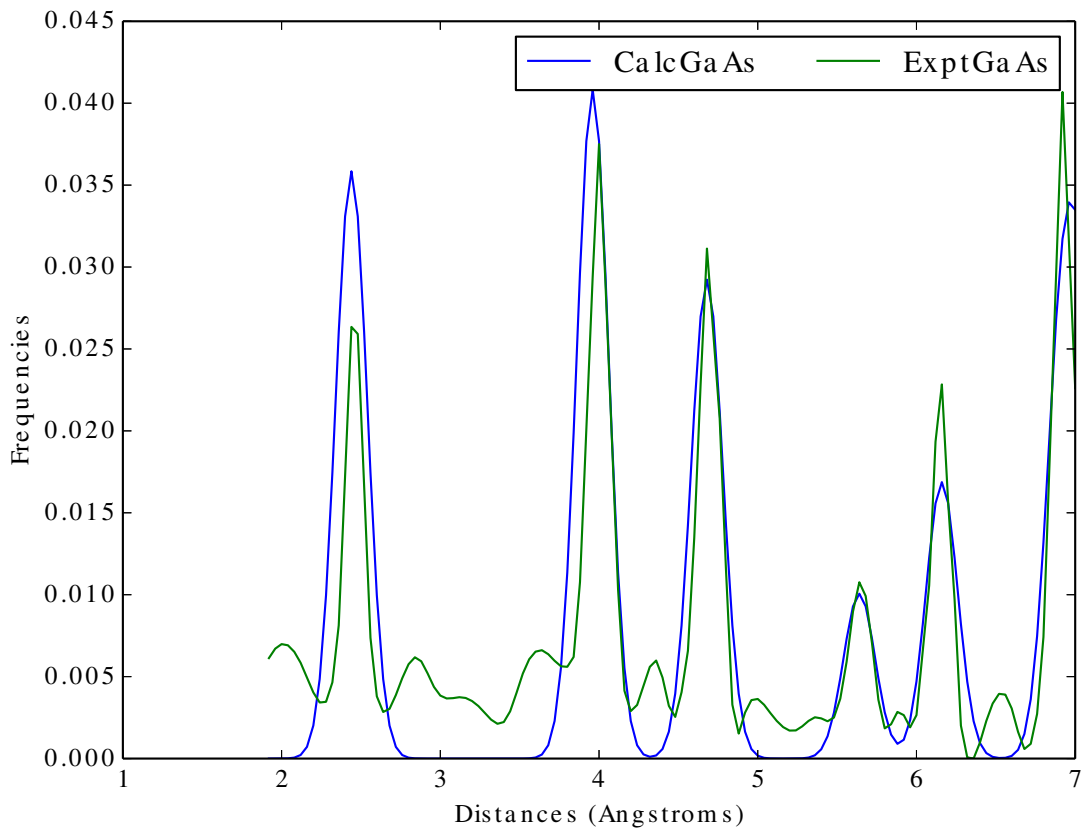


Figure 65: ExptGaAs, CalcGaAs

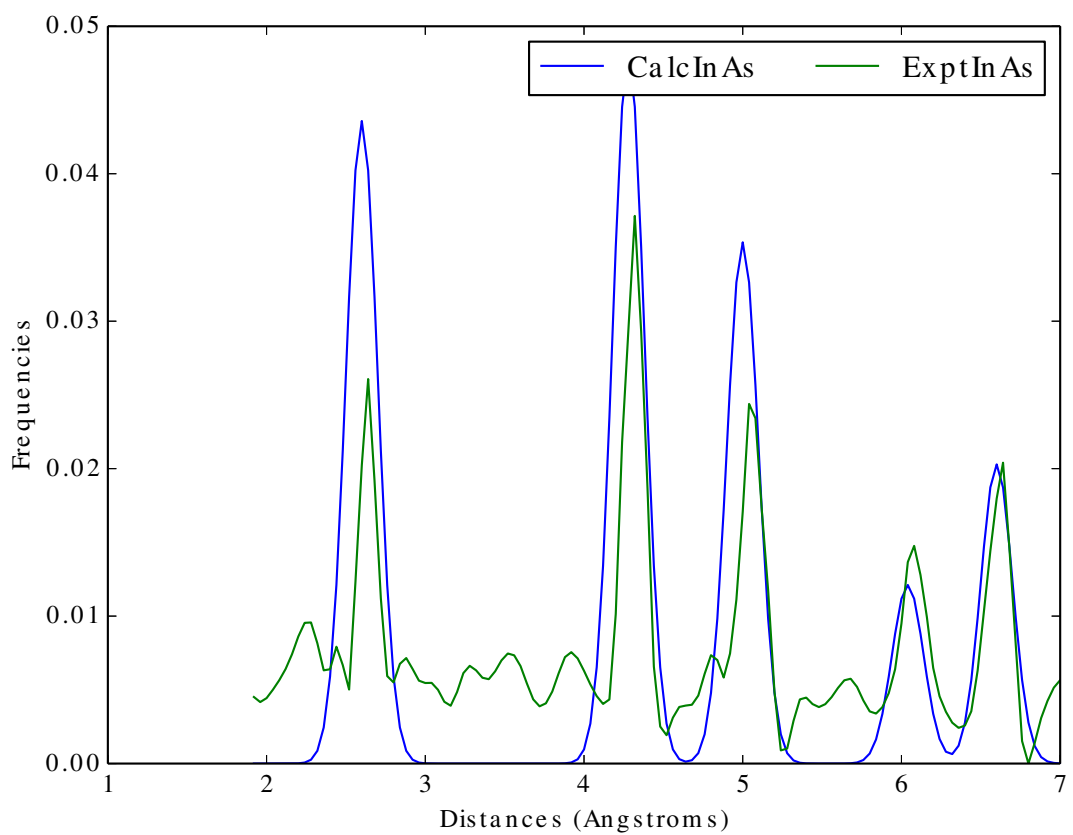


Figure 66: ExptInAs, CalcInAs

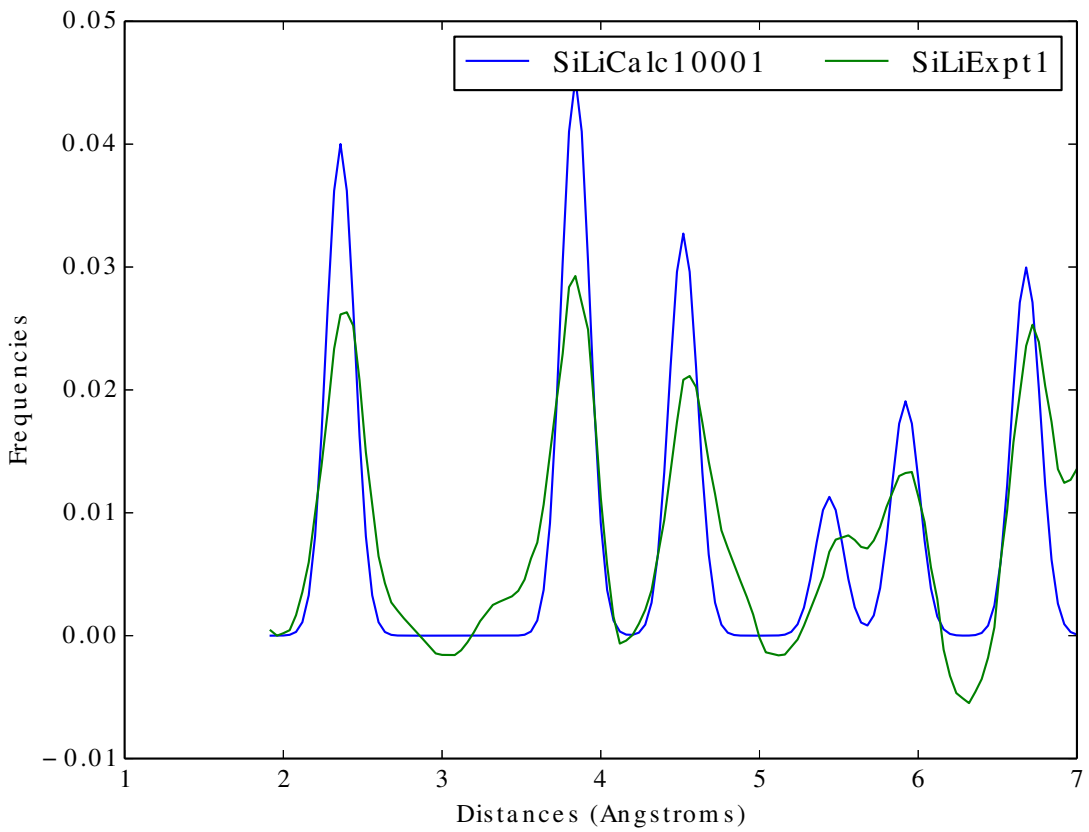


Figure 67: SiLiExpt1, SiLiCalc10001

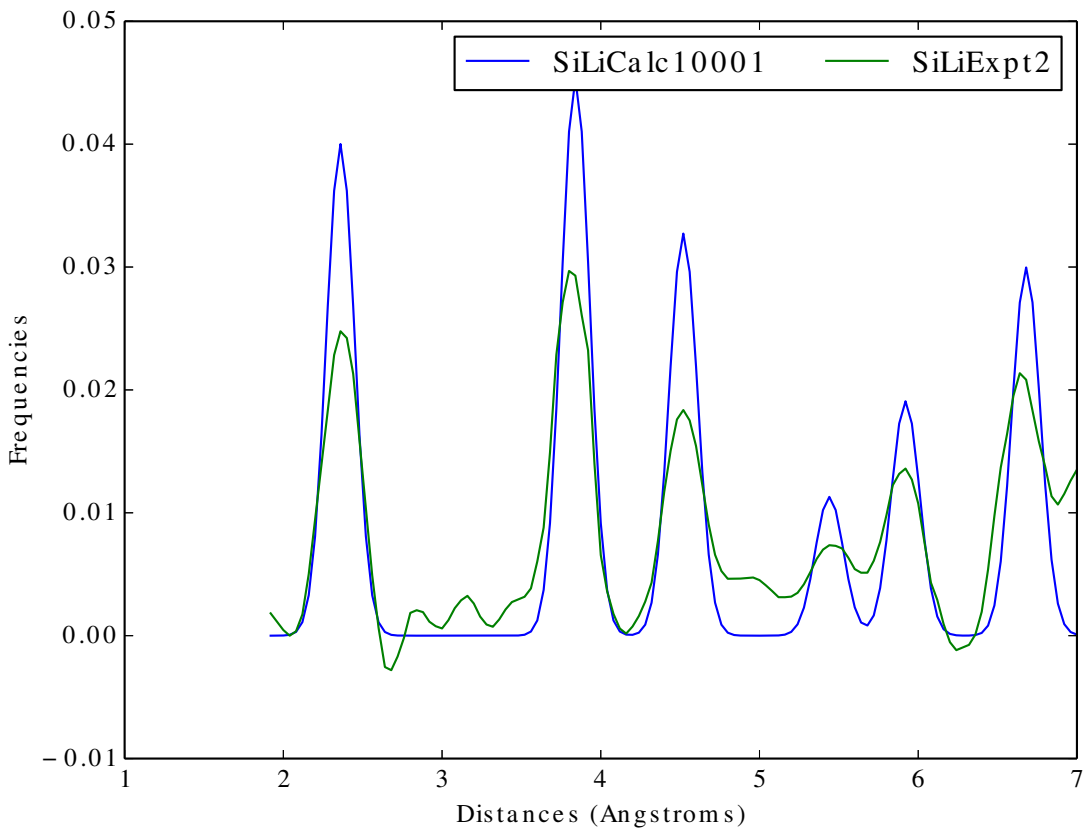


Figure 68: SiLiExpt2, SiLiCalc10001

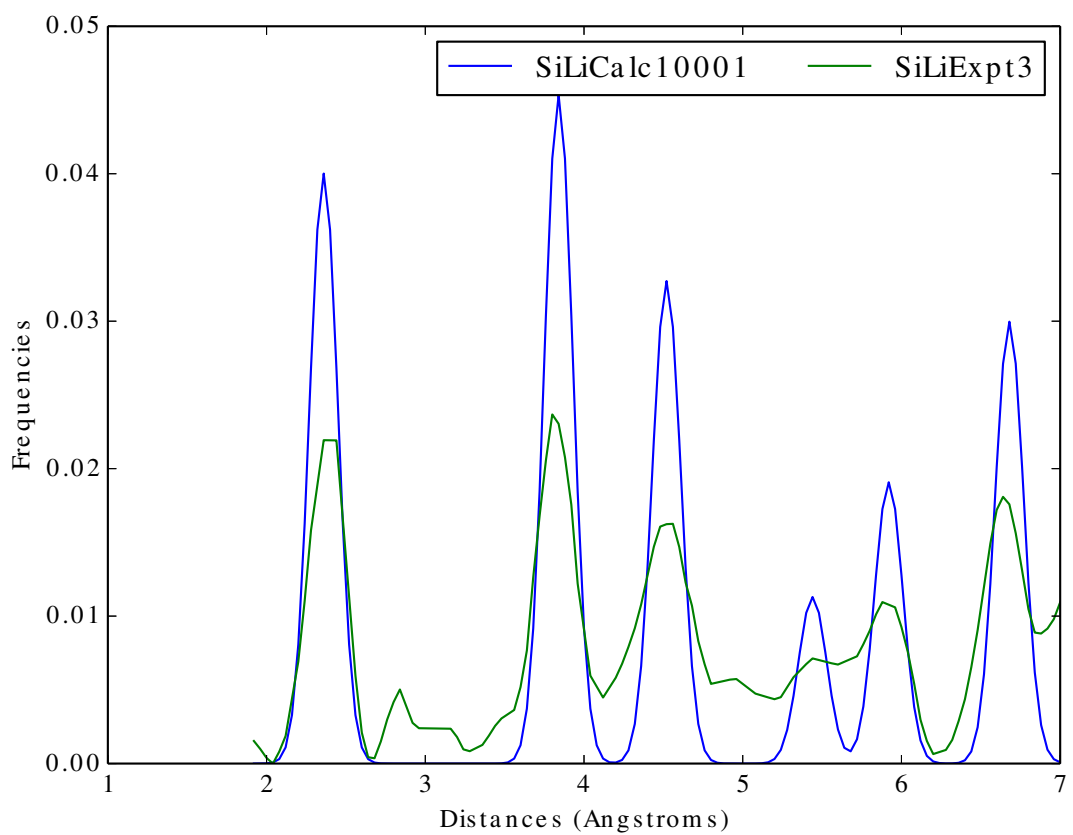


Figure 69: SiLiExpt3, SiLiCalc10001

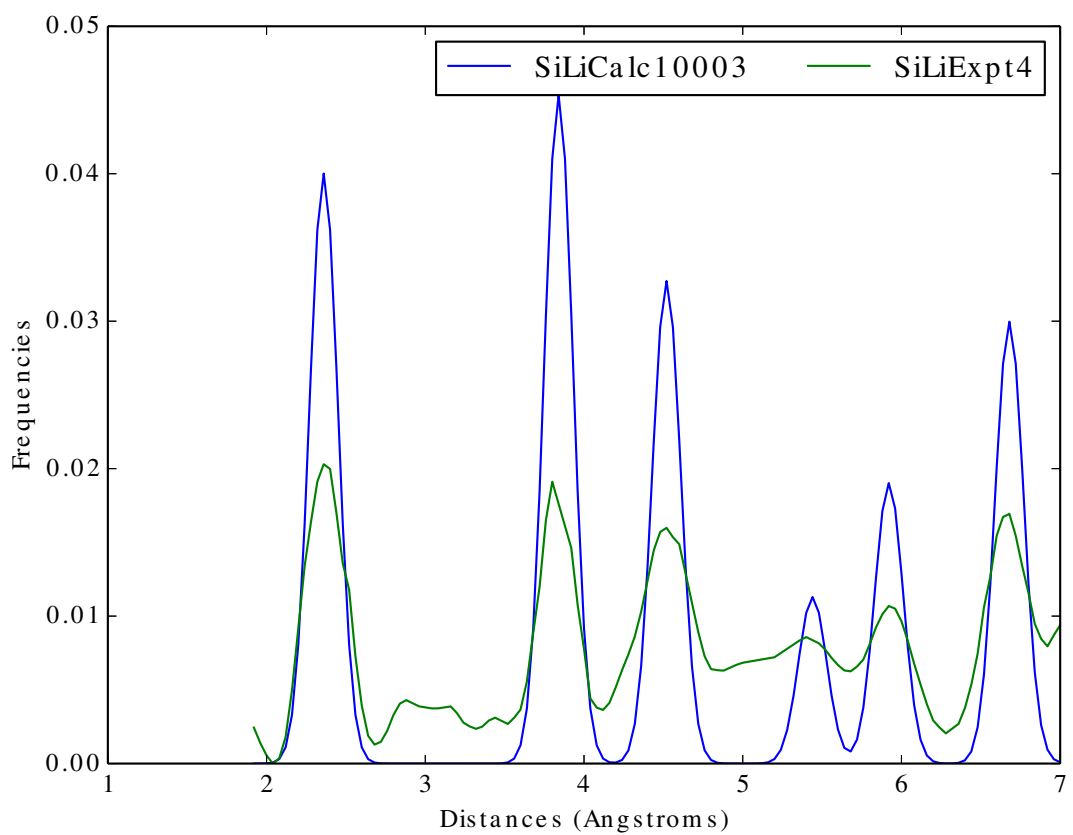


Figure 70: SiLiExpt4, SiLiCalc10003

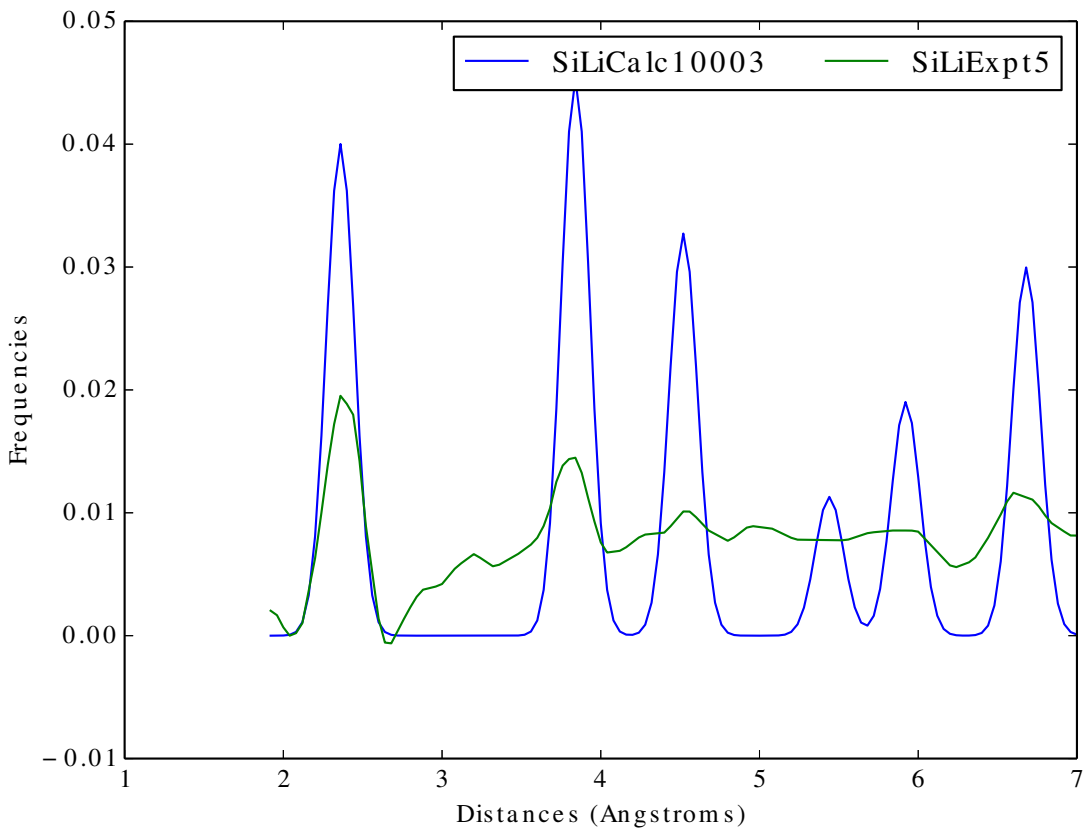


Figure 71: SiLiExpt5, SiLiCalc10003

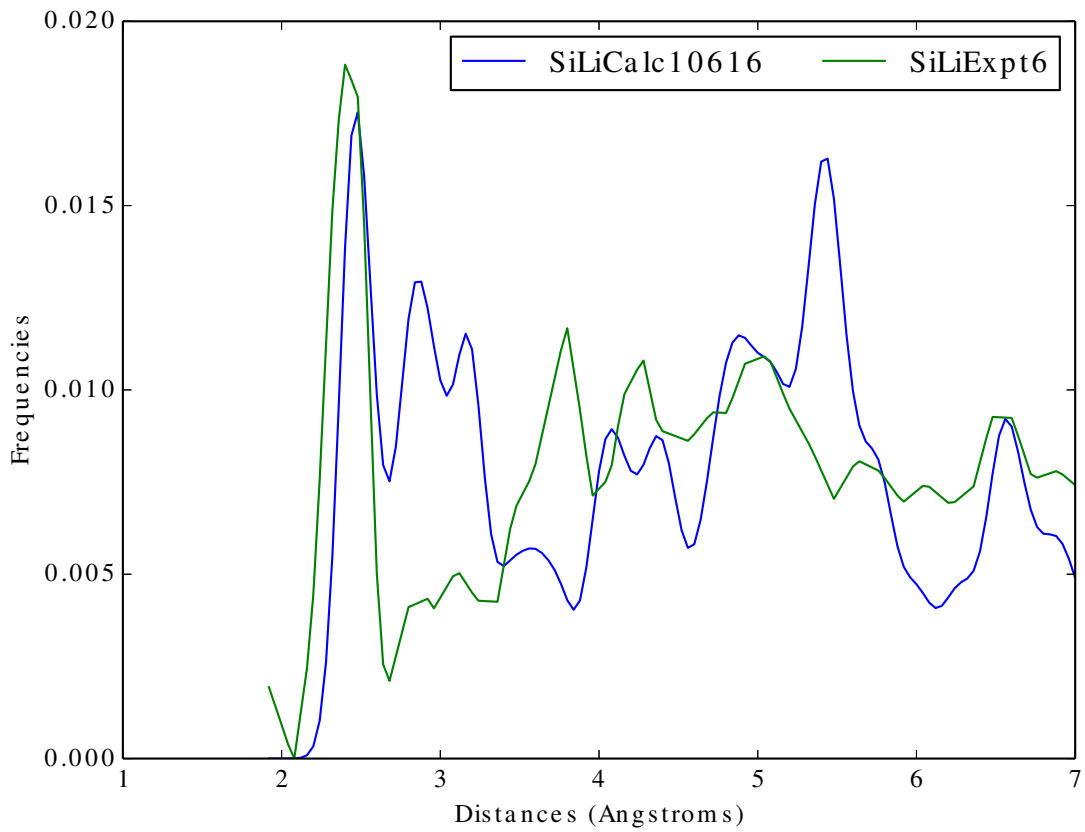


Figure 72: SiLiExpt6, SiLiCalc10616

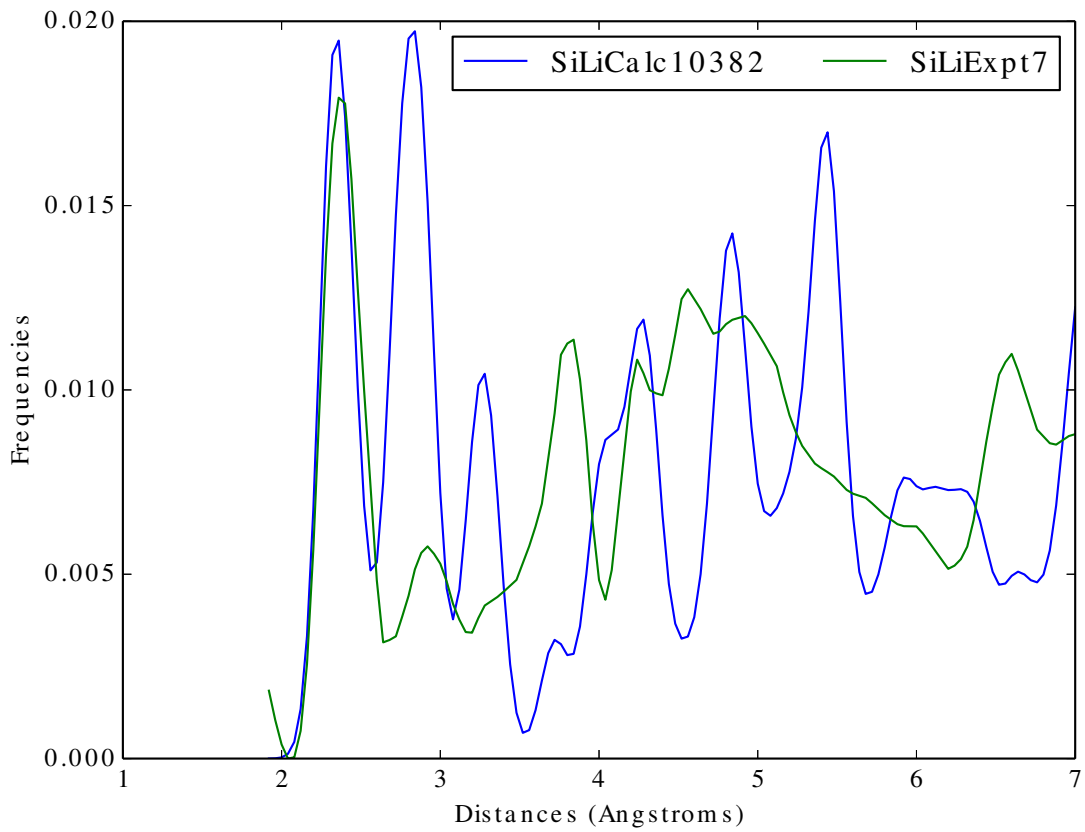


Figure 73: SiLiExpt7, SiLiCalc10382

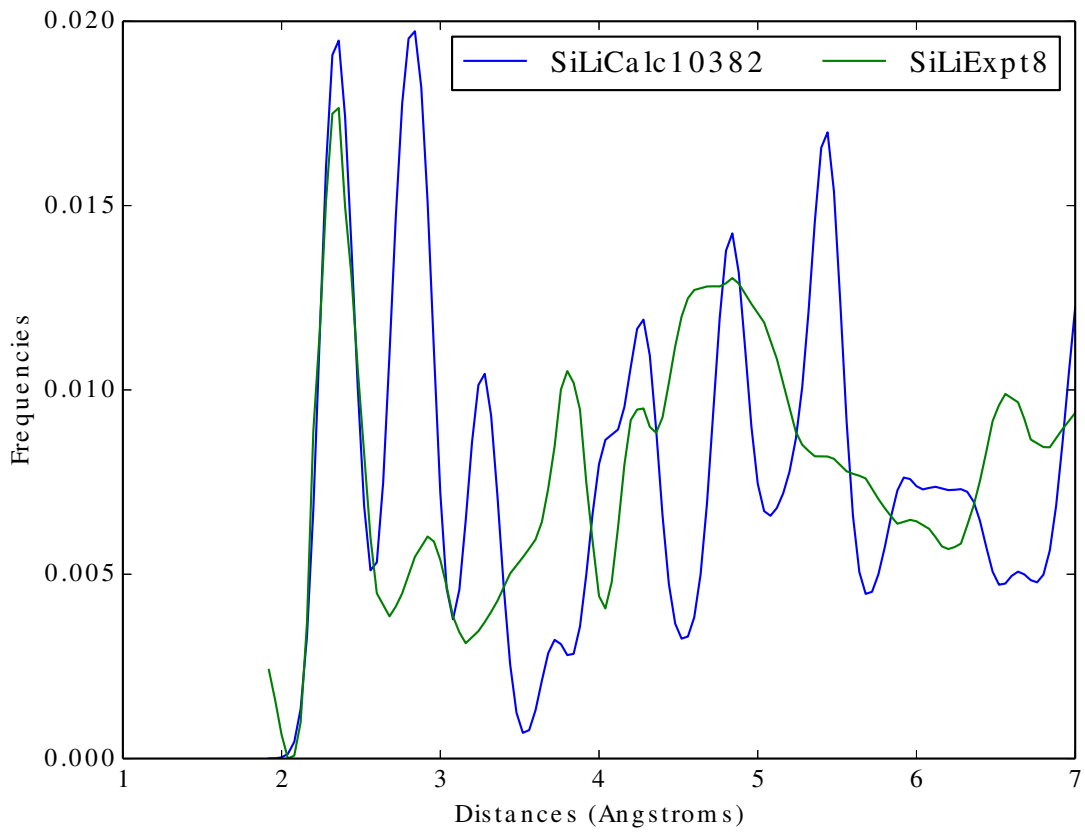


Figure 74: SiLiExpt8, SiLiCalc10382

5.2 Synthetic Experimental Image Recognition

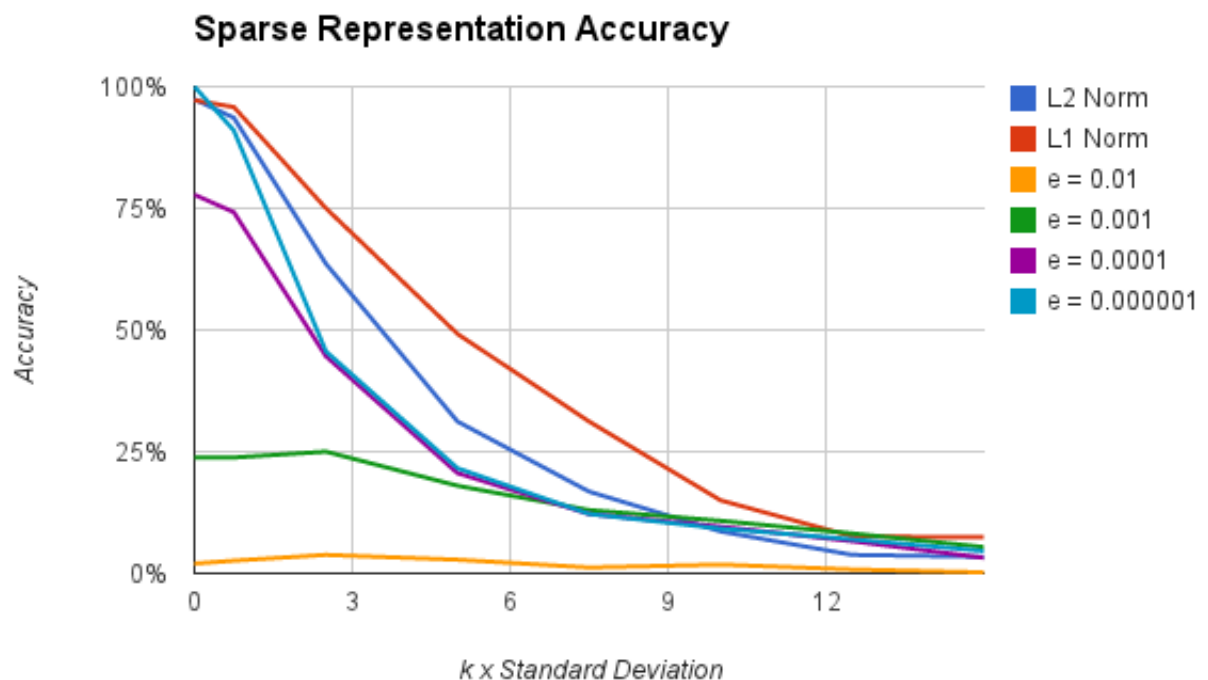


Figure 75: Synthetic Experimental Image Recognition Accuracy

6 Code

The code used to produce the results in this document as well as the document itself can be found here: <https://github.com/chadvoegele/xraysprectrapy>

7 Sources

http://en.wikipedia.org/wiki/Atom_vibrations

http://en.wikipedia.org/wiki/Radial_distribution_function

http://en.wikipedia.org/wiki/Weierstrass_transform

http://matplotlib.org/api/mlab_api.html

http://en.wikipedia.org/wiki/Principal_components_analysis

First Principles Simulations of the Electrochemical Lithiation and Delithiation of Faceted Crystalline Silicon
of Faceted Crystalline Silicon

Maria K. Y. Chan, C. Wolverton, and Jeffrey P. Greeley

Journal of the American Chemical Society 2012 134 (35), 14362-14374

Pair Distribution Functions Analysis.

Petkov, V. 2012.

Characterization of Materials. 1-14.

"Face recognition using eigenfaces,"

Turk, M.A.; Pentland, A.P.,

Computer Vision and Pattern Recognition, 1991. Proceedings CVPR '91.,

IEEE Computer Society Conference on , vol., no., pp.586,591, 3-6 Jun 1991

"Robust Face Recognition via Sparse Representation,"

Wright, J.; Yang, A.Y.; Ganesh, A.; Sastry, S.S.; Yi Ma,

Pattern Analysis and Machine Intelligence, IEEE Transactions on ,

vol.31, no.2, pp.210,227, Feb. 2009